

DEGRADATION BEHAVIOR OF INDOCYANINE
GREEN DYE DURING HIGH INTENSITY
LASER IRRADIATION

By

JASON WAYNE CRULL

Bachelor of Science

University of Central Oklahoma

Edmond, Oklahoma

1994

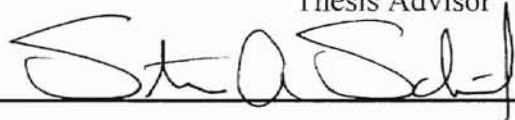
Submitted to the Faculty of the
Graduate College of the
Oklahoma State University
in partial fulfillment of
the requirement for
the Degree of
MASTER OF SCIENCE
December, 1997

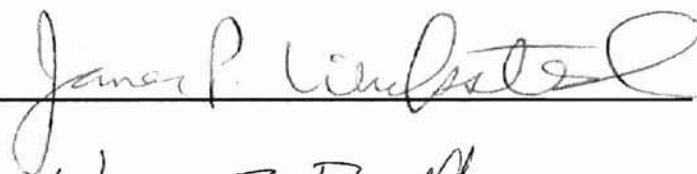
DEGRADATION BEHAVIOR OF INDOCYANINE
GREEN DYE DURING HIGH INTENSITY
LASER IRRADIATION

Thesis Approved:



Thesis Advisor







Dean of the Graduate College

ACKNOWLEDGMENTS

I would like to express my thanks and undying gratitude to both of my Major Advisors: Dr. Stephen W. S. McKeever and Dr. Steven A. Schafer. I would like to thank Dr. Schafer for not only letting me work for him as a graduate student but also as an undergraduate for two summers prior to my attendance to Oklahoma State University. Dr. Schafer's patience and understanding are greatly appreciated during the times when things were not working correctly, especially when it was my fault. I would like to thank Dr. McKeever for taking me under his wing during Dr. Schafer's absence and giving me the opportunity to finish the work I started under Dr. Schafer. Dr. McKeever's patience in waiting for me to finish this thesis is greatly appreciated, along with his understanding and support when I informed him that I would be leaving the Physics Department upon completion of this thesis to pursue a career in industry. I would also like to thank Dr. James P. Wicksted for his willingness to be on my graduate committee and for letting me share an office with his graduate students.

Someone who deserves special thanks is Dr. Jin Fu Zhou. Dr. Zhou deserves credit for the design and construction of the spectrophotometer setup used in the experiment, as well as the software that converted the images collected from the spectrophotometer into the data that I analyzed in this thesis. Dr. Zhou sacrificed his own

valuable time to help me, and delayed his own experiments so that I could have access to the equipment and computers. Thank you for everything, Dr. Zhou.

I would also like to express my fondest thanks to my wife, Lynett, for always telling me not to give up, and that I could do it if she could, and for making me feel like the smartest person on the planet, even if we both know it is not true. I thank Scarlet, for the opportunity of being called “Daddy.” I also need to thank my parents Wayne and Janis Crull, for supporting me in all my decisions, inspiring me to learn all that I can in life, and for making me work with the best “Jack of All Trades.” I also need to thank my mother-in-law, Joyce Rock, for the nearly daily constant reminder that my thesis was not yet done and that the deadlines were fast approaching.

Last, but not least, I would like to thank all of my friends in the physics department: from the graduate students that started here the same time that I did, to those that just received their Ph.D.’s, to the secretaries, and all the other professors that had to deal with me and put up with my questions.

TABLE OF CONTENTS

Chapter	Page
1. INTRODUCTION	1
1.1. HISTORY OF INDOCYANINE GREEN	1
1.2. OPTICAL PROPERTIES OF INDOCYANINE GREEN	1
1.3. INDOCYANINE GREEN STABILITY	4
1.4. CONTRIBUTIONS OF THIS THESIS	4
2. EXPERIMENTAL PROCEDURES	10
2.1. INTRODUCTION	10
2.2. SAMPLE PREPARATION	10
2.2.1. AQUEOUS ICG SOLUTIONS	10
2.2.2. METHANOL ICG SOLUTIONS	12
2.2.3. MEASUREMENT UNCERTAINTY	12
2.3. EXPERIMENTAL SETUP	17
2.3.1. IRRADIATION SETUP	17
2.3.2. SPECTROPHOTOMETER SETUP	21
2.4. THEORETICAL PREDICTIONS	25
3. RESULTS AND DISCUSSION	29
3.1. EXPERIMENTAL RESULTS	29
3.1.1. METHANOL ICG SOLUTIONS	29
3.1.2. AQUEOUS ICG SOLUTIONS	37
3.2. DATA ANALYSIS	44
3.2.1. ANALYSIS PROCEDURES	44
3.2.2. ANALYSIS RESULTS	45
4. SUMMARY AND CONCLUSIONS	61
BIBLIOGRAPHY	64

APPENDICES	68
APPENDIX A - SOFTWARE FOR DATA ACQUISITION AND ANALYSIS	69
A.1. DATA ANALYSIS	69
A.2. DATA ACQUISITION	74
APPENDIX B - PREVIOUS PUBLICATION	87

LIST OF TABLES

Table	Page
2.1. Concentrations and measurements of ICG in aqueous solution	15
2.2. Concentrations and measurements of ICG in methanol solution	16
3.1. Best fit parameters for ICG in methanol solution	58
3.2. Best fit parameters for ICG in aqueous solution	59

LIST OF FIGURES

Figure	Page
1.1. The indocyanine green molecule	6
1.2. Normalized absorbance spectra of ICG in water at three concentrations	7
1.3. Normalized absorbance spectra of ICG in water + 3% HSA at three concentrations	8
1.4. Normalized absorbance spectra of ICG in methanol at three concentrations	9
2.1. Schematic representation of the irradiation setup	20
2.2. Schematic representation of spectrophotometer setup	24
3.1. Irradiated and unexposed samples of 1 μM ICG in methanol	32
3.2. Irradiated and unexposed samples of 3 μM ICG in methanol	33
3.3. Irradiated and unexposed samples of 10 μM ICG in methanol	34
3.4. Irradiated and unexposed samples of 30 μM ICG in methanol	35
3.5. Irradiated and unexposed samples of 100 μM ICG in methanol	36
3.6. Irradiated and unexposed samples of 1 μM ICG in aqueous solution	39
3.7. Irradiated and unexposed samples of 3 μM ICG in aqueous solution	40
3.8. Irradiated and unexposed samples of 10 μM ICG in aqueous solution	41
3.9. Irradiated and unexposed samples of 30 μM ICG in aqueous solution	42
3.10. Irradiated and unexposed samples of 100 μM ICG in aqueous solution	43

3.11. Photodegradation of 1 μM ICG in methanol	48
3.12. Photodegradation of 3 μM ICG in methanol	49
3.13. Photodegradation of 10 μM ICG in methanol	50
3.14. Photodegradation of 30 μM ICG in methanol	51
3.15. Photodegradation of 100 μM ICG in methanol	52
3.16. Photodegradation of 1 μM ICG in aqueous solution	53
3.17. Photodegradation of 3 μM ICG in aqueous solution	54
3.18. Photodegradation of 10 μM ICG in aqueous solution	55
3.19. Photodegradation of 30 μM ICG in aqueous solution	56
3.20. Photodegradation of 100 μM ICG in aqueous solution	57
3.21. Parameter m vs. concentration for methanol and aqueous solutions	60
A.1 Microsoft Excel worksheet used for calculating the κ and m values for the 10 μM ICG in aqueous solution	73

CHAPTER 1

INTRODUCTION

1.1 HISTORY OF INDOCYANINE GREEN

Indocyanine green dye (ICG) was developed in the 1950's at the Eastman Kodak Research Laboratories in New York by Drs. Leslie Brooker and Donald Heseltine and patented in 1959 [1-4]. ICG was quickly distinguished for two unique properties: it has high optical absorbance in a spectral region where human tissue is relatively transparent and it has very low toxicity [1-3]. One of the initial uses for ICG was as an indicator for cardiovascular circulation [1-3]. Indocyanine green has continued to be used in the medical community for such purposes as blood volume determination, liver function studies, object localization in tissue and fluorescence probing of enzymes and proteins [5]. More recently, ICG has been used in ophthalmic research and as a selectivity agent in the delivery of laser energy to biological tissues [6-20, 32-38].

1.2 OPTICAL PROPERTIES OF INDOCYANINE GREEN

The optical properties of indocyanine green arise from its chemical composition. The schematic diagram of the indocyanine green molecule seen in Figure 1.1 shows a chain of atoms, in the center of the ICG molecule, that are bound together by alternating single and double bonds that form what is called a conjugated chain [31]. This conjugated

chain behaves like an antenna, in that the π -orbital electrons in the chain may oscillate along the chain when excited with the appropriate energy. The strong absorption of light by ICG is considered to be due to the electrons in this conjugated chain absorbing the incident light energy [31].

At low concentrations, indocyanine green dye, when dissolved in water, blood plasma, or methanol, has a peak absorption near 800 nm; the exact location of the peak absorbance depends on the concentration of ICG and the solvent used. At high concentrations the dominant absorption peak is located near 700 nm; the 800 nm peak is still present, but it is no longer the dominant peak [25,26]. The wavelength at which peak absorption occurs will thus vary for different concentrations of ICG dissolved in different solvents. Similarly, the concentration at which the 700 nm peak becomes dominant depends on the solvent used. The change in wavelength at which the dominant peak occurs is not due to a shift of the peaks, but from a chemical change in the ICG solution that takes place at higher concentrations.

The change in the maximum absorbance peak is due to indocyanine green aggregation, the collection of one or more ICG molecules combining with other ICG molecules to form larger units, called oligomers. An oligomer of two molecules is called a dimer, an oligomer of three molecules is a trimer, and so on. An oligomer with n number of molecules is generally referred to as an n -mer. A single molecule of ICG can be considered an oligomer of only one molecule and is referred to as a monomer. The aggregation of ICG can occur through different species of oligomers, such as a monomer to monomer, or dimer to dimer, or monomer to dimer, *etc.*

Figures 1.2 - 1.4 show how the normalized absorption spectra changes at different

concentrations for different solvents; the absorbance has been normalized with the concentration to show the nature of the absorbance spectra at different concentrations on the same scale. Figure 1.2 shows a maximum absorbance at approximately 780 nm for the 36 and 17 μM concentrations, with each having a shoulder peak at 715 nm. This shoulder peak not only becomes the dominant peak at higher concentrations but it is also shifted; the maximum absorbance peak is located at 700 nm at a concentration of 101 μM . While the peak at the 700 - 715 nm range shifts to lower wavelengths at higher concentrations, the 780 nm peak remains fixed at low and high concentrations.

Figure 1.3 shows the normalized absorbance spectrum for ICG in a solution of water and human serum albumin (water + 3% HSA, by weight). The peak absorbance remains stationary at approximately 795 nm at low and high concentrations, with a barely visible shoulder peak around 725 nm.

Figure 1.4 shows the normalized absorbance behavior of ICG in methanol. The dominant absorption peak is located at approximately 787 nm, with the shoulder peak in the 715 nm range showing no change with concentration.

As indicated in Figure 1.2, indocyanine green aggregates will form at low concentrations due to the hydrophobic nature of the dye. The aggregates form from the dipole-dipole interactions and van der Waals forces between the dye and the water molecules in aqueous solutions [26]. At higher concentrations aggregation dominates giving rise to the increase of the 700 nm absorption peak. When ICG is dissolved in either methanol or a solution of water and human serum albumin (HSA) the dye becomes more stable and aggregates form less readily. ICG in aqueous solutions with HSA do form aggregates at high enough concentrations. The concentration at which the absorption

peak due to aggregate formation becomes dominant depends on the ICG concentration and the amount of HSA present in the solution. However, solutions of ICG in methanol, in concentrations above 120 μM , have not demonstrated aggregate formation.

1.3 INDOCYANINE GREEN STABILITY

When in the dry, solid state form, powdered indocyanine green is stable for over a year when kept at room temperature. However, once indocyanine green has been dissolved in water, the dye will rapidly degrade, even in the absence of light [1,30]. However, if indocyanine green is in a solution of water and protein, such as human serum albumin (HSA), the degradation rate is greatly reduced [30]. When in the blood, ICG is stable over a period of several days [1].

Indocyanine green dissolved in methanol, although of no use in medical treatments, has the advantage of being easy to handle and store and, most importantly, being stable for periods of weeks. In this thesis, the indocyanine green dye samples were either dissolved in methanol or in a solution of deionized water and 3% HSA, by weight.

1.4 CONTRIBUTIONS OF THIS THESIS

Indocyanine green has long been studied for its absorption properties, fluorescence properties, and degradation properties when exposed to light or heat [1-5, 23-28, 30, 32-33]. Studies have also been performed to determine the effectiveness of the dye in medical applications, especially in laser tissue welding [6-20, 22,34-38]. This thesis expands on the work done by Crull and Schafer that studies the effect that high intensity

laser irradiation has on the stability/degradation of ICG [29]. This thesis considers the effect that laser radiation, which may be typical in laser welding applications, has on the degradation of ICG in an otherwise stable environment.

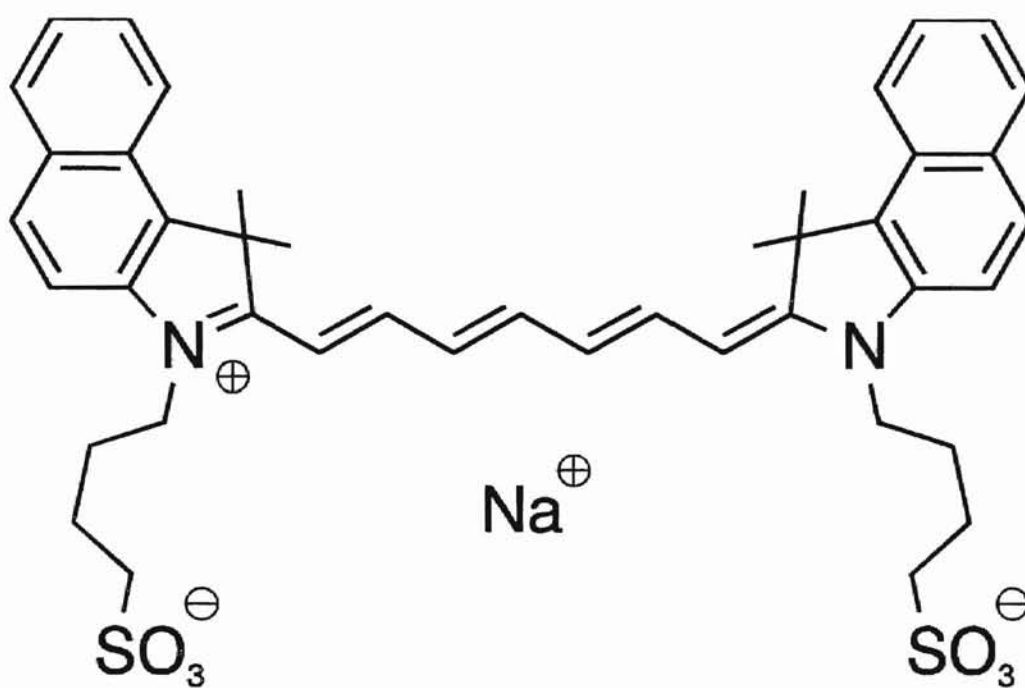


Figure 1.1 The indocyanine green molecule. Unlabeled vertices represent Carbon atoms.

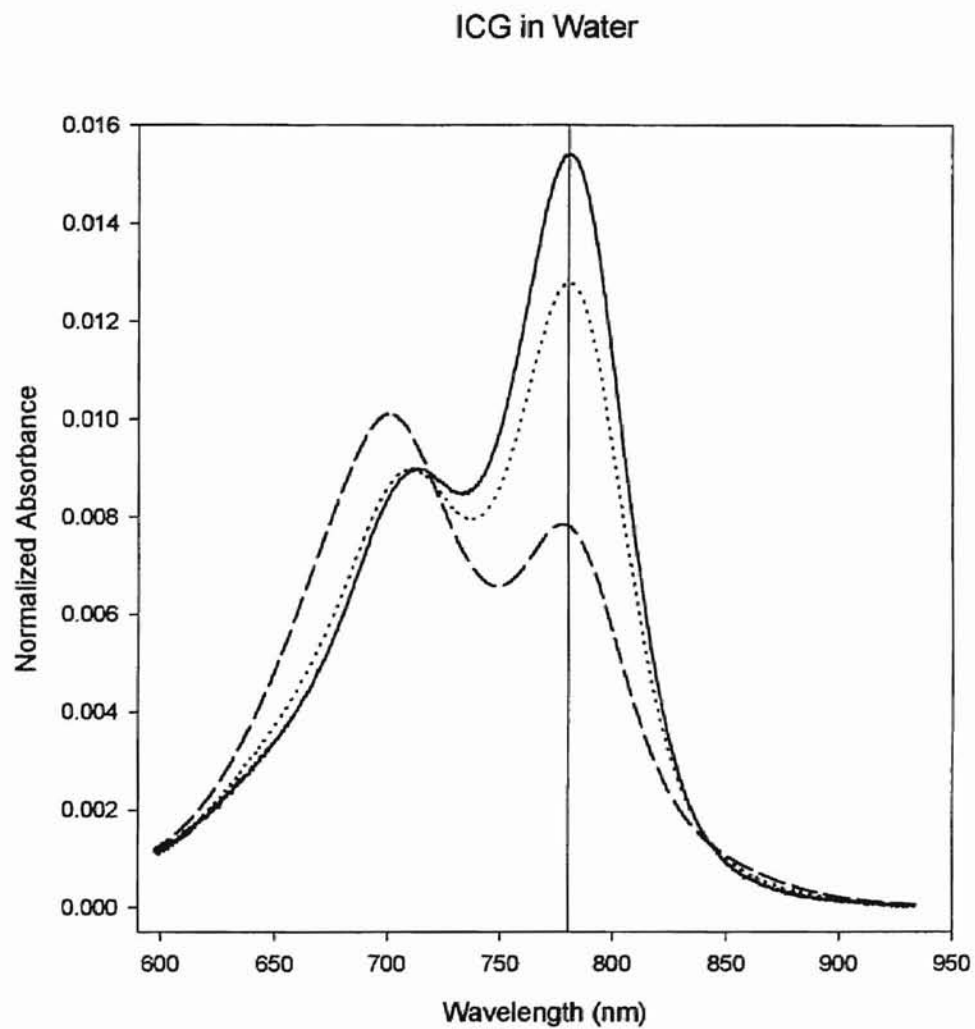


Figure 1.2 Normalized absorbance spectra of ICG in water for three concentrations: 17 μM (solid line), 36 μM (dotted line), and 101 μM (dashed line). The vertical line is at approximately 780 nm.

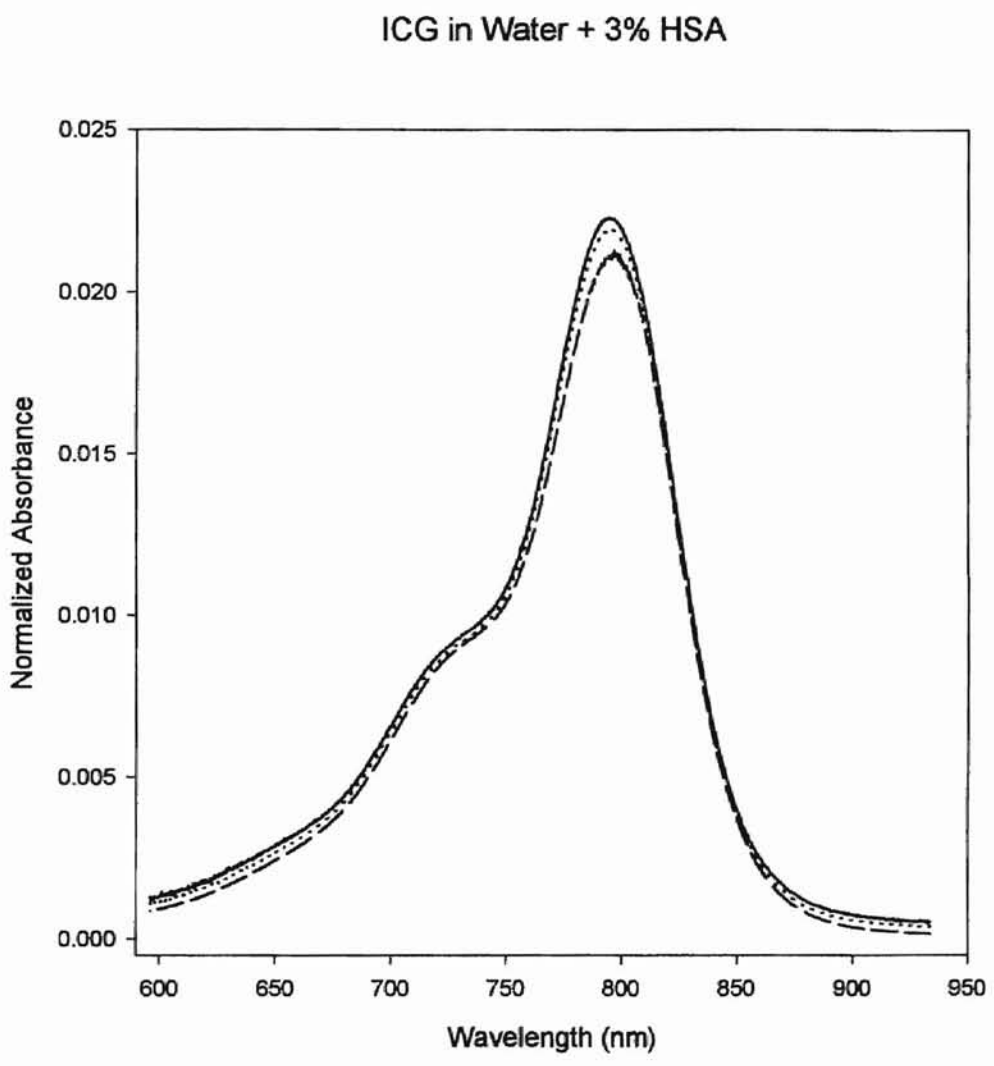


Figure 1.3 Normalized absorbance spectra of ICG in water + 3% HSA for three concentrations: 16 μM (solid line), 31 μM (dotted line), and 106 μM (dashed line).

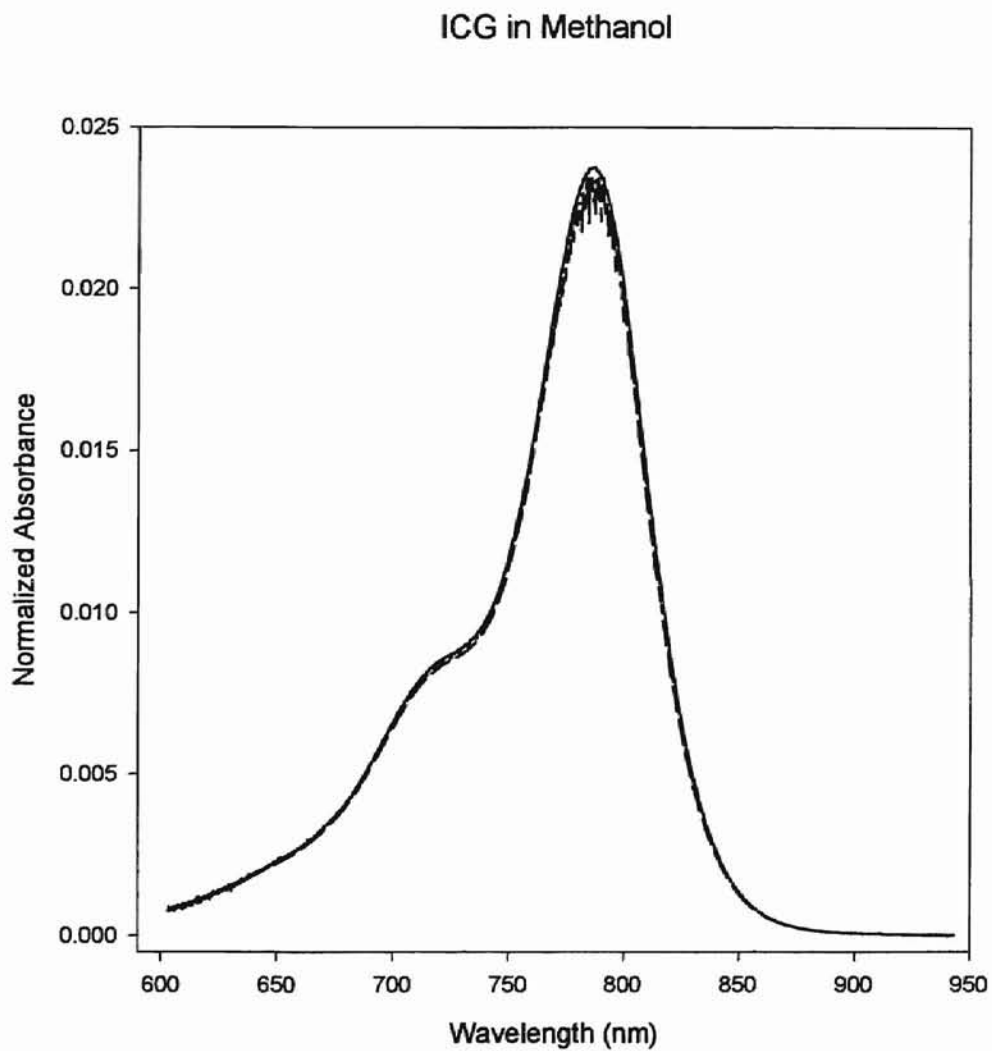


Figure 1.4 Normalized absorbance spectra of ICG in methanol for three concentrations: 32 μM (solid line), 65 μM (dotted line), and 128 μM (dashed line).

CHAPTER 2

EXPERIMENTAL PROCEDURES

2.1 INTRODUCTION

Before this work, it was believed that indocyanine green dye in methanol solutions was stable even upon exposure to high intensity laser irradiation. It was also believed that ICG in solutions with stabilizing proteins were stable while in the body. However, work done by LaJoie, *et al.*, has suggested that ICG may photodegrade even in the presence of stabilizing proteins, if the illumination intensity is high enough [20,29]. To date, no references are available describing the degradation effects that high intensity laser irradiation has on ICG while in the body.

This thesis will describe studies of how indocyanine green degrades upon exposure to high intensity laser irradiation when in methanol solutions and aqueous solutions with stabilizing proteins present.

2.2 SAMPLE PREPARATION

2.2.1 AQUEOUS ICG SOLUTIONS

The 538 μM stock solution of aqueous ICG was prepared by dissolving 12.5 mg of laser-grade indocyanine green (formula weight: 774.97 g/mole) in 30 mL of a solution

of deionized water + 3% by weight human serum albumin (HSA). The indocyanine green was obtained from Kodak under the trade name IR-125; the deionized water was obtained from a Barnstead NANOpure ultrapure water system; the pipettes used in measuring the volume of liquid used were Oxford® BenchMate™ continuously adjustable pipettes. The human serum albumin (HSA) was purchased from Sigma Chemical; the percentage of HSA-to-water in the solution is 3% by weight, or 4.8482g HSA in 160 mL water (see section 2.2.3 for measurement uncertainties). The bottle of stock solution was sealed and shaken by hand for approximately 30 seconds. To allow the indocyanine green to fully dissolve in solution and to allow the bubbles formed from shaking the container to diminish, the stock solution was placed in a dark, room temperature (20 °C) box for nine hours. From this stock solution 15 mL of 1 μ M, 3 μ M, 10 μ M, 30 μ M, and 100 μ M final concentrations of ICG were prepared in similar bottles (see Table 2.1 for details); the above mentioned samples were stirred by grasping the bottles at the neck and swirling the bottles circularly in the horizontal plane to eliminate the bubble formation encountered while shaking the stock solution.

Two polystyrene cuvettes (Fisher Chemical standard DSP cuvettes) were then filled with identical concentrations and covered by Parafilm-M to minimize loss due to evaporation. One cuvette was set aside in a dark box for a control sample while the other was irradiated with laser energy. This same procedure was followed for all above mentioned concentrations.

2.2.2. METHANOL ICG SOLUTIONS

A concentrated solution of ICG in methanol was prepared by dissolving 15.0 mg of laser-grade indocyanine green, from Kodak (IR-125, lot # 0990 103070), and 32.6 mL of HPLC grade methanol, from Fisher Chemical, to create a 595 μM stock solution. The methanol was used without further purification. The lid was securely tightened on the glass container of ICG stock solution and shaken vigorously for 30 seconds. The solution was then placed in a dark, room temperature (25 °C) container for several hours to allow the dye to fully dissolve in the methanol. Final concentrations of 1 μM , 3 μM , 10 μM , 30 μM , and 100 μM were prepared in similar containers (see Table 2.2) and placed in a dark, room temperature container for eight hours (overnight) before use. Two polystyrene cuvettes were each filled with 3.5 mL of the desired concentration; one cuvette was stored in a dark container for a control while the other was irradiated with laser energy.

2.2.3 MEASUREMENT UNCERTAINTY

The greatest uncertainty in measuring the concentration of the samples is in measuring the initial amount of indocyanine green powder to be used in the solutions. The display on the digital scale used reads to the tenth of a milligram, or 0.0001 g. However, this digit is not significant. The maximum error for this scale is thus ± 0.5 mg, leading to a 4% and 3.3% error in the mass of the ICG used in creating the stock aqueous and methanol solutions, respectively. To calculate the molar concentration (moles/liter), the mass of the ICG to be used is divided by the formula weight of ICG (assumed to be exact)

such that $n = m/FW$, where n is the number of moles, m is the mass and FW is the formula weight. Thus, the error in the number of moles, Δn , is just the error in the mass of ICG divided by the formula weight, or $\Delta n = \Delta m/FW$.

The uncertainty in the volume of solvent used in making the solutions is determined from the pipette manufacturer's specifications. The uncertainty varies with the settings on the pipettes; for example, a setting of 1000 μL has an uncertainty of $\pm 0.8\%$, or $\pm 8 \mu\text{L}$ whereas a setting of 10 μL has an uncertainty of $\pm 3.0\%$, or $\pm 0.3 \mu\text{L}$.

The calculation of the stock solution concentration, C , is determined from the equation $C = n/V$, where n is the number of moles of ICG and V is the volume of the solvent. The error in the stock concentration, ΔC is

$$\Delta C = \frac{\Delta n}{\Delta V} - \frac{n \Delta V}{V^2}, \quad (2.1)$$

where ΔV is the error in the volume of solvent.

The concentrations used in the experiment are prepared by diluting concentrations of the stock solution and, therefore, require a different equation that relates the final concentration to the initial stock concentration. The equation for the diluted concentration is

$$C_f = C_i \frac{V_i}{V_f} \quad (2.2)$$

where C_f is the final diluted concentration, C_i is the initial (stock) concentration, V_i is the volume of stock solution, and V_f is the total volume of the final (diluted) solution. The total volume of the final solution is the sum of the volume of the stock solution used and the volume of the solvent used, or $V_f = V_i + V_s$, where V_s is the volume of the solvent.

The uncertainty in the final concentration is therefore dependent on the uncertainty in C_i , V_i , and V_s . The formula for the uncertainty in C_f , is

$$\Delta C_f = \frac{C_i \Delta V_i}{V_i + V_s} + \frac{\Delta C_i V_i}{V_i + V_s} - \frac{C_i V_i (\Delta V_i + \Delta V_s)}{(V_i + V_s)^2}. \quad (2.3)$$

Tables 2.1 (b) and 2.2 (b) show the maximum uncertainties in the measurements for the data shown in the corresponding Tables 2.1 (a) and 2.2 (a) for aqueous solutions and methanol solutions, respectively.

Final Concentration	Stock Solution used (538 μM)	Water + 3% HSA Solution used
1 μM	27.9 μL	14.9721 mL
3 μM	83.6 μL	14.9164 mL
10 μM	0.279 mL	14.721 mL
30 μM	0.836 mL	14.164 mL
100 μM	2.788 mL	12.212 mL
538 μM	30.000 mL	

Maximum Concentration Uncertainty	Stock Solution Volume Uncertainty	Water + 3% HSA Solution Volume Uncertainty
(1 μM) \pm 0.005 μM	\pm 0.4 μL	\pm 0.120 mL
(3 μM) \pm 0.013 μM	\pm 1.04 μL	\pm 0.120 mL
(10 μM) \pm 0.352 μM	\pm 3.2 μL	\pm 0.120 mL
(30 μM) \pm 1.006 μM	\pm 0.008 mL	\pm 0.112 mL
(100 μM) \pm 3.238 μM	\pm 0.024 mL	\pm 0.099 mL
(538 μM) \pm 17.20 μM	\pm 0.240 mL	

TABLE 2.1. (a) Concentrations of indocyanine green (ICG) samples in water + 3% HSA. Final concentrations are obtained by mixing the given amount of 538 μM stock solution with the given amount of water + 3% HSA solution. (b) Uncertainty in the measurements shown in (a).

Final Concentration	Stock Solution used (595 μM)	Methanol used
1 μM	25.2 μL	14.975 mL
3 μM	75.6 μL	14.924 mL
10 μM	0.336 mL	19.664 mL
30 μM	1.010 mL	18.992 mL
100 μM	3.360 mL	16.640 mL
595 μM	32.60 mL	

Maximum Concentration Uncertainty	Stock Solution Volume Uncertainty	Methanol Volume Uncertainty
(1 μM) \pm 0.033 μM	\pm 0.4 μL	\pm 0.120 mL
(3 μM) \pm 0.099 μM	\pm 1.2 μL	\pm 0.120 mL
(10 μM) \pm 0.312 μM	\pm 4.8 μL	\pm 0.160 mL
(30 μM) \pm 0.763 μM	\pm 8.3 μL	\pm 0.152 mL
(100 μM) \pm 2.530 μM	\pm 0.028 mL	\pm 0.136 mL
(595 μM) \pm 14.98 μM	\pm 0.264 mL	

TABLE 2.2. (a) Concentrations of indocyanine green (ICG) in methanol samples. Final concentrations are obtained by mixing the given amount of 595 μM stock solution with the given amount of methanol.
(b) Uncertainty of the measurements shown in (a).

2.3. EXPERIMENTAL SETUP

2.3.1. IRRADIATION SETUP

A pulsed Alexandrite laser (Light Age model 101PAL) was used as the source of laser radiation. The Alexandrite laser is tunable over a range from approximately 720 nm to 780 nm. The laser output is maximal when the laser is set at a wavelength of 750 nm; hence, the wavelength chosen for the experiment was 750 nm. The laser operates at a pulse repetition rate of 20 Hz with each pulse being approximately 60 μ s long (full width at half maximum, FWHM), henceforth called long pulses. Each long pulse is actually a packet of multiple, shorter pulses that have individual pulse widths on the order 90 ns (FWHM).

The laser may also be operated in a Q-switched mode which shortens the pulses, but keeps the total energy per pulse constant. These Q-switched pulses are a single pulse with pulse width around 90 ns (FWHM). The experimental setup for both long pulse and Q-switched irradiations is the same.

In order to accommodate the laser, all the optics, the sample, and both detectors on one optics table, the setup required the "U" shape form as seen in Figure 2.1. The beam exits the laser and is redirected to the opposite end of the optics table via two dielectric coated mirrors (Virgo Optics). A glass microscope-slide is placed in the path of the beam and is used as a beam splitter. This glass slide reflects approximately 3% of the incident laser beam.

The diverging lens positioned after the first beam splitter and before the ICG sample is used to provide a larger spot size at the surface of the cylindrical lens. The

cylindrical lens modifies the beam into an elliptical shape; this enables the expanded beam to irradiate a broader portion of the sample with minimal loss of laser radiation to the periphery; the spot size on the cuvette is approximately 0.5 cm wide by 2.5 cm tall. To ensure a uniform distribution of energy deposition throughout the ICG sample, a miniature magnetic stir bar was placed inside the cuvette and driven by a Hellma CUV-O-STIR® (model 333).

The amount of energy delivered to the ICG sample cannot be detected directly, for the energy of the laser pulses is far greater than the damage threshold of the available detectors. To calculate the amount of energy delivered to the ICG sample, an alternate method was devised that entailed measuring a smaller portion of the energy delivered to the sample. The amount of energy deposited into the ICG sample is determined by measuring the both the amount of energy transmitted and energy reflected by the second beam splitter; the light that is incident to the second beam splitter is just the light reflected from the first beam splitter. The second beam splitter is placed at an angle identical to the first beam splitter ($45^\circ \pm 1^\circ$ with respect to the incident beam); therefore, the percent of light reflected by the second beam splitter should be identical to the percentage of light reflected by the first beam splitter. The ratio of transmitted to reflected energy (T:R ratio) of the first beam splitter is then identical to the T:R ratio of the second beam splitter.

The laser pulses from the alexandrite laser vary in shape and position due to thermal fluctuations of the alexandrite crystal, hence any non-uniformity of the detector surfaces (typical of a foreign object on the detector surface or a damaged area of the detector) can cause the measured T:R ratio to vary from pulse to pulse. To minimize the fluctuations in the measured T:R ratio, the lens placed before the second beam splitter is

used to diverge the beam going to both detectors by the same amount in order for the beam to cover the greatest surface area on both detectors. This enlarged beam spot size (approximately 0.5 cm in diameter) is large enough to cover most of the detector surface without clipping by the detector aperture.

Since the measured T:R ratio varies slightly from pulse to pulse, the appropriate ratio used to calculate the energy delivered to the ICG sample is the average of the T:R ratios for each pulse of that irradiation data set. Once the T:R ratio of the second beam splitter is determined, the amount of energy delivered to the ICG sample can be calculated by multiplying the T:R ratio with the energy detected by Detector A. This assumes that no loss due to surface reflections occur at the lenses, cuvette, back surfaces of the beam splitters, and the detector heads. To minimize any loss due to these surface reflections, a minimal amount of optics was used for the irradiation setup.

The detectors (Laser Precision RJP-735) monitor the energy per pulse in real time. The energy meter (Laser Precision RM-6600) is connected to an IBM compatible 486 personal computer via a National Instruments NI-488.2 interface board. A computer program reads the data from the energy meter, displays the real-time data on a computer monitor, and saves the data to a local hard disk. The data acquisition software was written in Microsoft QuickBasic Version 4.5 and was run under DOS 6.20.

The polystyrene cuvettes used in this experiment have 88% transmission in the 700-800 nm range and show no signs of any reaction with the methanol solvent for a period of over one month. The cuvettes show no signs of reaction at all with the aqueous solutions of indocyanine green.

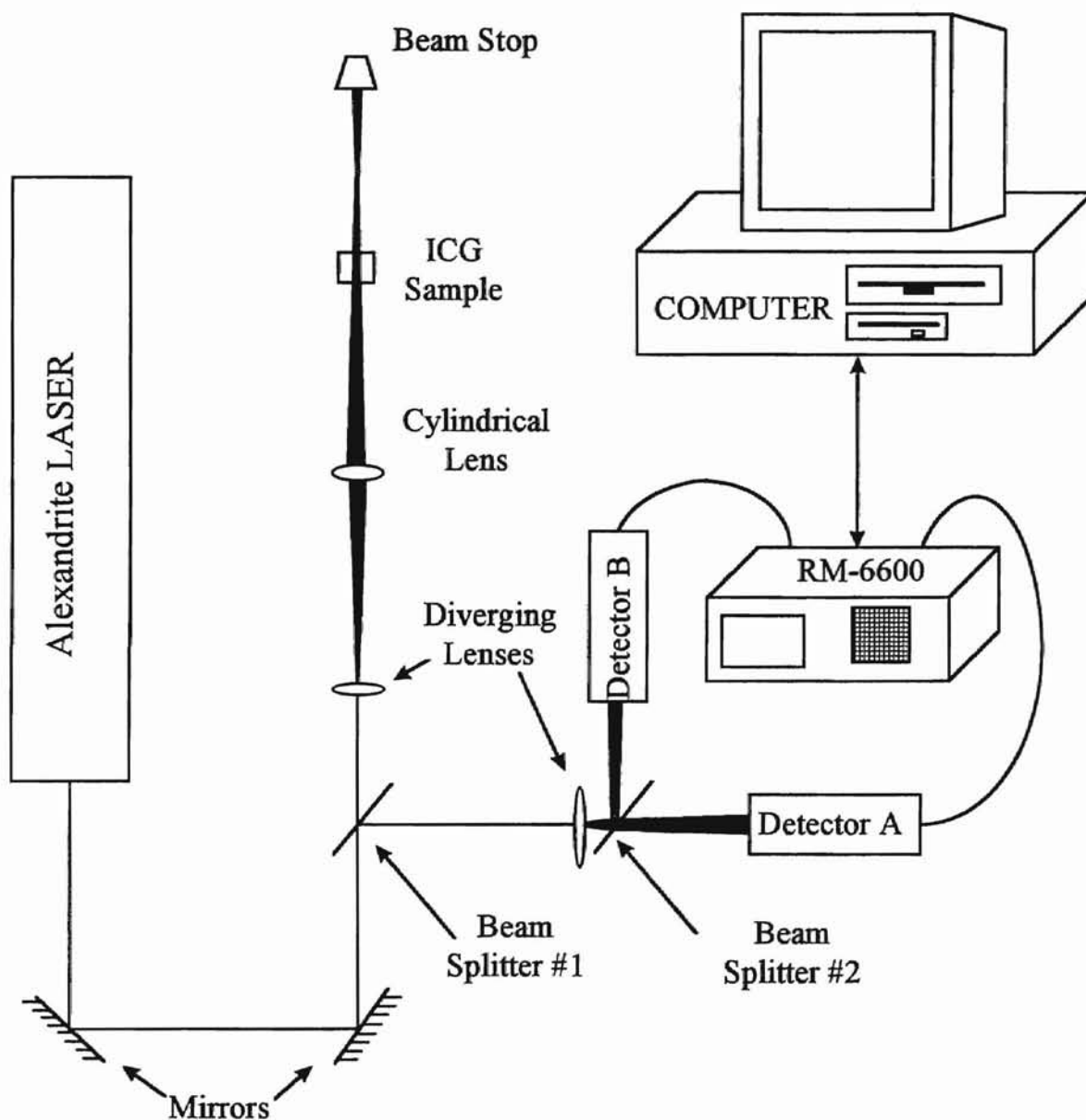


FIGURE 2.1. Schematic representation of the irradiation experimental setup.

2.3.2 SPECTROPHOTOMETER SETUP

At intervals during irradiation the cuvette containing the ICG sample was removed from the irradiation setup and inserted into the single-beam spectrophotometer shown in Figure 2.2. The infrared lamp (an electrically-heated platinum wire) emits light in the wavelength range of interest for ICG optical absorption (approximately 600-930 nm). A 35 mm, f/8 camera lens is used to focus the light onto the cuvette; the spot size on the cuvette is approximately 2 mm x 35 mm. After the light passes through the cuvette it enters the spectrometer (Instruments SA HR320) through a 136 μm wide slit. The transmitted spectrum is then imaged by a thermo-electrically cooled CCD camera (Photometrics CH 250; 1317 x 1035 pixels). The camera exposure time for optimal signal to noise ratio was 15 seconds for the 1, 3, 10 and 30 μM concentrations in methanol and all concentrations in the water/HSA solution and 20 seconds for the 100 μM concentration in methanol. An exposure time that is too long saturates the camera, hence data in regions with high optical transmittance (low absorbance) is lost. An exposure time which is set too short loses information in regions with low optical transmittance (high absorbance) by not collecting enough data; the signal is then of the order of magnitude of the noise in the system. The optimal exposure time mentioned above was determined by experiment.

Due to the high optical absorbance of indocyanine green at concentrations of 30 and 100 μM , the optical transmission of ICG in the 10 mm path length cuvettes is too low

to detect accurately. Therefore, for the 30 and 100 μM concentrations, a small amount of the irradiated ICG was transferred from the original 10 mm path length cuvette to a 1 mm path length quartz cuvette via a syringe. The unexposed ICG and reference solvent was transferred to similar 1mm path length cuvettes and left in the same cuvettes for the duration of the experiment. These shorter path length cuvettes were then used in the spectrophotometer. After data were collected with the spectrophotometer, the irradiated dye was transferred back to the longer path length cuvette for further irradiation.

In order to correct for any absorbance or scattering due to the solvent or the cuvette, a reference sample in a similar cuvette containing the appropriate solvent (either methanol or water + HSA solution) was imaged as well. For the samples that were imaged in the 1mm path length cuvettes, the reference spectrum was obtained using a similar 1 mm path length cuvette. To reduce any errors caused by the drift of the lamp or errors in the reading of the CCD image, the data was collected following the procedure described below for all measurements:

1. Reference cuvette
2. Irradiated ICG sample
3. Unexposed ICG sample
4. Reference cuvette
5. Irradiated ICG sample
6. Unexposed ICG sample.
7. Reference cuvette

The three reference data images are taken to account for any intensity or spectral drift that may occur in the lamp during the course of taking data. If any drift is detected in one of

the irradiated or unexposed images, the images from the second set of images were used. Fortunately, there were no significant drifts in either the first or second image files.

After one set of these seven images has been taken, the irradiated ICG sample was then returned to the irradiation setup for further exposures. Another computer then copied the image files, analyzed the copied files, and calculated the absorbance spectrum of both the irradiated ICG sample and the unexposed ICG sample.

The images from the CCD camera were then manipulated on a column-by-column basis by a program written in C++ that calculated the optical absorbance from the CCD image data using the equation

$$A = -\log_{10}\left(\frac{I_{\text{ICG}}}{I_{\text{reference}}}\right), \quad (2.4)$$

where A is the optical absorbance, I_{ICG} is the measured intensity of either the irradiated ICG sample or the unexposed ICG sample, and $I_{\text{reference}}$ is the measured intensity of the reference cuvette. From the number of pixels in the CCD camera and the wavelength range of the spectrum from the spectrometer, a resolution of approximately 0.25 nm per pixel is achieved using this setup.

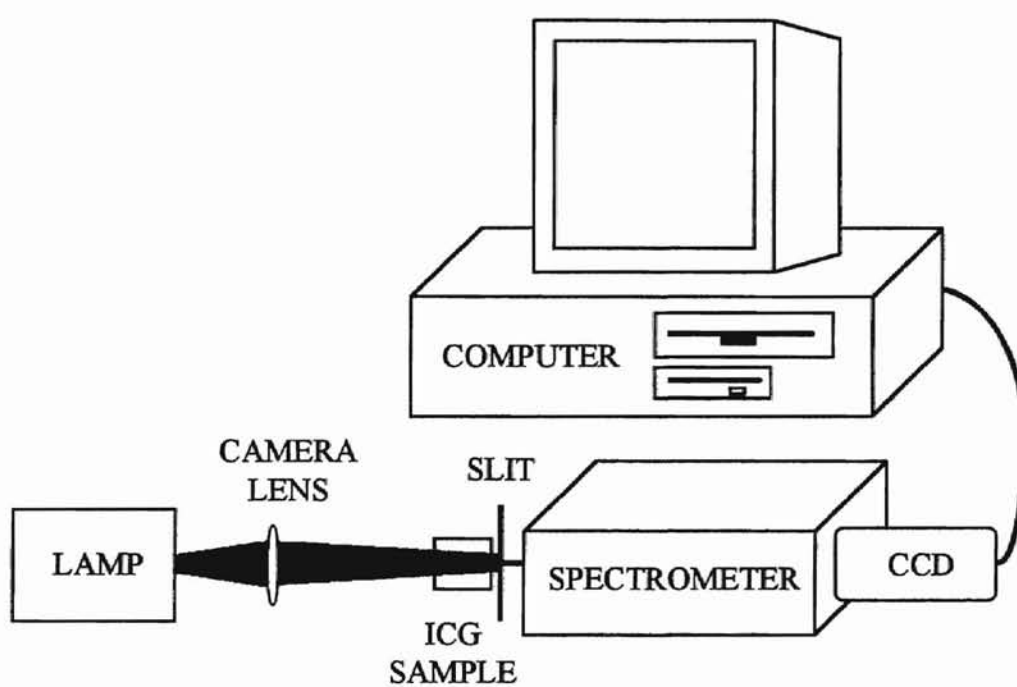


FIGURE 2.2. Schematic representation of spectrophotometer setup.

2.4 THEORETICAL PREDICTIONS

Since the first synthesis of indocyanine green, attempts have been made to create a model for the optical absorption properties of ICG as a function of concentration and the degradation/aggregation of ICG as functions of time, temperature, and concentration, to name a few [5,23,26,28-30]. In order to better understand the degradation process of indocyanine green, a theoretical model that suitably explains the data to be presented later in this thesis is required.

The first step in developing this theoretical model is to understand some basic physical properties of the situation that is to be described. First, it must be noted that the rate of energy delivered to the sample (the incident laser power, described in Section 2.3.1) remains approximately constant during the experiment, however, the energy absorption rate does not remain constant due to the decrease in the absorption coefficient during the course of irradiating the ICG samples with laser energy. If the degradation rate is assumed to be proportional to the energy absorption rate and if the absorption coefficient is assumed to depend on the amount of undegraded ICG, then it may be shown that

$$\delta\alpha \propto (1 - e^{-\alpha x}) \delta E \quad (2.5)$$

where $\delta\alpha$ is the change in absorption coefficient of the solution, δE is the delivered energy, and x is the path length of the cuvette. the quantity $1 - e^{-\alpha x}$ represents the fraction of the incident energy absorbed by the solution.

However, Equation (2.5) ignores some key factors in the degradation process.

One such factor is that the absorption coefficient increases as the concentration increases, but the rate of degradation decreases as concentration increases. So if the degradation rate is not only proportional to the energy deposition rate but also to the ICG concentration, the Equation (2.5) may be modified such that

$$\frac{d\alpha}{dE} = -k(1 - e^{-\alpha x})f(C), \quad (2.6)$$

where k is a constant of proportionality and $f(C)$ is a function of the ICG concentration, C .

At this point a digression must be made to consider a law that relates the transmitted intensity of an electromagnetic wave (light) through an absorbing medium to the incident intensity of that electromagnetic wave and the concentration of that absorbing medium.[39] This law will be referred to as Beer's Law in this thesis, but it is sometimes referred to as the Beer-Lambert law.[39]

Beer's law states that the relationship between transmitted and incident light through an absorbing medium is

$$I = I_0 10^{-aCx}, \quad (2.7)$$

where I is the transmitted intensity, I_0 is the incident intensity, C is the concentration, x is the path length, and a is the absorptivity (a new constant).[28]

Combining Equations (2.4) and (2.7), the relationship between absorbance and concentration becomes

$$-A = \log_{10} \frac{I}{I_0} = -aCx, \quad (2.8a)$$

or

$$A = aCx. \quad (2.8b)$$

The absorption coefficient, α , is defined from the equation

$$e^{-\alpha x} = 10^{-A} \quad (2.9a)$$

or

$$\alpha = \frac{A}{x} \ln(10). \quad (2.9b)$$

Substituting Equation (2.8b) into Equation (2.9b), the relationship between the absorption coefficient can be seen as $\alpha = a C \ln(10)$, or $\alpha \propto C$. Based on Beer's law alone, the relationship between absorbance and ICG concentration is obvious in Equation (2.8b). However, based on work done by Simmons and Shephard, the absorbance of indocyanine green deviates from Beer's law, especially at higher concentrations, when in a solution of either distilled water, whole blood, or blood plasma.[28] This study did verify that the absorbance of ICG does depend on the concentration of ICG, but did not attempt to find a corrected form of Equation (2.8b).

From the above mentioned considerations, it is known that the absorption coefficient is dependent on concentration, therefore, the function $f(C)$ in Equation (2.6) may be replaced by a function of α , or $f(C) = g(\alpha)$. Equation (2.6) may now be expressed as

$$\frac{d\alpha}{dE} = -k(1 - e^{-\alpha x})g(\alpha), \quad (2.10)$$

where $g(\alpha)$ is a function of the absorption coefficient of ICG.

One hypothesis regarding the function $g(\alpha)$ is that this function is also a function of the number of ICG molecules involved in the degradation process. For the simple case of no interaction between ICG molecules (no aggregation), Equation (2.10) would

simplify to

$$\frac{d\alpha}{dE} = -k'(1 - e^{-\alpha x}). \quad (2.11)$$

However, it is known that the degradation involves more than just one oligomeric species. For degradation involving only dimers the function $g(\alpha)$ will be proportional to α . Similarly, if the degradation process only involved trimers then $g(\alpha)$ would be $g(\alpha)$ proportional to α^2 . Generalizing this relationship, Equation (2.10) may be expressed as

$$\frac{d\alpha}{dE} = -\kappa(1 - e^{-\alpha x})\alpha^{m-1}, \quad (2.12)$$

where m is a positive, real number (not necessarily an integer) and κ is a new, real constant of proportionality; the units of κ are dependent on the value of m .

CHAPTER 3

RESULTS AND DISCUSSION

3.1 EXPERIMENTAL RESULTS

3.1.1 METHANOL ICG SOLUTIONS

As can be seen in Figure 3.1, a 1% reduction in peak absorbance of the 1 μM ICG solution is indicated after being irradiated with a small dose of energy, 3 J mL^{-1} . A 17% reduction in the absorbance peak is observed after a total irradiation of 100 J mL^{-1} . Figure 3.1 also shows that the absorbance of the unexposed ICG sample does not change over a period of about two hours, which is to be expected since ICG is stable in methanol for long periods of time.

The noise that appears in the 600 - 650 nm range of Figure 3.1 is attributed to many factors that are beyond control. The biggest factors that influence the above mentioned noise are the position of the cuvette containing the sample and the CCD efficiency. If the cuvette is tilted at some angle, however slight, the path of the light traveling through the sample into the spectrophotometer (see Section 2.3.2) is altered. If the path is altered enough, the transmitted light will no longer be focused to pass through the center of the slit (see Figure 2.2), which will cause a vertical shift in the absorbance spectrum. To correct for this shift, a baseline correction was done on the 900 - 950 nm

range of the data, since that region provides a more adequate baseline (the details of the baseline correction are given in Appendix A). The rest of the noise is mostly attributed to read errors in collecting the image acquired by the CCD and in the pixel-to-pixel efficiency of the CCD array. The pixel-to-pixel efficiency is best described by two neighboring CCD pixels that receive the same amount of light but convert that light to different amount of electrical charges which are then read by the computer. This CCD efficiency error in combination with a slightly tilted cuvette is believed to be the cause of the noise seen in the data. The intensity of the lamp is lowest in the 600 nm range, which will also contribute to some of the noise in that region.

The 3 μM ICG solution in Figure 3.2 shows a 74% reduction in its peak absorbance after being irradiated with just 803 J mL^{-1} . Again, the unexposed ICG in Figure 3.2 shows no change over a period of two hours.

The 10 μM ICG solution in Figure 3.3 shows an 80% reduction in its peak absorbance after 826 J mL^{-1} . Some minor noise is apparent at the maximum absorbance peak in Figure 3.3, but the unexposed dye shows to still be stable after a period of about 2.5 hours. This noise is attributed to such a low signal detected by the CCD camera due to the low transmittance of light through the sample in that spectral region.

In Figure 3.4 the reduction of the maximum absorbance from the 30 μM solution compared to the 10 μM solution is due to the absorbance of the 30 μM sample being measured in a 1 mm path length cuvette while the absorbance of the 10 μM solution was measured in a 10 mm path length cuvette. However, similar results can be seen: a 51% reduction of the maximum absorbance peak is the result of 744 J mL^{-1} exposure. The unexposed dye show some minor deviations from previous concentrations, mainly due to

some of the sample spilling on the outside of the cuvette containing the unexposed ICG when the samples were being transferred to and from the spectrophotometer setup. The “unexposed” cuvette then required the addition of more unexposed ICG to restore the level of solution inside the cuvette to match that of the other cuvettes. The outside of the cuvette was then wiped down with a KimWipe tissue and the experiment continued. The increase of the maximum absorbance peak is believed to be due to the extra absorption of adsorbed ICG on the outside surface of the cuvette from the spilled ICG that was not fully removed when the cuvette was initially wiped down; however, the data still indicates that the unexposed ICG does not degrade in the absence of laser irradiation. Since only the unexposed cuvette was affected by the accident, the data from the irradiated sample are still reliable.

The 100 μM ICG has a 40% reduction of the peak absorbance after irradiation of 1031 J mL^{-1} , as seen in Figure 3.5. Unfortunately, an accident similar to the one during the 30 μM experiment occurred with the 100 μM unexposed cuvette midway through this experiment. Again, the data still clearly indicates that the ICG in the methanol solutions are stable over the course of the experiment, about 3 hours.

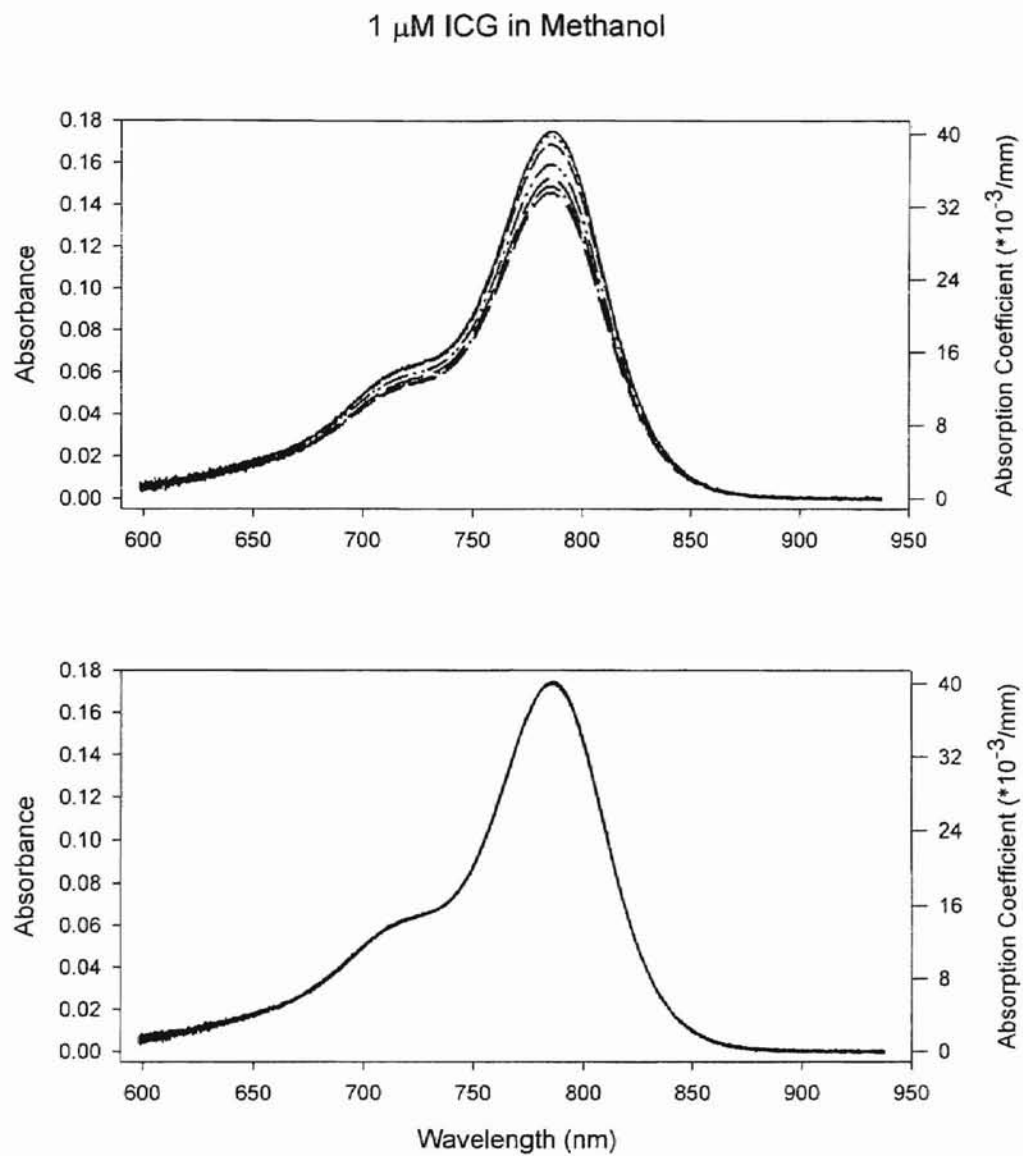


FIGURE 3.1 1 μM ICG in Methanol. Top graph shows absorbance spectrum after 0, 3, 19, 40, 61, 82, and 99 J mL^{-1} . Bottom graph shows absorbance spectrum of non-irradiated 1 μM ICG taken at same time as the irradiated sample.

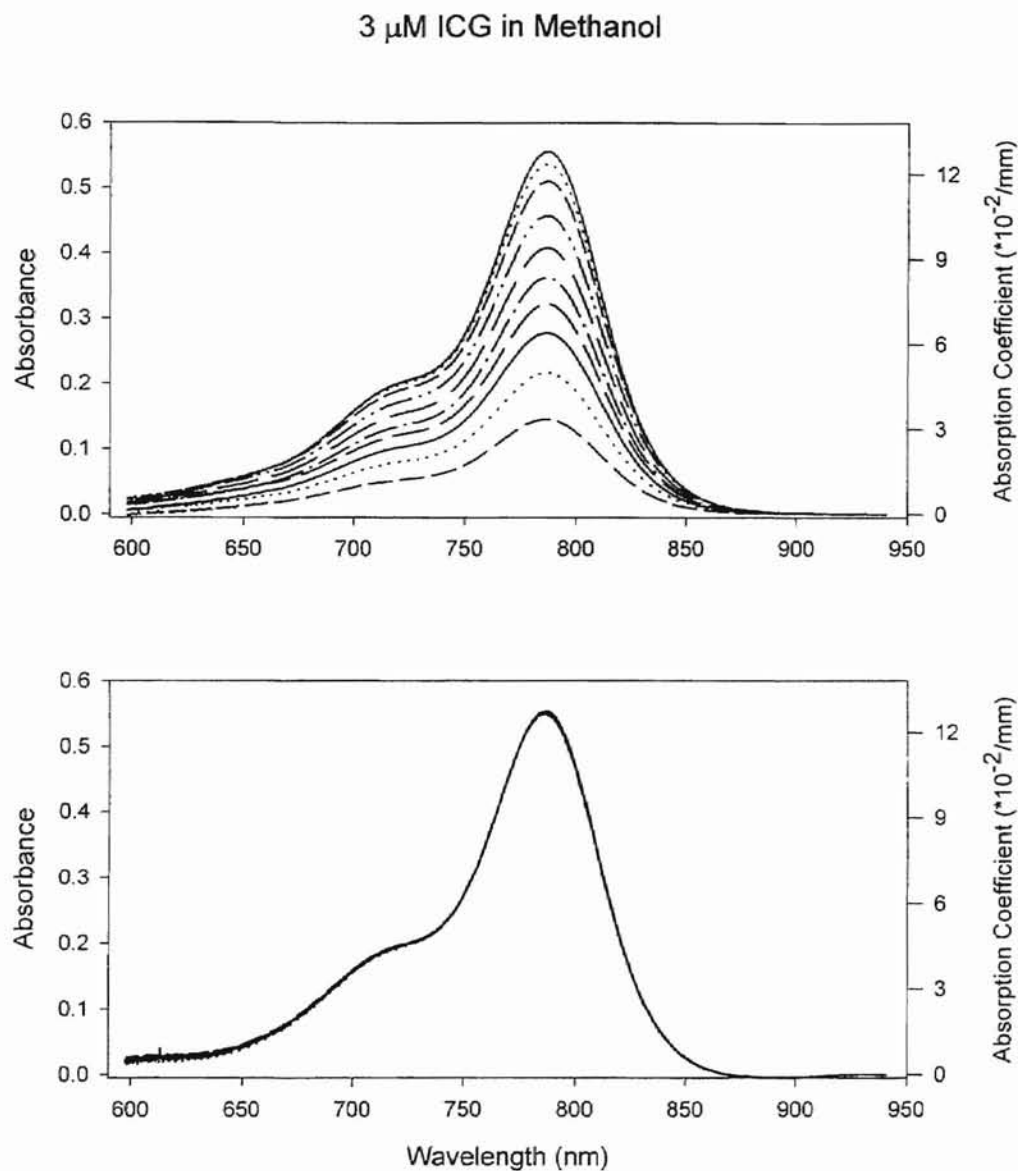


FIGURE 3.2 3 μM ICG in Methanol. Top graph is the absorbance spectrum after irradiation of 0, 16, 48, 96, 156, 232, 323, 430, 584, and 803 J mL^{-1} . Bottom graph shows absorbance of a non-irradiated sample taken at the same time as the above irradiated sample.

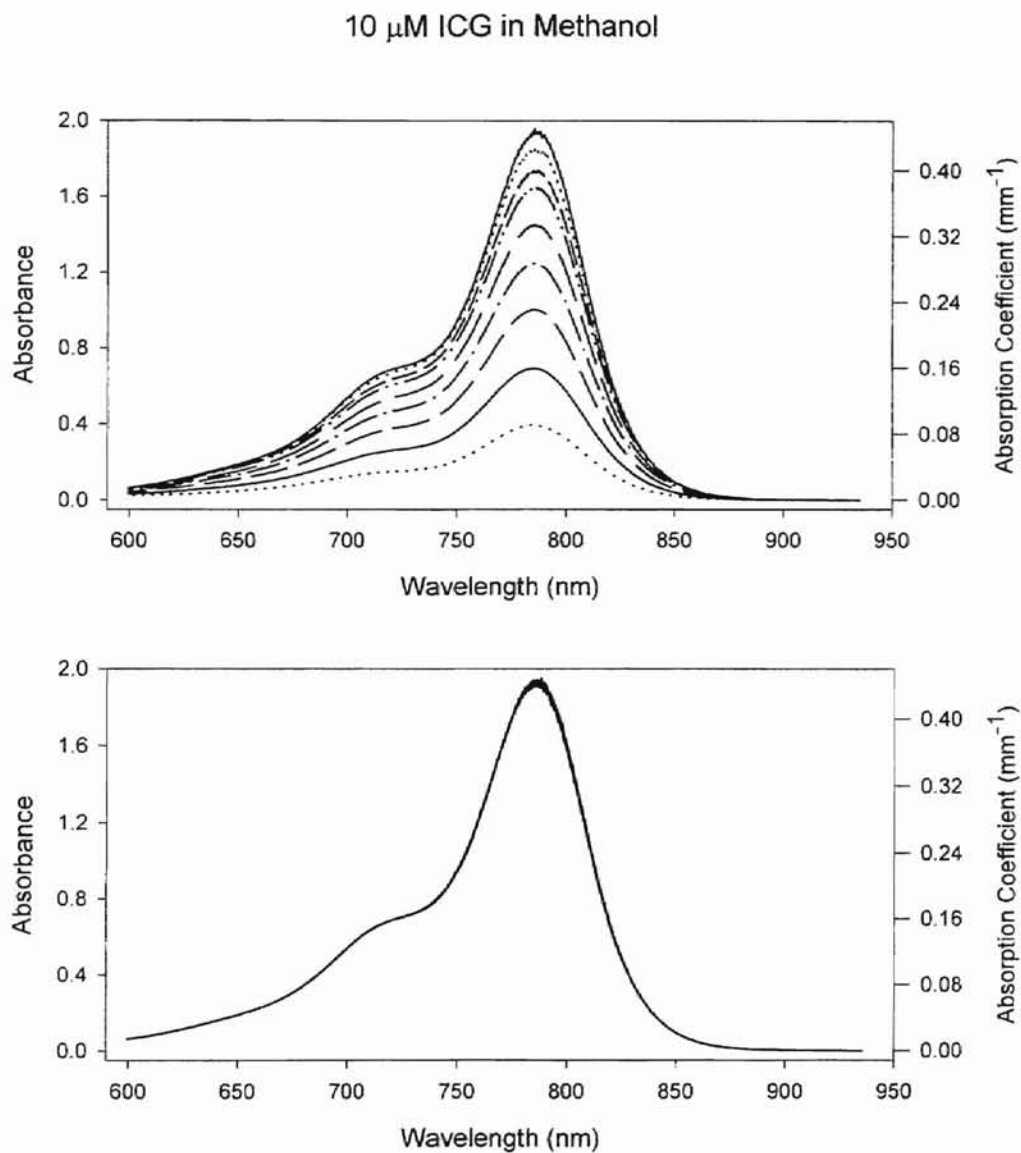


FIGURE 3.3 10 μM ICG in methanol. The ICG dye solution in the top graph was irradiated with 0, 18, 44, 86, 141, 231, 368, 561, 826 J mL^{-1} . Bottom graph shows absorbance on non-irradiated ICG for the duration of the experiment.

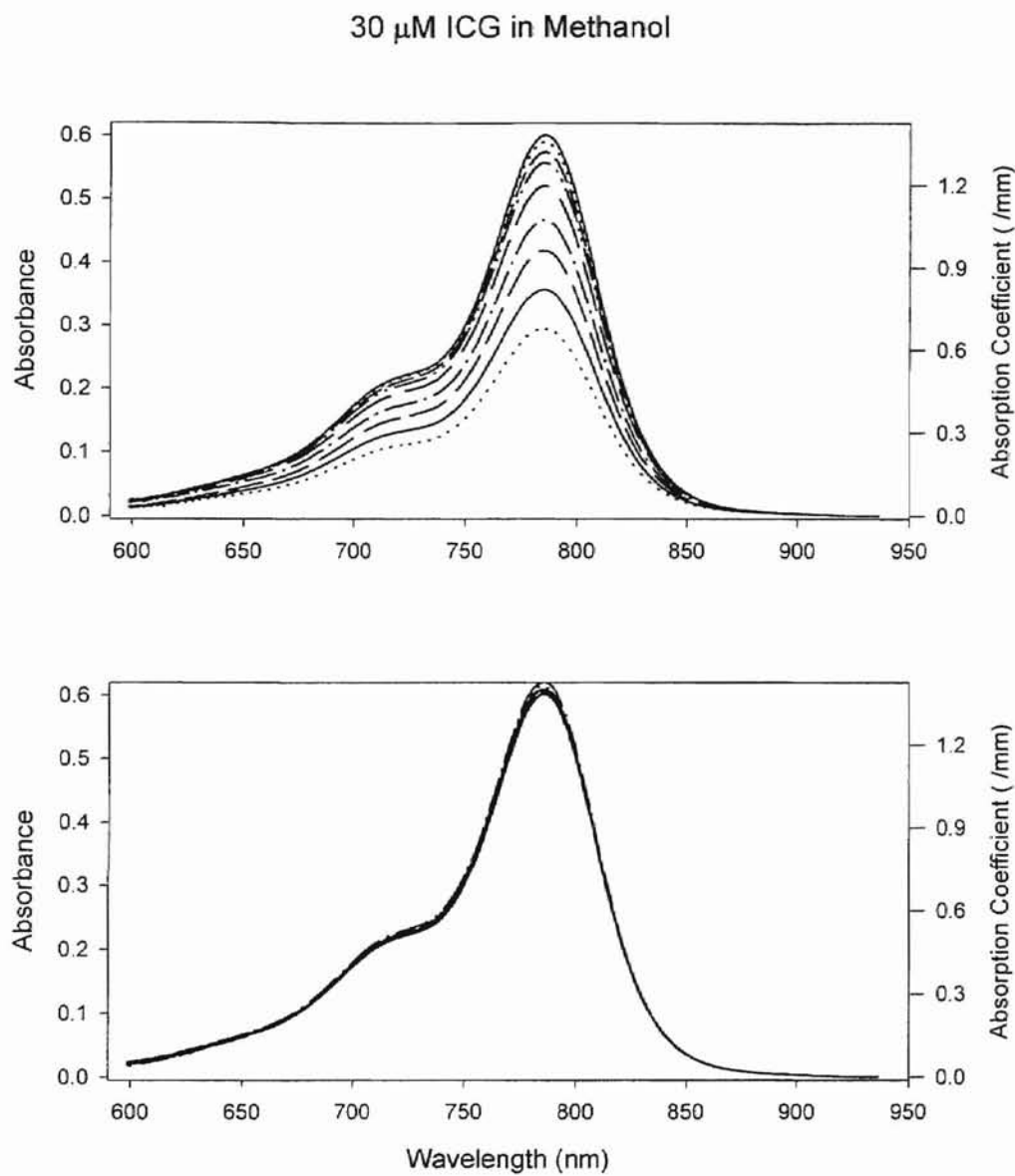


FIGURE 3.4 30 μM ICG in methanol. Top graph shows absorbance after irradiation with 0, 16, 40, 73, 127, 202, 319, 487, 744 J mL^{-1} . Bottom graph shows the absorbance of the non-irradiated ICG for the duration of the experiment.

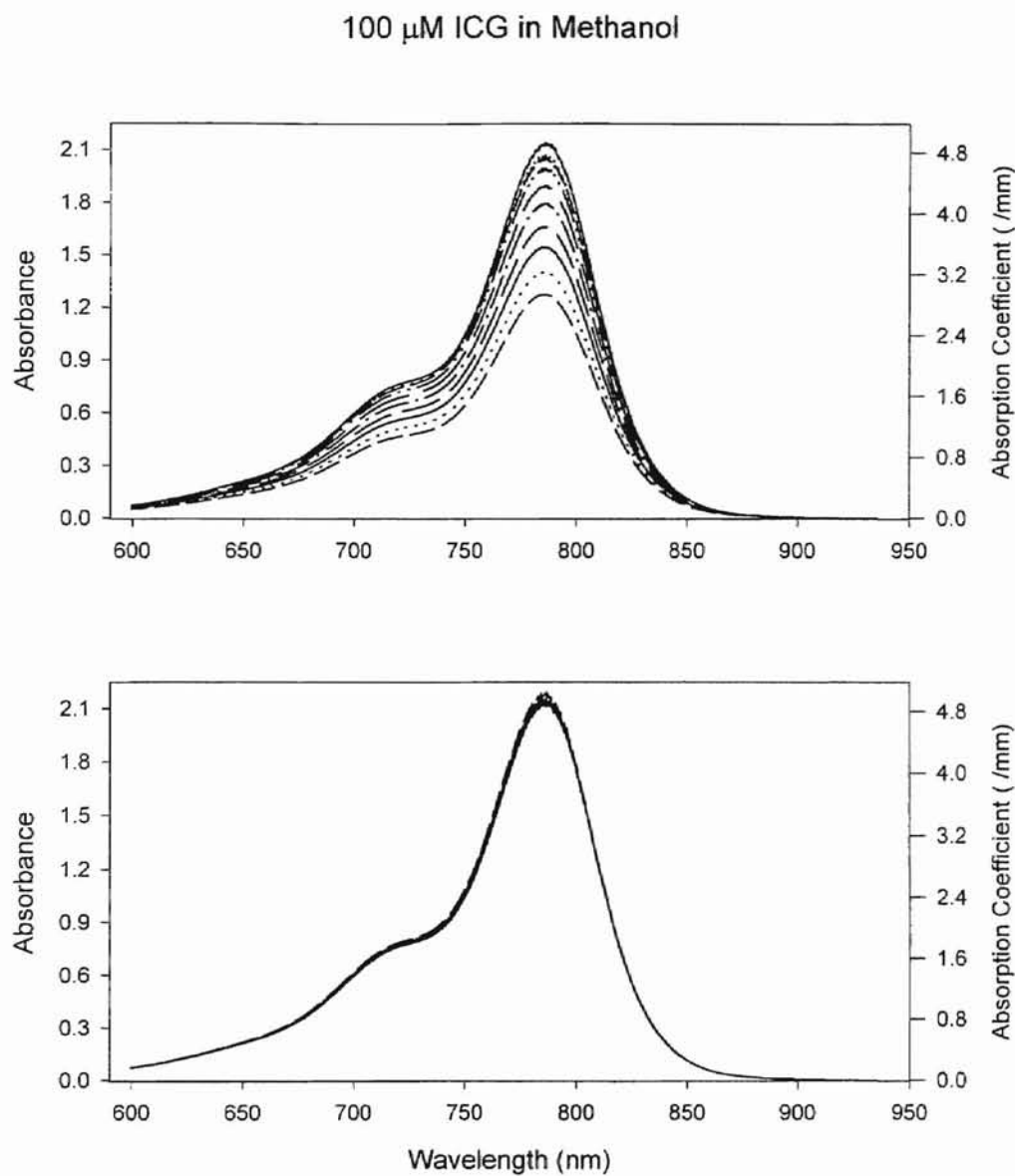


FIGURE 3.5 100 μM ICG in methanol. Top graph shows absorbance after irradiation of 0, 17, 79, 134, 216, 337, 513, 769, 1031 J mL^{-1} . Bottom graph shows absorbance of non-irradiated ICG for the duration of the experiment.

3.1.2 AQUEOUS ICG SOLUTIONS

A dramatic change of the absorbance spectrum is visible for 1 μM ICG in the water + 3% HSA solution when irradiated for less than 30 seconds for a total of 13 J mL^{-1} . After the ICG sample was irradiated for a total of 113 J mL^{-1} the peak absorbance dropped 89% from original, as seen in Figure 3.6. The non-irradiated sample shows only a 2.6% deviation from the original maximal absorbance value for the duration of the experiment.

The 3 μM ICG solution in Figure 3.7 shows a 91% decrease in peak absorbance due to 149 J mL^{-1} irradiation. The unexposed ICG shows no change of absorbance spectrum for the duration of the experiment.

Figure 3.8 shows a 93% reduction in peak absorbance of the 10 μM ICG solution after 171 J mL^{-1} irradiation. The absorbance spectrum of the unexposed ICG solution shows no change of the peak absorbance; however, the horizontal shift of the peak absorbance of one of the spectra is attributable to an error in reading the CCD array by the computer, as discussed in Section 3.1.2. The deviation of another of the spectra along the outer edges of the spectral peak can be attributed to a similar error in collecting the data from the CCD array.

The peak absorbance of the unexposed 30 μM ICG solution diminishes by 78% after being irradiated by 166 J mL^{-1} of laser energy. The unexposed 30 μM ICG solution in Figure 3.9 shows no degradation over the course of the experiment.

The 100 μM ICG solution has a 32% reduction of its peak absorbance after being irradiated by 198 J mL^{-1} of laser energy, with no change of the absorbance spectra for the duration of the experiment, as seen in Figure 3.10.

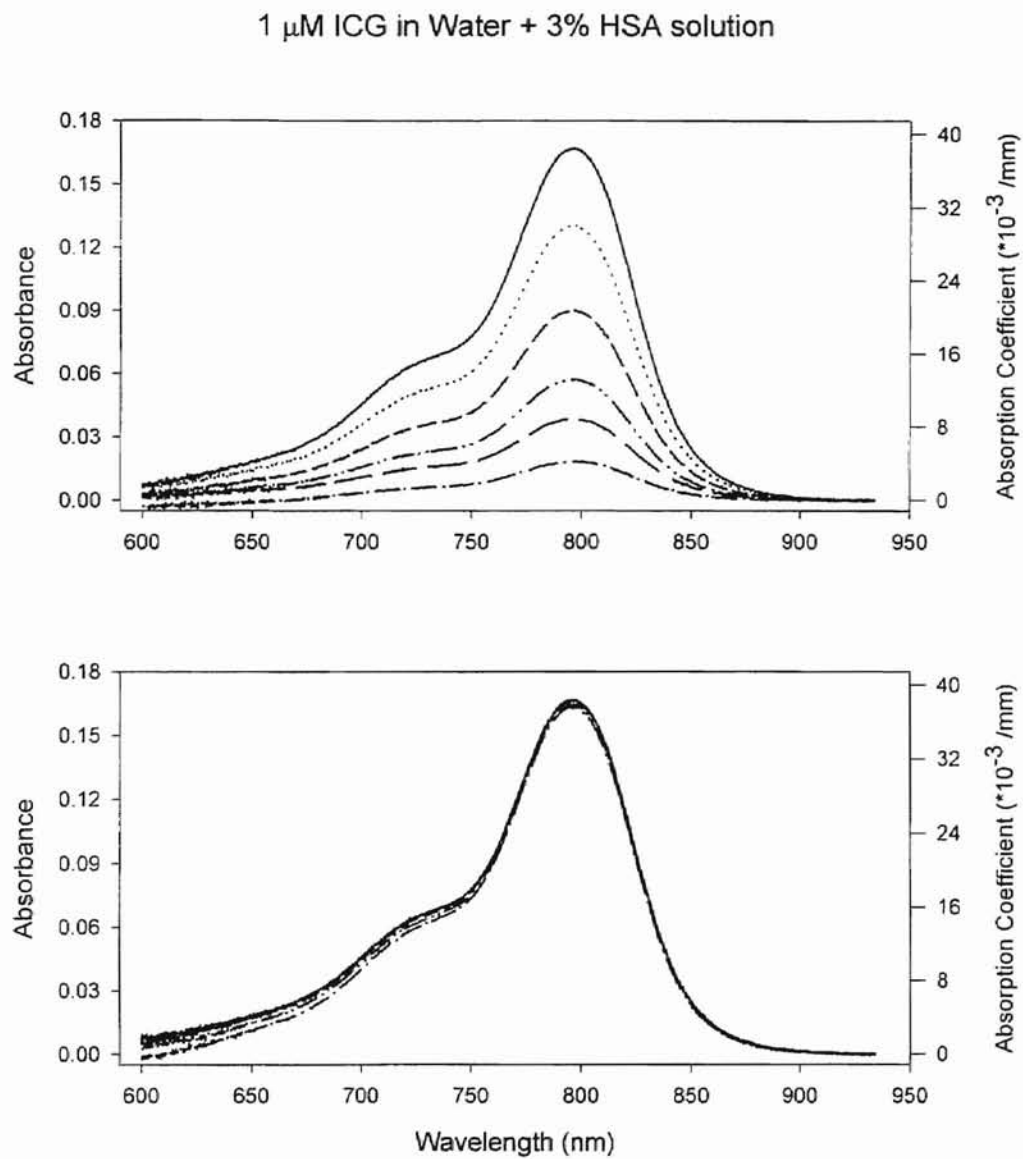


FIGURE 3.6. 1 μM ICG in water + 3% HSA. Upper graph shows change of absorbance spectra after energy dose of 0, 13, 32, 59, 82, 113 J mL^{-1} . Lower graph shows absorbance spectra of unexposed 1 μM ICG.

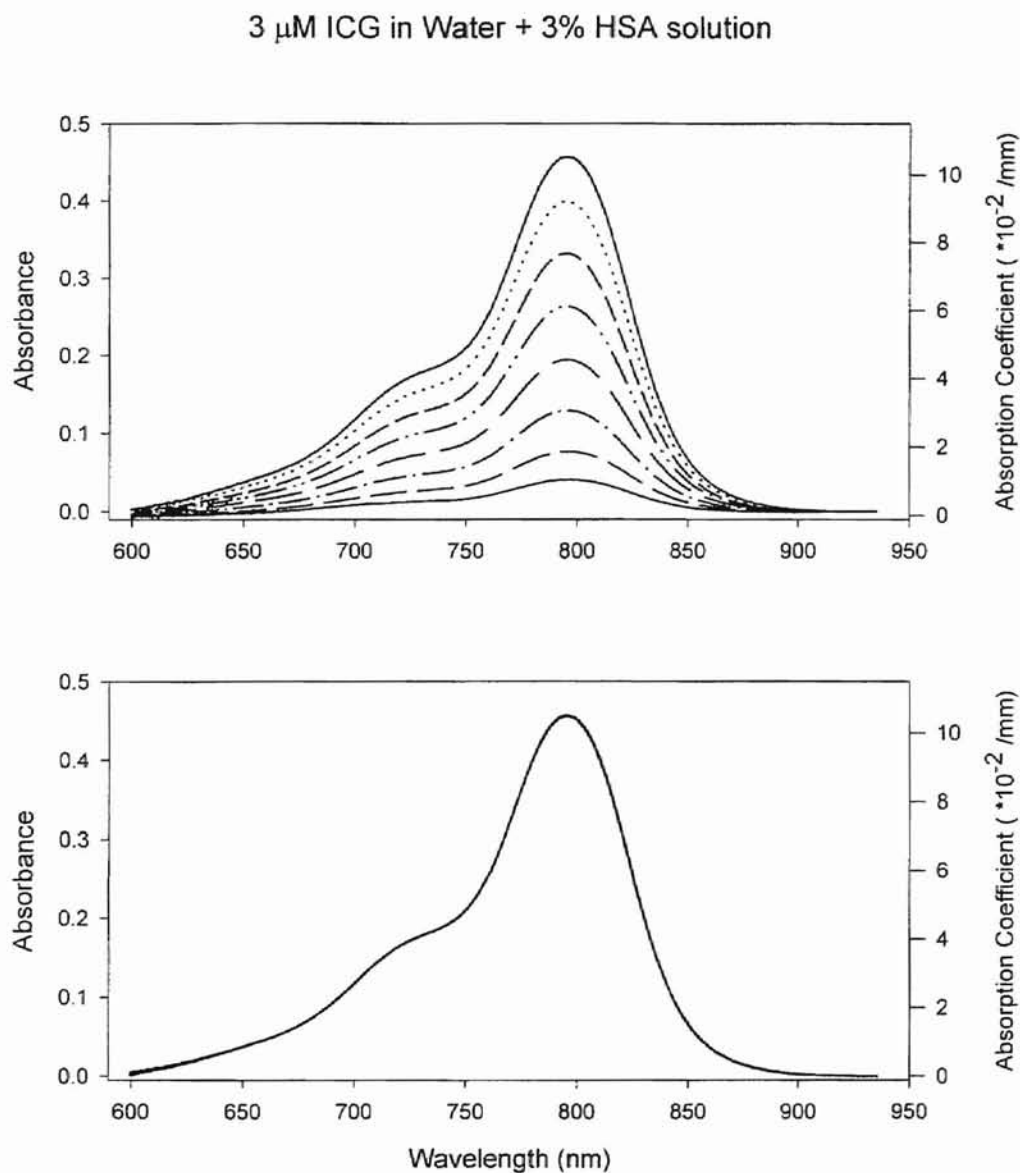


FIGURE 3.7. Top graph shows optical absorbance of photodegraded 3 μM ICG in water + 3% HSA. From highest to lowest absorbance, delivered energy dose is 0, 9, 21, 37, 57, 81, 111, 149 J mL^{-1} . Bottom graph shows optical absorbance of non-irradiated 3 μM ICG in water + 3% HSA.

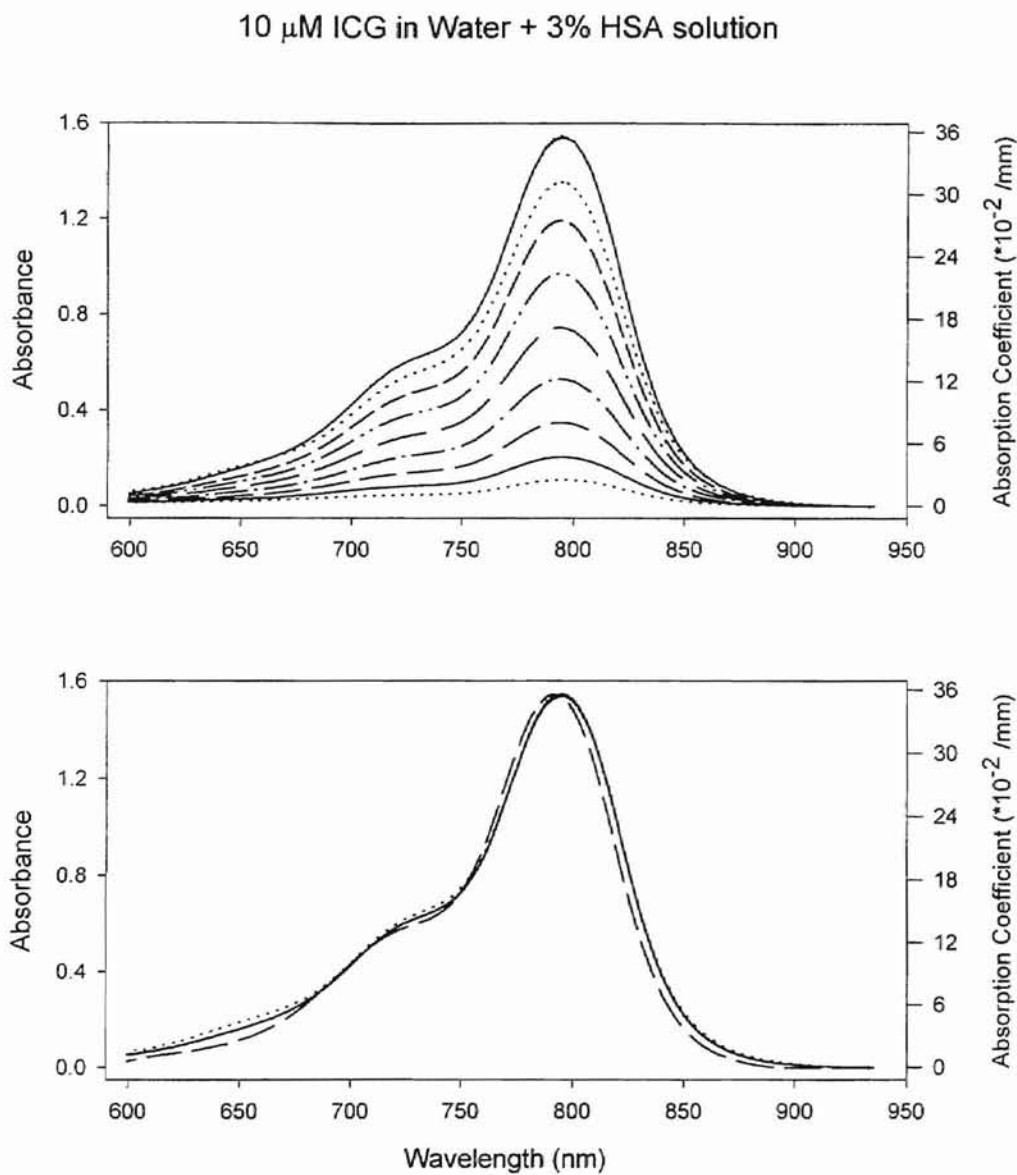


FIGURE 3.8. Top graph shows optical absorbance of photodegraded 10 μM ICG in water + 3% HSA. From highest to lowest absorbance, delivered energy dose is 0, 10, 22, 37, 55, 77, 103, 134, 171 J mL^{-1} . Bottom graph shows optical absorbance of unexposed 10 μM ICG in water + 3% HSA.

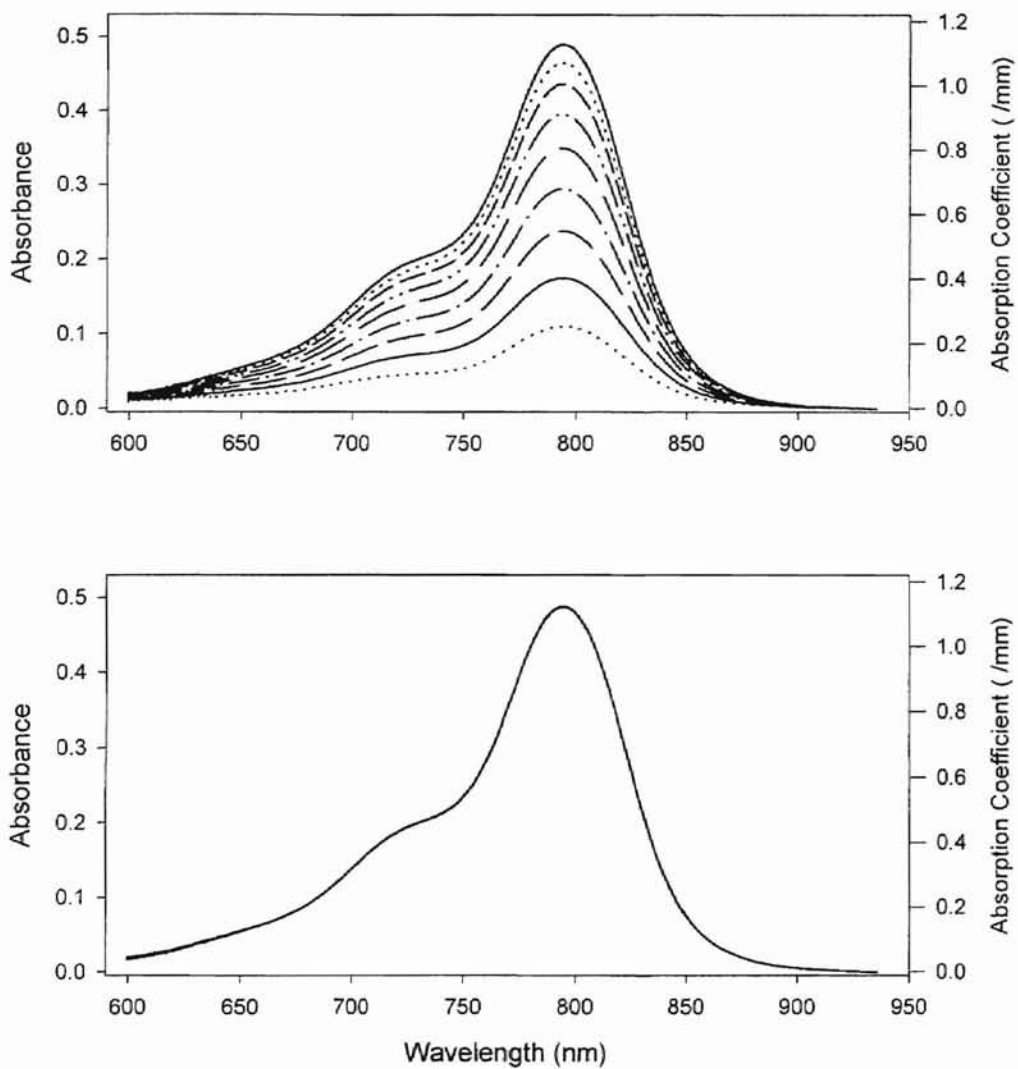
30 μM ICG in Water + 3% HSA solution

FIGURE 3.9. Top graph shows optical absorbance of photodegraded 30 μM ICG in water + 3% HSA. From highest to lowest absorbance, delivered energy dose is 0, 9, 21, 36, 54, 75, 100, 130, 166 J mL^{-1} . Bottom graph shows optical absorbance of unexposed 30 μM ICG in water + 3% HSA.

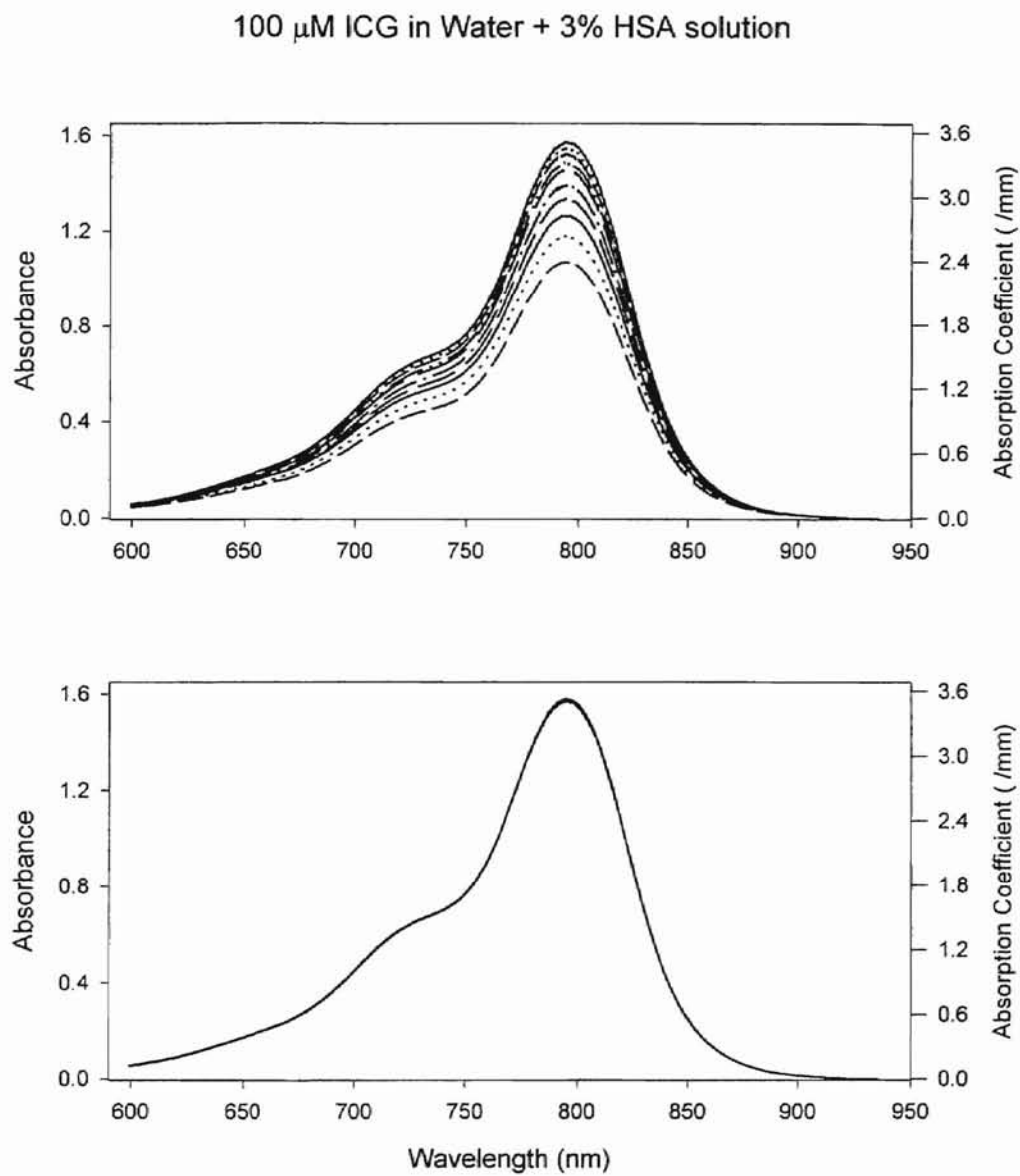


FIGURE 3.10. Top graph shows the optical absorbance of photodegraded 100 μ M ICG in water + 3% HSA. From highest to lowest absorbance, delivered energy dose is 0, 9, 21, 32, 49, 69, 94, 123, 158, 198 J mL⁻¹. Bottom graph shows the optical absorbance of unexposed 100 μ M ICG in water + 3% HSA.

3.2 DATA ANALYSIS

3.2.1 ANALYSIS PROCEDURES

The data presented in Sections 3.1.1 and 3.1.2 represent the change in absorbance (and absorption coefficient) as a function of delivered energy. To understand the mechanics behind the degradation process, the above data must be analyzed. The theoretical predictions in Section 1.4 describe how the change in absorption coefficient changes as a function of delivered energy, however, as can be seen in the data, the absorption coefficient is different for different wavelengths, which begs the question: at which wavelength is the absorption coefficient chosen?

Instead of choosing the absorption coefficient at the wavelength used for the irradiations, the absorption coefficient for the wavelength at which the initial non-irradiated (0 J mL^{-1} delivered energy dose) sample had the highest absorbance was chosen since the degradation behavior is more easily observed when the peak absorbance is used. The wavelength which produces the highest initial absorbance will be constant for any given sample regardless of the irradiation wavelength used, which was another factor in choosing which wavelength at which the absorption coefficient would be calculated. The absorbance at the irradiation wavelength could have been chosen for the analysis. However, since maximum absorbance is not at the irradiation wavelength, the proportional amount of decrease of the absorbance spectrum at the irradiation wavelength will be less than the proportional amount of decrease at the maximum absorbance.

The maximum absorbance for the initial non-irradiated solution can be found by inspection, but the statistics function in Jandel Sigma Plot was used instead. The wavelength that corresponded to this maximum absorbance was then considered to be the wavelength at which the maximum absorbance occurred for the further irradiated samples for that concentration and solvent. For example, the initial maximum absorbance of the 3 μM ICG in methanol sample is 0.556 (arbitrary units) at 786.9 nm; at 786.9 nm, the absorbance for the 16 J mL^{-1} exposure is 0.536, the absorbance for the 48 mL^{-1} exposure is 0.511 at 786.9 nm, and so on. The maximum absorbance for all further exposures for the 3 μM ICG in methanol sample was the absorbance at 786.9 nm.

Once the maximum absorbance values were found, the values were copied from the Sigma Plot file and pasted into a Microsoft Excel worksheet. Inside the Excel worksheet, the absorption coefficient was calculated from the absorbance data. The total energy delivered for each exposure was then copied from the appropriate data file (collected from the computer in Figure 2.1) to corresponding cells in the Excel worksheet. From this absorption coefficient data and the delivered energy data, the parameters κ and m from Equation (2.12) were then found by Excel's solver function. For a more detailed explanation of the above mentioned procedure, see Appendix A.

3.2.2 ANALYSIS RESULTS

The calculated values for κ and m that best fit the data are presented in Tables 3.1 and 3.2 for solutions of ICG in methanol and water + 3% HSA, respectively. It can be noted that the values for m increase with concentration, with the only exception occurring at a jump between the 10 μM and 30 μM ICG concentrations in the water + 3% HSA

solution. After this jump the trend for m to increase as concentration increases is still evident, for the 100 μM concentration has a larger m value than the 30 μM . One possible explanation for this anomaly may be due to the absorbance data being collected with the samples in a smaller path length cuvette made from a different material or from aggregate formation at these higher concentrations. The change of cuvette from the 10 mm plastic cuvettes to the 1 mm quartz glass cuvette may cause some ICG adsorption to the surface of the quartz glass cuvette which would change the absorbance of that sample, thus causing a jump in the values for m .

Another trend which is evident after inspection of the data is that slower degradation rates lead to a higher m values; again, the only exception occurs at a jump between the 10 μM and 30 μM ICG concentrations in water + 3% HSA. Even with this one exception, the slower degradation of the 100 μM versus the 30 μM concentration (the 100 μM has a higher m value than the 30 μM) indicates that a higher m value causes less degradation for a given amount of delivered energy (slower degradation).

Figures 3.11 through 3.20 show graphs of Equation 2.12 fitted to the maximum absorption coefficient data. The hypothesis on the significance of m is as follows: m is the mean number of ICG molecules involved in the degradation. For example, if $m = 2$, then there would be an average of two molecules involved in the degradation process. Therefore, for a value of $m = 1.35$, the degradation process involves many different numbers of molecules, say mainly monomers and dimers, with contributions from higher oligomers.

Another hypothesis is that m indicates the mean number of photons that interacts with each indocyanine green molecule. For example, with $m = 1$, one photon interacts

with one molecule. With $m = 3$, then the energy from three photons are absorbed by each ICG molecule. A solution with a higher m value will require a greater number of photons to be absorbed for the degradation process, leaving fewer photons available for other ICG molecules; therefore, a solution with a higher value of m will degrade slower than a solution with a lower value of m . Figure 3.21 shows a plot of the calculated m values as a function of concentration for both the methanol solutions and the water + 3% HSA solutions.

The values for κ are not directly comparable since the units for κ depend on the value of m . If two concentrations of ICG were to have equal values of m , or approximately equal values of m , then a different value of κ represents a different decay constant: the higher the value of κ the faster the degradation, and the lower the value of κ the lower the degradation, for a given m .

As mentioned in Section 3.2.1, the proportional amount of decrease of the absorption coefficient at a wavelength other than the wavelength which produces the highest absorbance. Therefore, the value of m at a different wavelength will be slightly lower than those calculated above.

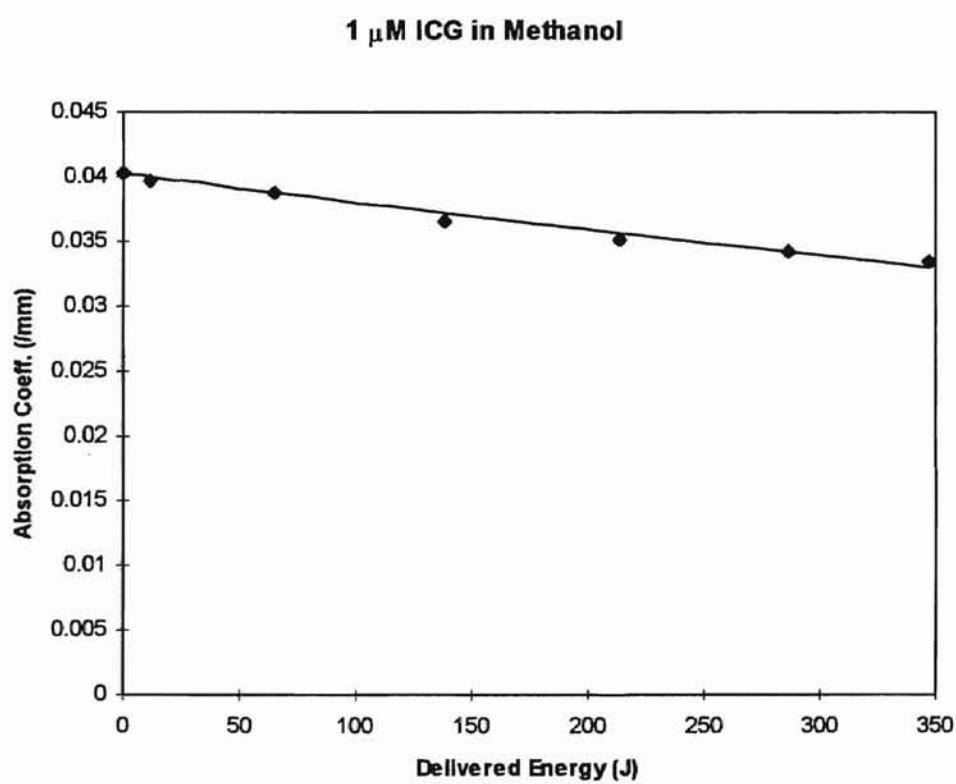


FIGURE 3.11 Photodegradation of 1 μ M ICG in methanol. Best-fit parameters are $\alpha_0 = 0.0403$, $m = 1.46$, $\kappa = 3.10 \times 10^{-4}$.

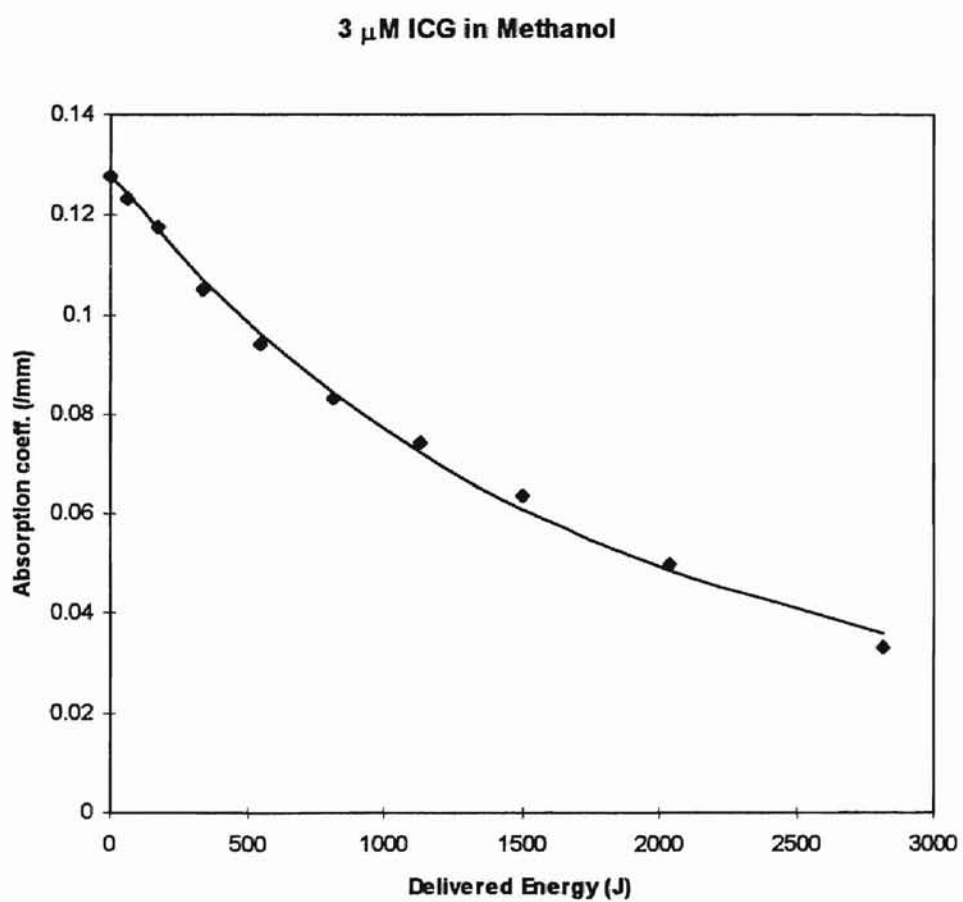


FIGURE 3.12 Photodegradation of 3 μ M ICG in methanol. Best-fit parameters are $\alpha_0 = 0.128$, $m = 1.63$, $\kappa = 3.49 \times 10^{-4}$.

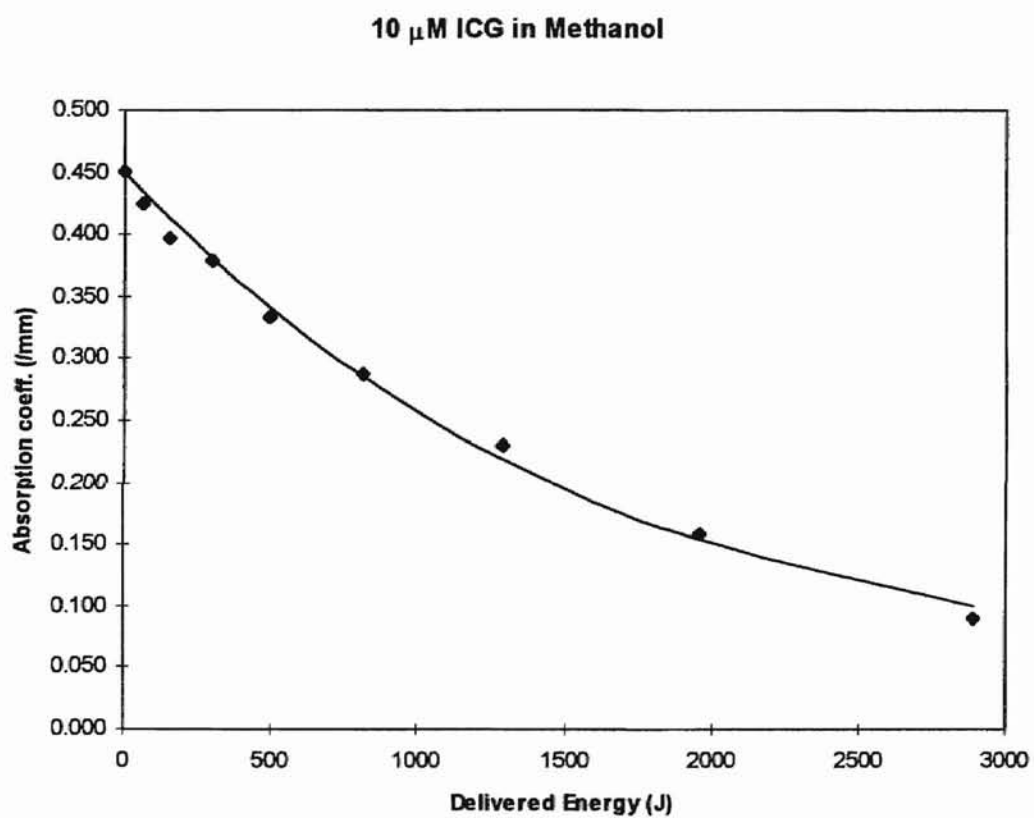


FIGURE 3.13 Photodegradation of 10 μ M ICG in methanol. Best-fit parameters are $\alpha_0 = 0.450$, $m = 1.89$, $\kappa = 5.18 \times 10^{-4}$.

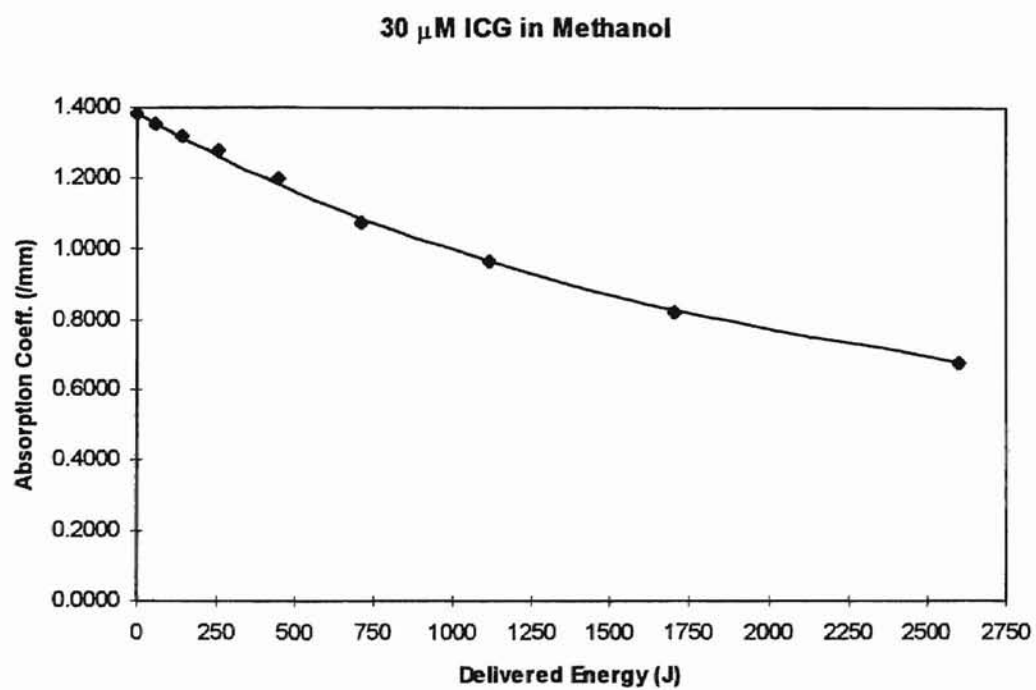


FIGURE 3.14 Photodegradation of 30 μ M ICG in methanol. Best-fit parameters are $\alpha_0 = 1.38$, $m = 2.31$, $\kappa = 4.59 \times 10^{-4}$.

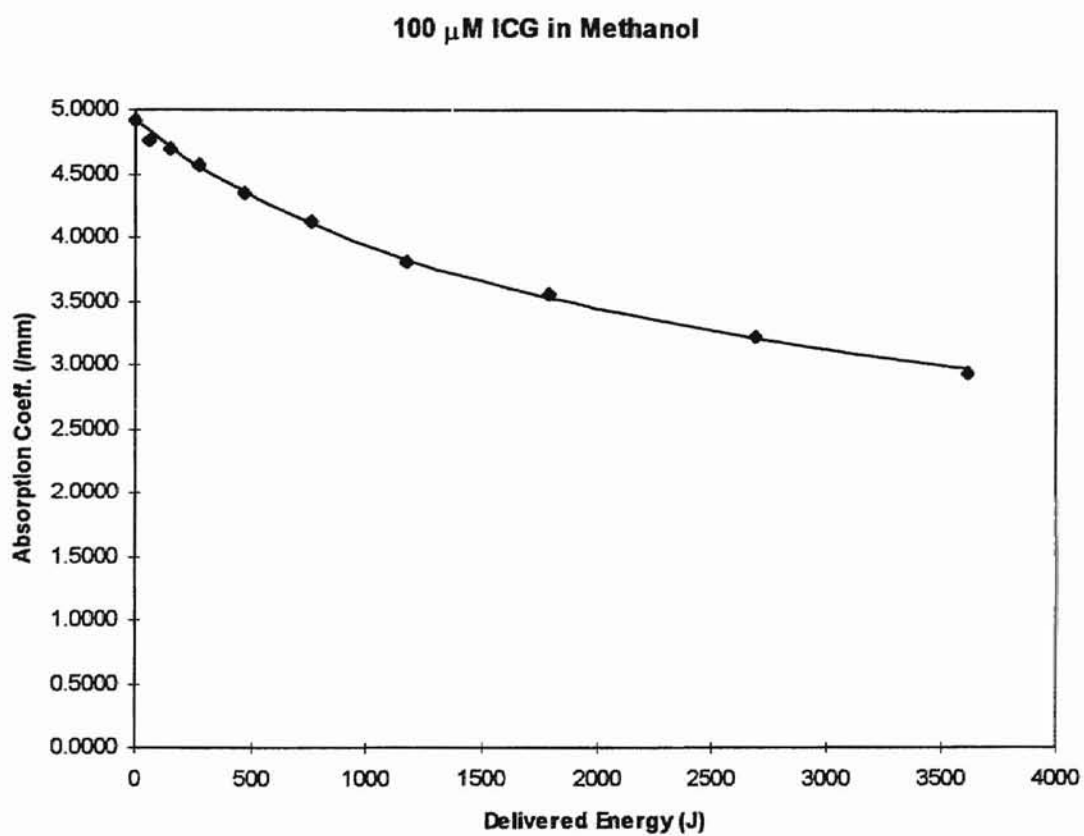


FIGURE 3.15 Photodegradation of 100 μ M ICG in methanol. Best-fit parameters are $\alpha_0 = 4.93$, $m = 4.75$, $\kappa = 3.93 \times 10^{-6}$.

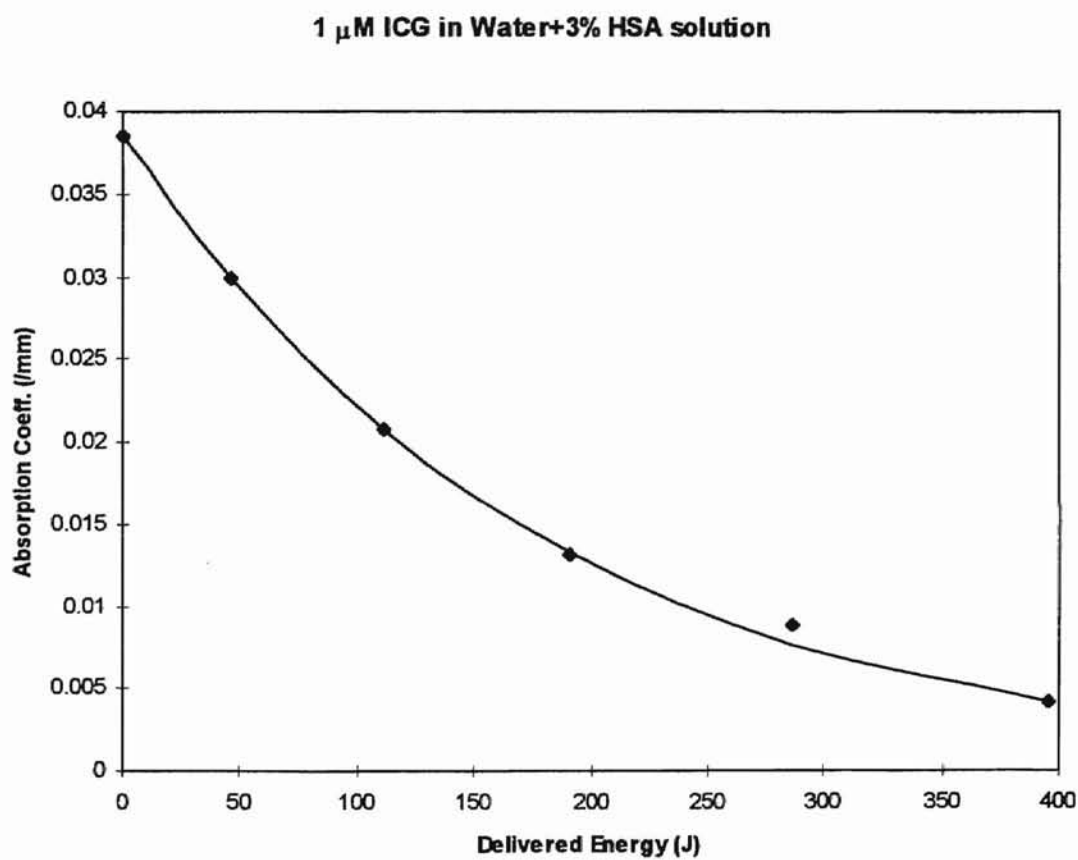


FIGURE 3.16 Photodegradation of 1 μ M ICG in Water + 3% HSA solution. Best fit parameters are $\alpha_0 = 0.0385$, $m = 1.07$, $\kappa = 8.20 \cdot 10^{-4}$.

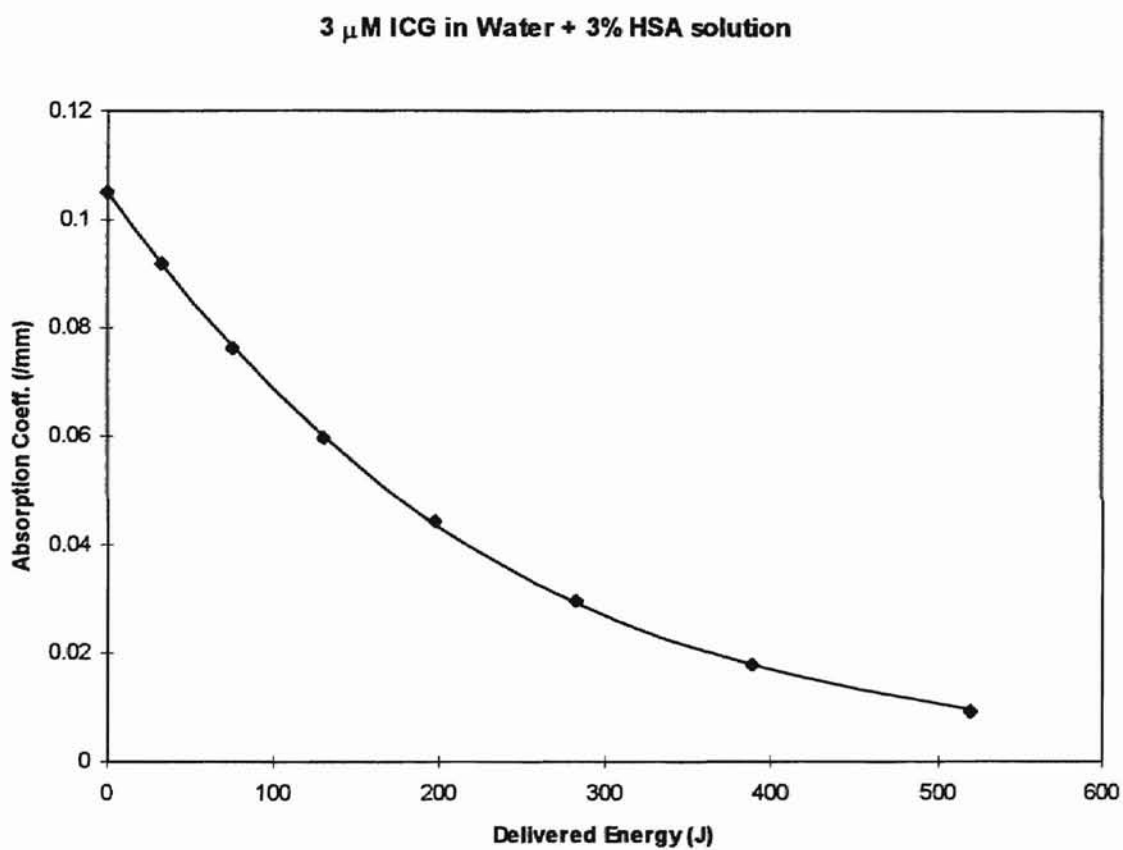


FIGURE 3.17 Photodegradation of 3 μM ICG in Water + 3% HSA solution. Best fit parameters are $\alpha_0 = 0.105$, $m = 1.14$, $\kappa = 8.98 \times 10^{-4}$.

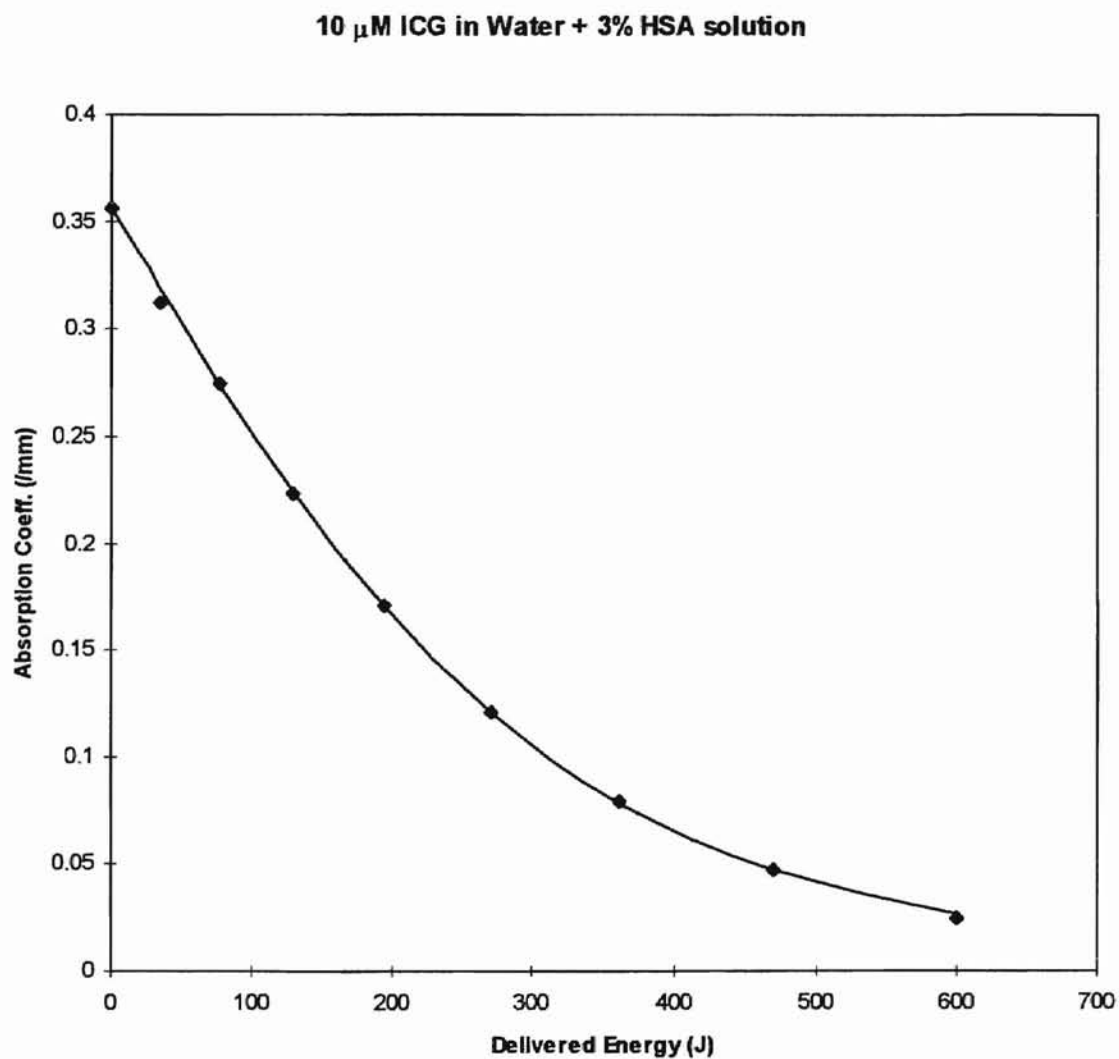


FIGURE 3.18 Photodegradation of 10 μ M ICG in Water + 3% HSA solution. Best fit parameters are $\alpha_0 = 0.356$, $m = 1.35$, $\kappa = 1.69 \times 10^{-3}$.

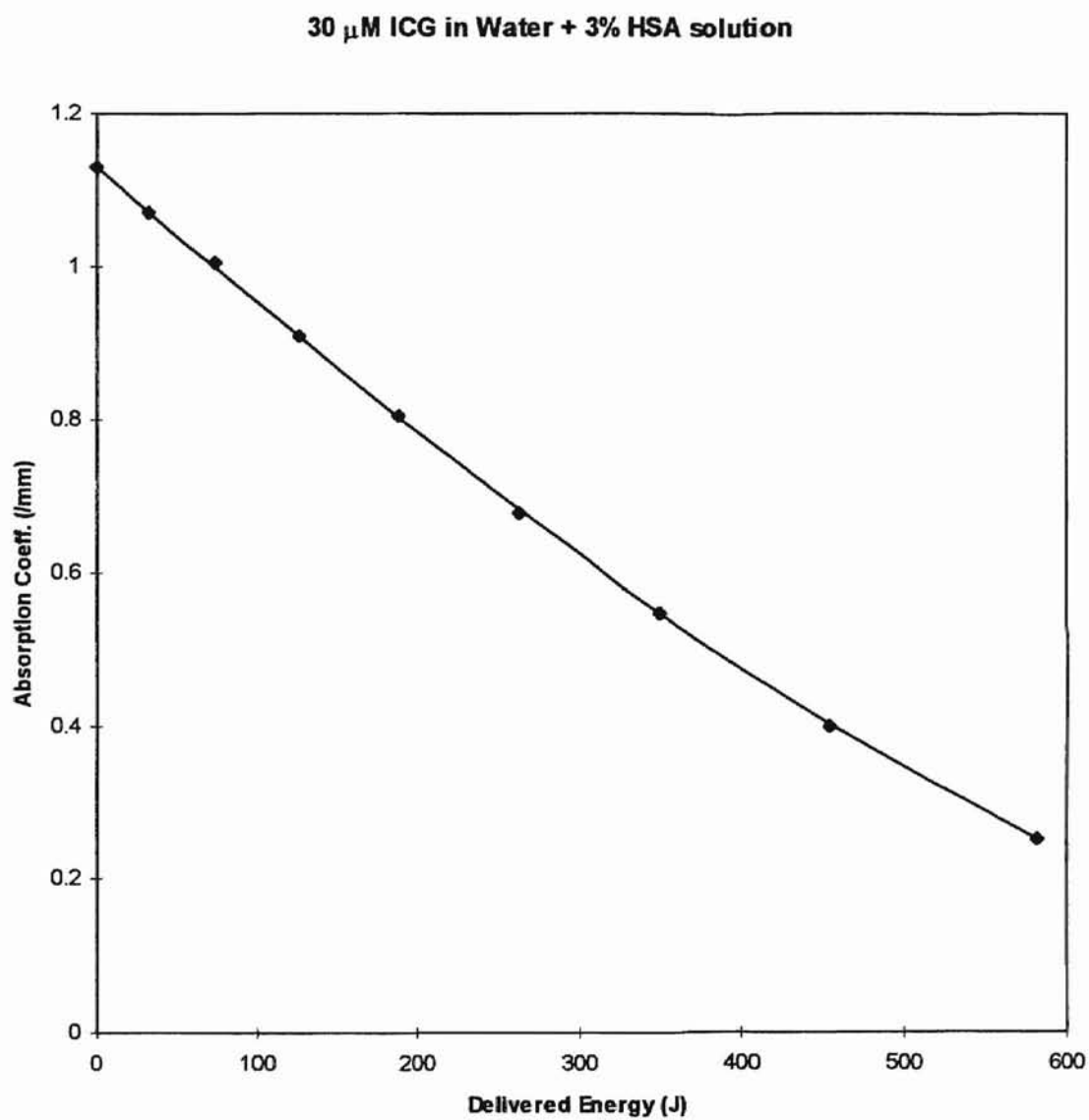


FIGURE 3.19 Photodegradation of 30 μ M ICG in Water + 3% HSA solution. Best fit parameters are $\alpha_0 = 1.13$, $m = 0.597$, $\kappa = 2.75 * 10^{-3}$.

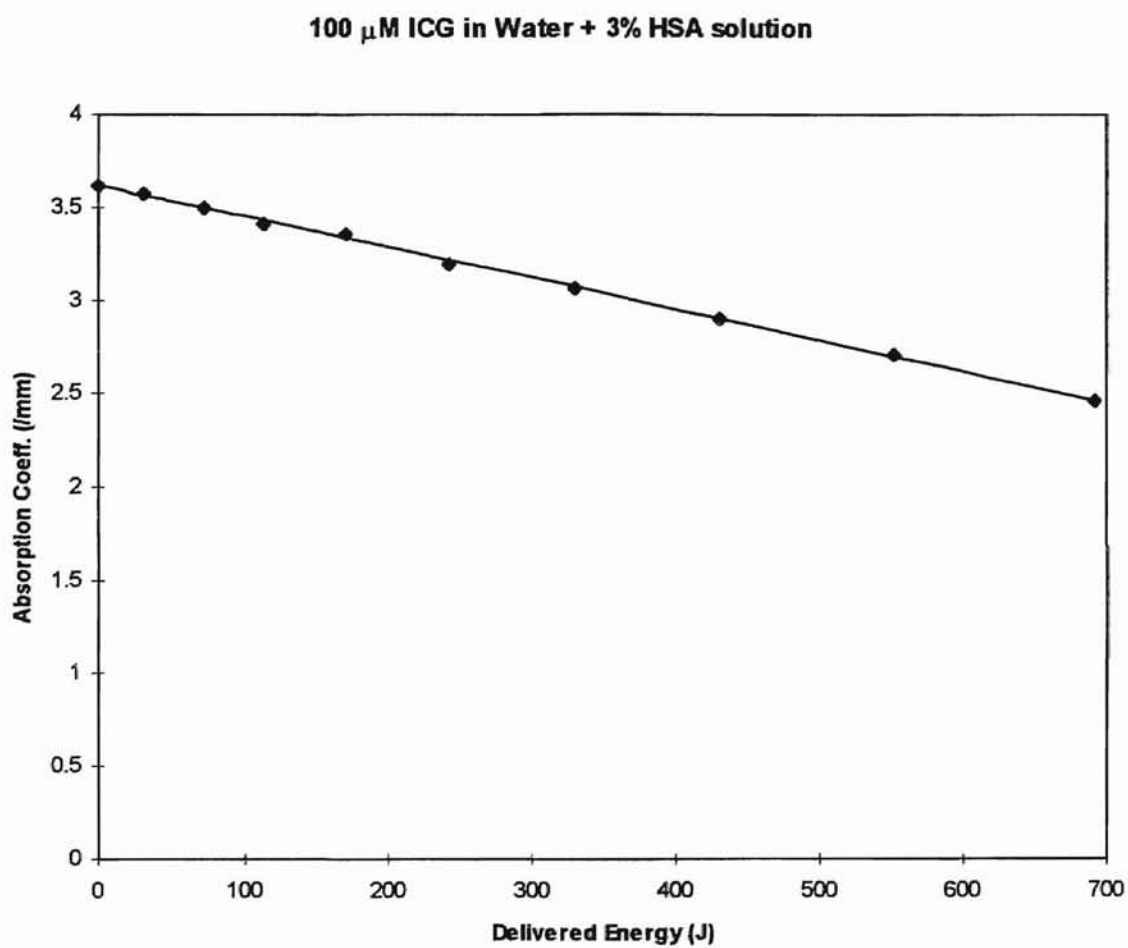


FIGURE 3.20 Photodegradation of 100 μ M ICG in Water + 3% HSA solution. Best fit parameters are $\alpha_0 = 3.62$, $m = 0.782$, $\kappa = 2.24 \cdot 10^{-3}$.

Concentration (μM)	α_0 (mm^{-1})	m	κ ($\cdot 10^{-4} \text{ J}^{-1} \cdot \text{mm}^{\text{m}-2}$)
1	0.0403	1.46	3.10
3	0.128	1.63	3.49
10	0.450	1.89	5.18
30	1.38	2.31	4.59
100	4.93	4.75	0.0393

TABLE 3.1 ICG in methanol values calculated for m and κ for the given α_0 (initial absorption coefficient). Units for m are dimensionless and the units for κ are $\text{J}^{-1} \cdot \text{mm}^{\text{m}-2}$.

Concentration (μM)	α_0 (mm^{-1})	m	κ ($\cdot 10^{-4} \text{ J}^{-1} \cdot \text{mm}^{\text{m}-2}$)
1	0.0385	1.07	8.20
3	0.105	1.14	8.98
10	0.356	1.35	16.9
30	1.13	0.597	27.5
100	3.62	0.782	22.4

TABLE 3.2 ICG in water + 3% HSA values calculated for m and κ for the given α_0 (initial absorption coefficient). Units for m are dimensionless and the units for κ are $\text{J}^{-1} \cdot \text{mm}^{\text{m}-2}$.

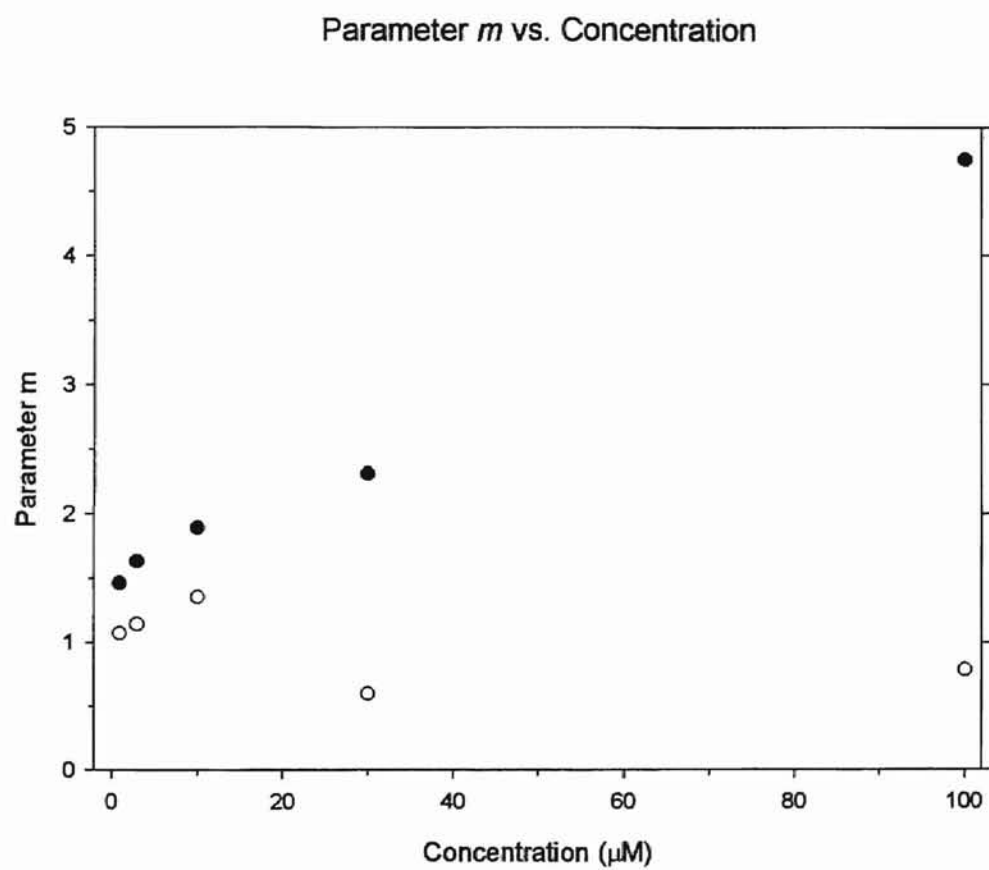


FIGURE 3.21 Plot of parameter m as a function of ICG concentration. Solid circles indicate ICG solutions in methanol, hollow circles represent ICG in water/HSA solution.

CHAPTER 4

SUMMARY AND CONCLUSIONS

In Chapter 1 a brief history of the dye indocyanine green (ICG) was given, along with some examples of its many uses in the medical field. ICG is well suited for its use in medical applications due to its low toxicity and high absorbance in a range where biological tissues have low absorbance. The only disadvantage of ICG is that when it does degrade (degrading into at least a dozen different products), the toxicity of the degradation products is not known [26].

Using the irradiation and data collection techniques described in Chapter 2, the absorption spectra of indocyanine green was obtained for the amount of laser light energy delivered to the sample. From the data presented in Chapter 3, it is clearly seen that ICG exposed to high intensity laser irradiation degrades more rapidly than samples left in a dark container (which show no signs of degradation during the course of the experiment). Higher concentrations of ICG degrade more slowly than lower concentrations of ICG. Also, ICG dissolved in methanol degrades much more slowly than ICG dissolved in a solution of deionized water and human serum albumin (HSA).

When the data collected in Chapter 3 was fitted to the theoretical model developed in Chapter 2, a correlation between the rate of degradation and the parameter m given in Equation (2.12) is observed: higher concentrations of ICG, which degrade more slowly,

have higher m values, which indicate that at higher concentrations there are more and more molecules involved in the degradation process. The proportionality constant, κ , also given in Equation (2.12), is a decay constant whose units are dependent on m . The values for κ from one concentration to the next are not directly comparable, since different concentrations have different m values.

In a previously published article by the author, which was a preliminary study of the material presented in this thesis (see Appendix B), a few other interesting properties of ICG were also discovered [29]. The first was that ICG exhibits saturable absorption properties when exposed to Q-switched laser pulses (described in Chapter 2). In this preliminary study, the pulse width (FWHM) of the direct laser was 94 ns; when a 10 μM solution of ICG in methanol was placed in the beam path, the pulse width of the beam that was transmitted through the ICG sample decreased to 77 ns.

During the course of the saturable absorption study, the ICG sample was observed to fluoresce with the laser in Q-switched mode, but ceased to fluoresce when the laser operated in the long pulse mode, indicating fluorescence due to multiphoton absorption. Due to the saturable absorption of ICG as described above, the decay rate of the ICG sample irradiated with Q-switched pulses is lower than samples irradiated with the long pulses. The value of m for the Q-switched irradiated samples were approximately three times larger than the value of m for a sample of equal concentration (10 μM ICG in methanol) that was irradiated with the long pulses; this lower degradation rate for the Q-switched irradiated samples giving a larger value of m is consistent with the observations in this thesis.

Studies involving irradiation of ICG samples at different wavelengths for both long pulses and Q-switched pulses have yet to be done on both methanol solutions and water/HSA solutions. Studies that have yet to be done include the determination of the degradation products of ICG, the toxicity of these degradation products, and the degradation of ICG irradiated with high intensity laser energy while in human tissue, blood, or blood plasma.

BIBLIOGRAPHY

1. I.J. Fox and E.H. Wood, "Indocyanine green: physical and physiologic properties," *Proceedings of the Staff Meetings of the Mayo Clinic* **35**, No. 2, pp. 732-745, Dec 7, 1960.
2. I.J. Fox, L.G.S. Brooker, D.W. Heseltine, H.E. Essex, E.H. Wood, "A tricarbo-cyanine dye for continuous recording of dilution curves in whole blood independent of variations in blood oxygen saturation," *Proceedings of the Staff Meetings of the Mayo Clinic* **32**, No. 18, pp. 478-484, Sept. 4, 1957.
3. I.J. Fox and E.H. Wood, "Applications of dilution curves recorded from the right side of the heart or venous circulation with the aid of a new indicator dye," *Proceedings of the Staff Meetings of the Mayo Clinic* **32**, No. 9, pp. 541-550, Sept. 18, 1957.
4. D.W. Heseltine and L.G.S. Brooker, "Tricarbo-cyanine infrared absorbing dyes," U.S. Patent 2,895,955; 1959.
5. R. Philip, A. Penzkofer, W. Baumler, R.M. Szeimies and C. Abels, "Absorption and fluorescence spectroscopic investigation of indocyanine green," *Journal of Photochemistry and Photobiology A: Chemistry* **96**, pp. 137-148, 1996.
6. N. Moazami, M.C. Oz, L.S. Bass and M.R. Treat, "Reinforcement of colonic anastomoses with a laser and dye-enhanced fibrinogen," *Arch. Surg.* **125**, pp. 1452-1454, 1990.
7. M.C. Oz, J.P. Johnson, S. Parangi, R.S. Chuck, C.C. Marboe, L.S. Bass, R. Nowygrod and M.R. Treat, "Tissue soldering by use of indocyanine green dye-enhanced fibrinogen with the near infrared diode laser," *J. Vasc. Surg.* **11**, pp. 718-725, 1990.
8. T.M. Wider, S.K. Libutti, D.P. Greenwald, M.C. Oz, J.S. Yager, M.R. Treat and N.E. Hugo, "Skin closure with dye-enhanced laser welding and fibrinogen," *Plastic Reconst. Surg.* **88**, pp. 1018-1025, 1991.
9. J.S. Auteri, M.C. Oz, V. Jeevanandam, J.A. Sanchez, M.R. Treat and C.R. Smith, "Laser activation of tissue sealant in hand-sewn canine esophageal closure," *J. Thorac. Cardiovasc. Surg.* **103**, pp. 781-783, 1992.

10. L.S. Bass, N. Maozami, J. Pocsidio, M.C. Oz, P. LoGerfo and M.R. Treat, "Changes in type I collagen following laser welding," *Lasers Surg. Med.* **12**, pp. 500-505, 1992.
11. S.D. Decoste, W. Farinelli, T. Flotte and R.R. Anderdon, "Dye-enhanced laser welding for skin closure," *Lasers Surg. Med.* **12**, pp. 25-32, 1992.
12. D.P. Poppas, T.J. Choma, C.T. Rooke, S.D. Klioze and S.M. Schlossberg, "Preparation of human albumin solder for laser tissue welding," *Lasers Surg. Med.* **13**, pp. 557-580, 1993.
13. L.S. Bass, N. Moazami, A. Avellino, W. Trosaborg and M.R. Treat, "Feasibility studies for laser solder neuroorrhaphy," *SPIE Proc.* **2128**, pp. 472-475, 1994.
14. U.M. Reali, R. Gelli, V. Fiannotti, F. Gori, R. Pini, F. Toncelli and U. Vanni, "Diode laser-assisted microvascular anastomosis: clinical and histological analysis on long period follow up," *SPIE Proc.* **2128**, pp. 476-483, 1994.
15. J.R. Mourant, G.D. Anderson, I.J. Bigio and T.M. Johnson, "Laser welding of bone: successful *in vitro* experiments," *SPIE Proc.* **2128**, pp. 484-488, 1994.
16. M.L. Kayton, S.K. Libutti, M. Bessler, L.D.F. Allendorf, S.D. Eiref, G. Marx, X. Mou, A. Morales, M.R. Treat and R. Nowygrod, "A comparison of laser-activated tissue solders and thrombin-activated cryoprecipitate for wound closure," *SPIE Proc.* **2128**, pp. 527-531, 1994.
17. S. Thomsen, E. Chan, I. Stubig, T. Menovsky and A.J. Welch, "Importance of wound stabilization in early wound healing of laser skin welds," *SPIE Proc.* **2395**, pp. 490-496, 1995.
18. R. Trickett, A. Lauto, J. Dawes and E. Owen, "Laser activated protein solder for peripheral nerve repair," *SPIE Proc.* **2395**, pp. 542-546, 1995.
19. K.E. Bartels, R.J. Morton, D.T. Dickey, E.L. Stair, M.E. Payne, S.A. Schafer and R.E. Nordquist, "Use of diode laser energy (808 nm) for selective photothermolysis of contaminated wounds," *SPIE Proc.* **2395**, pp. 602-606, 1995.
20. E.N. LaJoie, A.D. Barofsky, K.W. Gregory and S.A. Prahl, "Welding artificial biomaterial with a pulsed diode laser and indocyanine green dye," *SPIE Proc.* **2395**, pp. 508-516, 1995.
21. K.J. Baker, "Binding of sulfobromophthalein (BSP) sodium and indocyanine green (ICG) by plasma α_1 lipoproteins," *Proc. Soc. Exp Biol. Med.* **122**, pp. 957-963, 1966.

22. K.B. Saunders, J.I.E. Hoffman, M.I.M. Noble and R.J. Domenech, "A source of error in measuring flow with indocyanine green," *J. Appl. Physiol.* **28**, No. 2, pp. 190-198, Feb. 1970.
23. J. Gathje, R.R. Steuer, and K.R.K. Nicholes, "Stability studies on indocyanine green dye," *J. Appl. Physiol.* **29**, No. 2, pp. 181-185, Aug. 1970.
24. M.R. Tripp, G.M. Cohen, D.A. Gerasch and I.J. Fox, "Effect of protein and electrolyte on the spectral stabilization of concentrated solutions of indocyanine green," *Proc. Soc. Exp. Biol. Med.* **143**, pp. 879-883, 1973.
25. M.L.J. Landsman, G. Kwant, G.A. Mook and W.G. Zijlstra, "Light-absorbing properties, stability, and spectral stabilization of indocyanine green," *J. Appl. Physiol.* **40**, No. 4, pp. 575-583, Apr. 1976.
26. J.F. Zhou, M.P. Chin and S.A. Schafer, "Aggregation and degradation of indocyanine green," *SPIE Proc.* **2128**, pp. 495-505, 1994.
27. D. Dimitrov, L.S. Bass, M.R. Treat, "Thermal breakdown of indocyanine green," *SPIE Proc.* **2395**, pp. 486-489, 1995.
28. R. Simmons and R.J. Shephard, "Does indocyanine green obey Beer's law?" *J. Appl. Physiol.* **30**, No. 4, pp. 502-507, Apr. 1971.
29. J. Crull and S.A. Schafer, "Indocyanine green degradation during high-intensity laser irradiation," *SPIE Proc.* **2671**, pp. 243-250, 1996.
30. F. Barbier and G.A. De Weerd, "Chromatography and I.R. spectrography of indocyanine green," *Clinica Chimica Acta*, **10**, pp. 549-554, 1964.
31. L.G.S. Brooker, "Spectra of dye molecules," *Reviews of Modern Physics*, **14**, pp. 275-293, 1942.
32. T. Desmettre, S. Mordon, J.M. Devoisselle, "Indocyanine green dye (ICG) fluorescence and absorption properties as a function of time," *Vision Research*, **35**, p. 3325, Oct. 1995.
33. S. Yoneya, T. Saito, Y. Komatsu, J. Duvall-Young, "The binding properties of indocyanine green (ICG) significance in ICG imaging," *Vision Research*, **36**, p. 2421, Oct. 1996.
34. A. Espallat, D. Vilaplana, M. Jornet, A. Dukes, "Indocyanine-green angiography and occult choroidal neovascularization in age-related macular degeneration," *Vision Research*, **36**, p. 2422, Oct. 1996.

35. M. Vadala, G. Lodato, "Hypertensive choroidal changes in indocyanine green angiography," *Vision Research*, **36**, p. 2423, Oct. 1996.
36. K. Ishikawa, S. Yoneya, T. Saitoh, J.D. Young, "Evaluation of drusen, concerning a risk factor of age-related macular degeneration, with indocyanine green angiography," *Investigative Ophthalmology & Visual Science*, **37**, No. 3, p. 5171, Feb 15, 1996.
37. D.U. Bartsch, A.J. Mueller, W.R. Freeman, "Simultaneous indocyanine green and sodium fluorescein angiography using a confocal scanning laser ophthalmoscope," *Investigative Ophthalmology & Visual Science*, **37**, No. 3, p. 5173, Feb 15, 1996.
38. T. Desmettre, S. Mordon, S. Soulié, J.M. Devoisselle, J.M. Weisslinger "Shift of the fluorescence peak of indocyanine green (ICG) after injection: *in vivo* study on a vascular model," *Investigative Ophthalmology & Visual Science*, **37**, No. 3, p. 5174, Feb 15, 1996.
39. D.F. Swinehart "The Beer-Lambert law," *Journal of Chemical Education*, **39**, No. 7, p. 333, July 1962.

APPENDICES

APPENDIX A

SOFTWARE FOR DATA ACQUISITION AND ANALYSIS

A.1 DATA ANALYSIS

The first step in analyzing the data is to obtain the maximum values for the absorption coefficient for all degradation curves for each concentration; this was accomplished by the use of the statistics tool in SigmaPlot (Version 3.0). The statistics tool in SigmaPlot finds and displays the maximum value from the absorbance data from all irradiated samples of each concentration. The wavelength at which the maximum absorbance occurs for the unexposed “irradiated” sample (the sample that has been exposed to $0 \text{ J}\cdot\text{mL}^{-1}$ energy dosage) for a given concentration is then used for the wavelength the peak absorbance occurs for all other irradiated samples of the same given concentration. For example, the maximum absorbance for the $3 \text{ }\mu\text{M}$ ICG in methanol sample before exposure to laser radiation ($0 \text{ Joules delivered energy}$) occurs at 786.9 nm ; this absorbance at this wavelength for all the following irradiated absorbance spectra is then used as the maximum absorbance for subsequent irradiated samples--but only for the $3 \text{ }\mu\text{M}$ ICG in methanol sample. Due to slight shifts of the maximum spectral peak which can occur from one concentration to the next from aggregate formation or from simple background noise in the CCD camera, the wavelength which produces the maximum absorbance is re-calculated for each concentration in each solvent.

The maximum absorbance data is then copied to Microsoft Excel worksheet, where the absorption coefficient is calculated from the absorbance data (the absorption coefficient is the absorbance divided by the path length of the cuvette used). The absorption coefficients are then used with the laser irradiation data collected by the computer in Figure 2.1.

The amount of energy delivered to a sample before removal from the irradiation setup (removed for absorption data collection in the spectrophotometer setup), henceforth called an exposure, is calculated from the data file from the above mentioned computer. The appropriate transmitted to reflected ratio (described in Section 2.3.1) for a particular exposure is calculated by importing the data collected by a computer program (source code in Section A.2) into Sigma Plot. The raw Detector A data is then divided by the raw Detector B data (A:B ratio), with the results posted in another Sigma Plot column using Sigma Plot's user defined transforms. The average of the A:B ratio is then the average of the transmitted to reflected (T:R) ratio. Since the program that collects the Detector A and B data automatically sums all of the collected Detector A and B data, the T:R ratio is multiplied with the final sum of the total energy collected by Detector A. This then becomes the total amount of energy delivered to the ICG sample.

The experimentally obtained values for the absorption coefficient, α , and delivered energy, E , are now placed in the appropriate Excel worksheet cells, which are now to be used for the determination of the κ and m parameters given in Equation (2.12). Figure A.1 shows a sample of an Excel worksheet that was used to calculate the κ and m values for the 10 μM ICG in the water + 3% HSA solution.

In order to solve for the values of κ and m numerically, Equation (2.12) is modified slightly, which now becomes

$$d\alpha = -\kappa(1 - e^{-\alpha x})\alpha^{m-1} dE, \quad (\text{A.1})$$

which is then approximated by

$$\Delta\alpha = -\kappa(1 - e^{-\alpha x})\alpha^{m-1} \Delta E. \quad (\text{A.2})$$

For the numerical computations, $\Delta E = 1$ Joule. Since $\Delta E = 1$ and $\Delta\alpha = \alpha_i - \alpha_{i-1}$, then Equation (A.2) takes on the form

$$\alpha_i = \alpha_{i-1} - \kappa(1 - e^{-\alpha_{i-1}x})\alpha_{i-1}^{m-1} \quad (\text{A.3})$$

The initial value of the absorption coefficient, α_0 , is the initial absorbance of the unexposed “irradiated” sample (α_0 is labeled as **a0** in the Excel worksheet). Initial guesses for the values of κ and m are chosen and placed in two Excel worksheet cells (cells B15 and B16, respectively, in Figure A.1) and labeled **k** and **m**, for obvious reasons.

Initially, row 21 in the Excel worksheet has the value of E_0 and α_0 , then row 22 has values for E_1 and α_1 , row 23 has values for E_2 and α_2 , and so on. Since $\Delta E = 1$, then in a generalized form, $E_i = E_{i-1} + \Delta E = i$, where i runs from 1 to 600 (for this particular concentration, since the total energy delivered in the experiment was 600 J, and E_0 is just zero. The value for α_0 is also given, so that the value for α_i is $\alpha_i = \alpha_{i-1} - \Delta\alpha$, where $\Delta\alpha$ is given by Equation A.2. The values for α_i are then calculated by Equation A.3 by using the previously calculated value of α_{i-1} and the values of **k** and **m** given in the worksheet.

Now the experimentally obtained values of the absorption coefficient are compared to the theoretically obtained values of α that were calculated using Equation (A.3). In

column E, under the heading “Theoretical,” the theoretically obtained value of α (for which the “Theoretical Energy” value matches the “Total Delivered Energy (a/b)” value) is pasted in the cell next to the experimental value of α for the same delivered energy value. For example, cell E3 contains the value of cell B21 (corresponding to the theoretical value for 0 Joules delivered energy), cell E4 contains the value of cell B55 (corresponding to the theoretical value for 34 Joules of delivered energy), and so on.

Once the theoretical values are next to the experimental values, the absolute difference between the experimental and theoretical values are calculated in column F of the Excel worksheet under the label “ $\text{Sqrt}(R^2)$.” The values in this column are the square root of the square of the difference between the experimental data and the calculated values. Cell D14 represents the sum of each absolute difference calculated in cells F3 through F11. Using the Solver tool in Microsoft Excel, the value of cell D14 is minimized by changing the values of **k** and **m** given in cells B15 and B16, respectively. The initial values of **k** and **m** were usually taken to be 0.001 and 1, respectively, or values obtained from a previous fitting (i.e. the values for **k** and **m** for the 10 μM ICG in methanol may have been initially guessed to be the value for **k** and **m** obtained for the 3 μM ICG in methanol solution).

Individual Energy (a/b)	Total Delivered Energy (a/b)	Absorbance	Absorption coefficient (/mm)	Theoretical	Sqrt(R ²)
0	0	1.547176401	0.356250532	0.356250532	0
34.42390419	34	1.353806344	0.311725431	0.318356984	0.006631553
42.31976053	77	1.190696759	0.274168061	0.273443695	0.000724365
52.52638521	129	0.969122311	0.223148659	0.224073513	0.000924854
64.0853634	193	0.744837602	0.171505196	0.171508314	3.11756E-06
77.0553931	270	0.527460327	0.121452228	0.121009449	0.00044278
91.20933732	362	0.346762162	0.079844939	0.078090459	0.001754479
108.5709793	470	0.203523498	0.046863017	0.04686292	9.74268E-08
130.1179673	600	0.10810637	0.024892411	0.026477603	0.001585192
			Sum(Sqrt(R²))		
a0 =	0.356250532		0.012066438		
k =	0.00169123				
m =	1.351873593				
x =	10	mm			
Theoretical Energy	Theoretical Absorption Coeff.				
0	0.356250532				
1	0.355107708				
2	0.353966559				
3	0.352827088				
4	0.351689299				
5	0.350553196				
6	0.349418782				
7	0.348286062				
8	0.347155038				
9	0.346025716				
10	0.344898099				
11	0.34377219				
12	0.342647994				
13	0.341525514				
14	0.340404755				
15	0.33928572				
16	0.338168414				
17	0.33705284				
18	0.335939001				
19	0.334826903				
20	0.333716549				
21	0.332607944				
22	0.33150109				
23	0.330395992				
24	0.329292655				
25	0.328191082				
26	0.327091277				
27	0.325993244				
28	0.324896988				
29	0.323802512				
30	0.322709821				
31	0.321618918				
32	0.320529808				
33	0.319442495				
34	0.318356984				

FIGURE A.1. Microsoft Excel worksheet used for calculating the κ and m values for the 10 μM ICG in water + 3% HSA solution.

A.2 DATA ACQUISITION

The following is a listing of the Microsoft QuickBasic program written by the author used for collecting the energy delivered to the ICG sample. The data collected was for both the adjusted Detector A value (with an estimated average T:R ratio already multiplied to the data) and for the raw Detector A data so that the correct T:R ratio for that exposure could be calculated. The program was also written for a single detector setup that was not used for the experiments described in this thesis. The source code has a few “user friendly” implementations that were inserted to keep the author and other users of the program from performing such acts as inadvertently over-writing an existing data file or using an illegal file name that DOS 6.0 does not recognize. These lines of code along with the code that formats the data displayed on the computer monitor were added to simplify the use of the program, but are unnecessary for the overall collection of data.

```
'PROGRAM NAME: detectjc.bas
'
'DESC: This program tests the Rm-6600 GPIB bus using the NI AT-GPIB card.
'   The instrument must be set to Device Address 15 (factory default)
'   and the GPIB device name must be DEV15 (NI default).
'   The program will then collect and store data in a file and print
'   the data on screen.
'=====
'   This program works ONLY with the RM-6600 Universal Radiometer
'   by Laser Precision Copr.
'=====
'SYNTAX: n/a, main program
'
'INPUT: keyboard, Gpib
'
'OUTPUT: screen, Gpib, disk
'
'INCLUDE FILES: qbdecl4.bas, NI supplied QuickBasic 4.0/4.5 subprogram calls
'
'OTHER ACTIONS: none
'
'PROGRAMMER: Jason Crull
'
'previous revisions on: 8-2-96, 7-11-96, 5-7-96, 9-5-95, 9-26-95, 6-20-97
```

```
'$INCLUDE: 'c:\at-gpib\qbasic\qbdecl.bas'
```

```
DIM thepath(20) AS STRING
DECLARE SUB FindErr () 'subprogram to report board/device errors
DECLARE SUB Dev15Error () 'subprogram to report instrument errors
DECLARE SUB SetRange (Channel$, j$, range$, Joules$) 'subprogram to set detector range
DECLARE SUB NameCheck (name$, path$, notfound%, errcode%)
'NameCheck is a subprogram to check validity of filename of data file
DECLARE SUB PathCheck (path$, errcode%) 'check validity of file directory
```

```
AD$ = "AD" + CHR$(13) 'ASCII transfer without rm6600 screen updates
SD$ = "SD" + CHR$(13) 'ASCII transfer with Rm6600 screen updates
CMD$ = "" 'ASCII transfer command string
v% = 11 'variable that changes the minimum timeout
```

```
StartingPt:
```

```
ON KEY(5) GOSUB StopIt 'F5 key will stop program
KEY(5) ON
ON KEY(1) GOSUB StartingPt 'F1 key to go back one step in program
KEY(1) ON
CLS 'clear screen of all text and graphics
LOCATE 24, 1
PRINT "Hit <F5> to terminate program."
LOCATE 5, 5 'position cursor
PRINT "AD is ASCII transfer WITHOUT rm6600 screen updates (Faster)."
```

```
LOCATE 6, 5
PRINT "SD is ASCII transfer WITH rm6600 screen updates (Slower)."
```

```
LOCATE 8, 5
PRINT "Enter type of transfer A(D) or S(D) { default is A } : (A/S) "
```

```
DO
  Type$ = UCASE$(INKEY$)
  LOOP UNTIL (Type$ = "A") OR (Type$ = "S")
  CMD$ = AD$ 'This is the default setting. (jwc)
  IF (LEFT$(Type$, 1) = "A") THEN
    CMD$ = AD$ 'if first letter is A then AD
  END IF
  IF (LEFT$(Type$, 1) = "S") THEN
    CMD$ = SD$ 'if first letter is S then SD
  END IF
  KEY(1) OFF
```

```
GetNumberOfProbes:
```

```
CLS
LOCATE 23, 1
PRINT "Hit <F1> to go back one level in the program."
LOCATE 24, 1
PRINT "Hit <F5> to terminate program."
ON KEY(1) GOSUB StartingPt 'F1 key to go back one step in program
KEY(1) ON
numProbes% = 1
LOCATE 15, 1
PRINT "How many probes are you using with your detector ( 1 or 2) "
```

```
DO
  numProbes% = VAL(INKEY$)
  LOOP UNTIL ((numProbes% = 1) OR (numProbes% = 2))
  IF numProbes% = 1 THEN
    ch$ = "A"
    DO
      LOCATE 20, 1
      INPUT "Is your probe connected to Channel A or B (A or B, default is A)"; ch$
      ch$ = UCASE$(ch$)
      LOOP UNTIL ((ch$ = "A") OR (ch$ = "B"))
    END IF
```

```
TestTheRadiometer:
```



```

CLS                'clear screen of all text and graphics
' Assign a unique identifier to the first Gpib board (GPIB0) and store in
' variable Gp0%.
PRINT ""
PRINT "Testing the radiometer....."
PRINT ""
BDNAME$ = "GPIB0"      'put board name in string
CALL IBFIND(BDNAME$, Gp0%) 'find board, return number
IF Gp0% < 0 THEN CALL FindErr 'if board not found, then call the error routine
PRINT "The value returned in Gp0% was ", Gp0%
CALL IBSIC(Gp0%)      'Send Interface Clear to bd.
CALL IBSRE(Gp0%, 1)   'Set Remote Enable ON (1)

DName$ = "DEV15"      'put device name in string
CALL IBFIND(DName$, Dev15%) 'find device, return number
IF Dev15% < 0 THEN CALL FindErr 'if device not found, then call error routine
PRINT "The value returned in Dev15%", Dev15%
CPL% = &H100          'mask# for end of I/O transmission
ED% = &H2000          'mask # for end of a transmission
TIM% = &H4000         'mask # for time limit exceeded
CALL IBWAIT(Gp0%, CPL%) 'wait for end of I/O transmission

' Write the Identify instrument (ID) instruction to the Rm-6600 (DEV15).
' This string is meaningful to Laser Precision instruments only.
' (Note: the <CR> is optional. EOI must be sent with last byte on send.)

Write$ = "ID" + CHR$(13) 'build string to send
CALL IBWRT(Dev15%, Write$) 'Send command to Rm-6600

' If the data is valid, read the instrument identifier.

rd$ = SPACE$(25)      'create reply string for read
CALL IBRD(Dev15%, rd$) 'Read data from Rm-6600
PRINT "This is an Rm"; LEFT$(rd$, ibcnt%) 'Print string
CALL IBWAIT(Gp0%, CPL%)
PRINT ""
IF (ibcnt% = 0) THEN
  PRINT "The detector is not responding. Please make sure that the"
  PRINT "detector is on. If that is not the problem, run the program"
  PRINT "STOP.EXE or turn off the detector and turn it back on again."
  PRINT ""
  PRINT "If none of the above steps correct the problem then you are just out of luck!"
  PRINT ""
  PRINT ""
  END
END IF
PRINT "The test has been a success!"
KEY(1) OFF

```

```

'Start here when "Going Again" in the program

```

```

OPEN "c:\vm6600\filepath.dat" FOR INPUT AS #1 'File containing pre-set directories
i = 0
DO
  i = i + 1
  LINE INPUT #1, thepath(i)
LOOP UNTIL EOF(1) OR (i = 10)
CLOSE #1

```

```

PathTable:

```

```

KEY(5) OFF
DO 'This loop continues while ans$ = "Y" (Do you want to go again?)
  ans$ = ""
  DO
    KEY(5) ON
    CLS
    LOCATE 23, 1
    PRINT "Press <F5> to terminate program"

```

```

errcode% = 0
notfound% = 1
LOCATE 3, 1
PRINT "Choose a directory location to save your data,"
PRINT "or choose( "; i + 1; ") to enter you own customized directory."
FOR j = 1 TO i
LOCATE 5 + j, 4
PRINT "( "; j; ") "; thepath(j)
NEXT j
LOCATE 6 + i, 4
PRINT "( "; i + 1; ") <Enter your own directory--NO FLOPPY DRIVES> "
LOCATE 8 + j, 10
PRINT "Enter the number corresponding to the directory of your choice: "
ON KEY(1) GOSUB PathTable
KEY(1) ON
DO
  pathchoice% = VAL(INKEY$)
  LOOP UNTIL (pathchoice% >= 1) AND (pathchoice% <= i + 1)
  IF pathchoice% = i + 1 THEN
CLS
DO
LOCATE 22, 1
PRINT "Press <F1> then <RETURN> to go back one level."
LOCATE 23, 1
PRINT "Press <F5> then <RETURN> to terminate program"
LOCATE 10, 1
PRINT "Type in the directory of your choice: "
errcode% = 0
LOCATE 11, 2
PRINT "
"
LOCATE 11, 2
INPUT path$
CALL PathCheck(path$, errcode%)
LOOP UNTIL errcode% = 0
  ELSE
path$ = thepath(pathchoice%)
CALL PathCheck(path$, errcode%)
  END IF
LOOP UNTIL errcode% = 0
CLS
LOCATE 22, 1
PRINT "Press <F1> then <RETURN> to go back one level."
LOCATE 23, 1
PRINT "Press <F5> then <RETURN> to terminate program"
DO
CLOSE
LOCATE 9, 1
PRINT "Current directory "; path$
LOCATE 10, 1
PRINT "Enter filename for data storage: "
LOCATE 10, 35
INPUT name$ 'Store data
CALL NameCheck(name$, path$, notfound%, errcode%)
LOCATE 10, 35
PRINT "
"
IF errcode% <> 1 THEN
  IF LEN(path$) = 3 THEN
    filename$ = path$ + name$
  ELSE
    filename$ = path$ + "\" + name$
  END IF
  OPEN filename$ FOR OUTPUT AS #2
END IF
LOOP WHILE errcode% = 1

```

SetRange:

```

ON KEY(1) GOSUB PathTable
KEY(1) ON

```

```

CLS
LOCATE 23, 1
PRINT "Hit <F1> to go back one level in the program."
LOCATE 24, 1
PRINT "Hit <F5> to terminate program."
LOCATE 2, 5
PRINT " If an over-range is detected during the experiment, the detectors will"
PRINT " automatically reset and continue taking data using the same ranges; however,"
PRINT " during the short time it takes to reset the detectors, data will not be taken."

```

```

' these are the default settings used to display status during data acquisition, JWC
Arange$ = " Inactive "
Brange$ = " Inactive "

```

```

' Set the range of the detectors

```

```

IF numProbes% = 2 THEN
PRINT " "
PRINT " With what range do you wish to begin? "
CALL SetRange("A", JA$, Arange$, AJoules$)
RANA$ = "RA " + JA$ + CHR$(13)
CALL IBWRT(Dev15%, RANA$)      'send range to detector
CALL IBWAIT(Gp0%, CPL%)
CLS
LOCATE 23, 1
PRINT "Hit <F1> to go back one level in the program."
LOCATE 24, 1
PRINT "Hit <F5> to terminate program."
LOCATE 6, 5
CALL SetRange("B", JB$, Brange$, BJoules$)
RANB$ = "RB " + JB$ + CHR$(13)
CALL IBWRT(Dev15%, RANB$)    'send range to detector
CALL IBWAIT(Gp0%, CPL%)
CLS
ELSE

```

```

' Set range for only one Probe (A or B) present

```

```

IF ch$ = "A" THEN
CALL SetRange(ch$, JA$, Arange$, AJoules$)
RANA$ = "RA " + JA$ + CHR$(13)
CALL IBWRT(Dev15%, RANA$)    'send range to detector
CALL IBWAIT(Gp0%, CPL%)
ELSE
CALL SetRange(ch$, JB$, Brange$, BJoules$)
RANB$ = "RB " + JB$ + CHR$(13)
CALL IBWRT(Dev15%, RANB$)    'send range to detector
CALL IBWAIT(Gp0%, CPL%)
END IF
END IF
KEY(1) OFF

```

```

GetTheCal:

```

```

ON KEY(1) GOSUB SetRange
KEY(1) ON
CLS
LOCATE 23, 1
PRINT "Hit <F1> to go back one level in the program."
LOCATE 24, 1
PRINT "Hit <F5> to terminate program."
LOCATE 4, 1
PRINT "Do you wish to multiply one or both detectors by a"
PRINT "calibration factor (Y/N) "
DO
cal$ = UCASE$(INKEY$)
LOOP UNTIL (cal$ = "Y") OR (cal$ = "N")
Acal! = 1
Bcal! = 1

```

```

IF cal$ = "Y" THEN
  LOCATE 8, 4
  IF numProbes% = 2 THEN
    LOCATE 10, 6
    PRINT "What is the calibration factor for Probe A "
    LOCATE 11, 6
    INPUT " (Enter '1' for no calibration) "; Acal!
    LOCATE 13, 6
    PRINT "What is the calibration factor for Probe B "
    LOCATE 14, 6
    INPUT " (Enter '1' for no calibration) "; Bcal!
  ELSEIF ch$ = "A" THEN INPUT "What is the calibration factor for Probe A "; Acal!
  ELSEIF ch$ = "B" THEN INPUT "What is the calibration factor for Probe B "; Bcal!
  ELSE
    PRINT "You made a mistake"
    GOTO GetTheCal
  END IF
END IF
KEY(1) OFF

```

Setup the screen to display the data

```

CLS
ON KEY(1) GOSUB GetTheCal
KEY(1) ON
LOCATE 22, 1
PRINT "Hit <F1> to go back one level in the program."
LOCATE 23, 1
PRINT "Hit <F5> to terminate program."
LOCATE 4, 20
PRINT " Filename: "; filename$
LOCATE 5, 20
PRINT " A Range: "; Arange$
LOCATE 5, 44
PRINT "X"; Acal!
LOCATE 6, 20
PRINT " B Range: "; Brange$
LOCATE 6, 44
PRINT "X"; Bcal!
LOCATE 9, 10
PRINT "The displayed data is in Joules (J). "
LOCATE 11, 1
PRINT "Hit any key to start collecting data " '\
DO ' > wait until a key is pressed to begin
LOOP WHILE INKEY$ = "" ' /
KEY(1) OFF
KEY(5) OFF
' The following 6 lines clear previous data on screen
LOCATE 22, 1
PRINT " "
LOCATE 23, 1
PRINT " "
LOCATE 11, 1
PRINT " "
LOCATE 11, 1
PRINT "Collecting data"
dot0% = 17
dot1% = 0
LOCATE 13, 6
PRINT " Current Data" 'display data area
LOCATE 13, 40
PRINT "Total Accumulated"
LOCATE 13, 65
PRINT "OR ?"
IF numProbes% = 2 THEN
  LOCATE 14, 4
  PRINT "Detector A Detector B "
  LOCATE 14, 35
  PRINT "Detector A Detector B "

```

```

PRINT #2, "Filename: ", filename$
PRINT #2, "Detector A range: ", Arange$
PRINT #2, "Detector B range: ", Brange$
PRINT #2, "The 'calibration' factor (which has already been applied to the data) is:"
PRINT #2, "A_data * "; Acall
PRINT #2, "B_data * "; Bcall
PRINT #2, "The data (with calibration factor applied) is printed (in Joules) as follows: "
PRINT #2, "A_data, B_data, accumulated_A_data, accumulated_B_data, raw_A_data, raw_A_accumulated_data
(,overrange A &/or B)"
PRINT #2, "_____ "
energyA! = 0          ' resetting value for raw data from detector A
energyB! = 0          ' resetting value for raw data from detector B
CalEnergyA! = 0       ' resetting value for calibrated data from detector A
CalEnergyB! = 0       ' resetting value for calibrated data from detector B
ELSE
LOCATE 14, 4
PRINT "Detector " + ch$
LOCATE 14, 35
PRINT "Detector " + ch$
PRINT #2, "Filename: ", filename$
PRINT #2, "Detector "; ch$; " range: ", Arange$
PRINT #2, "The 'calibration' factor (which has already been applied to the data) is:"
PRINT #2, "A_data * "; Acall
PRINT #2, "The data (with calibration factor applied) is printed (in Joules) as follows: "
PRINT #2, "data, accumulated_data (,overrange)"
PRINT #2, "_____ "
END IF

CALL ibtmo(Dev15%, 11)          'changes default timeout in IBRD to 1s
' _____
' This loop is for the actual collection of data
' for TWO (2) Probes present
' _____
IF numProbes% = 2 THEN
' _____
' This DO loop takes data until a key is pressed
' _____
DO
CALL IBWRT(Dev15%, CMD$)          'Write command to Rm-6600
CALL IBRD(Dev15%, rd$)           'read energy meter

LOCATE 11, (dot0% + dot1%)
PRINT "."                          ' This prints a '.' at every collection of data or timeout for visual reference
' _____
' this prints a blank over energy A & B data to get rid
' of the old values and to print nothing when no data is taken
' _____

LOCATE 16, 5
PRINT " "
LOCATE 18, 5
PRINT " "
LOCATE 16, 62
PRINT " " ' gets rid of X's which indicates over-range
overrangeA$ = " "
overrangeB$ = " "
' _____
' This IF statement executes only if data is taken
' _____
IF (ibcnt% <> 0) THEN
' _____
' Do this if OR is detected
' _____
IF (INSTR(rd$, "OR") <> 0) THEN      'Check if Probe A or B has OR
leftrd$ = MID$(rd$, 1, ibcnt% / 2)
rightrd$ = MID$(rd$, ibcnt% / 2, ibcnt% - 11)
IF (INSTR(leftrd$, "OR") <> 0) THEN 'Check if OR is in Probe A
leftrd$ = AJoules$          'replace OR with max value of the current range
overrangeA$ = "AX "
END IF

```

```

IF (INSTR(rightrd$, "OR") <> 0) THEN 'Check if OR is in Probe B
    rightrd$ = BJoules$      'replace OR with max value of the current range
    overrangeB$ = "BX"
END IF
Aval! = VAL(leftrd$)      ' the data returned from the RM6600 is actual a text string
Bval! = VAL(rightrd$)    ' this converts the appropriate part of the text to numbers
CalEnergyA! = CalEnergyA! + Acal! * Aval!
energyA! = energyA! + Aval!
CalEnergyB! = CalEnergyB! + Bcal! * Bval!
energyb! = energyb! + Bval!
betterA! = Acal! * Aval!
betterB! = Bcal! * Bval!

```

```

Print Data to Screen and Disk when OR detected

```

```

LOCATE 16, 62
PRINT overrangeA$
LOCATE 16, 65
PRINT overrangeB$

```

```

Store the data to disk when OR detected

```

```

PRINT #2, betterA!, ";", betterB!, ";", CalEnergyA!, ";", CalEnergyB!, ";", Aval!, ";", energyA!, ";", overrangeA$, overrangeB$
LOCATE 16, 5
PRINT USING "#.####^AAA"; betterA!
LOCATE 16, 20
PRINT USING "#.####^AAA"; betterB!
LOCATE 16, 35
PRINT USING "#.####^AAA"; CalEnergyA!
LOCATE 16, 50
PRINT USING "#.####^AAA"; CalEnergyB!

```

```

Now reset the detector to clear the Over-Range
and reset the range values and timeout

```

```

CALL ibonl(Dev15%, 1)
CALL ibtmo(Dev15%, 11)      'changes default timeout in IBRD to 1s
CALL IBWRT(Dev15%, RANA$)   'send range to detector
CALL IBWAIT(Gp0%, CPL%)
CALL IBWRT(Dev15%, RANB$)   'send range to detector
CALL IBWAIT(Gp0%, CPL%)

```

```

ELSE
Finished handling OR "problem"

```

```

leftrd$ = MID$(rd$, 1, ibcnt% / 2)
rightrd$ = MID$(rd$, ibcnt% / 2, ibcnt% - 12)
Aval! = VAL(leftrd$)
Bval! = VAL(rightrd$)
energyA! = energyA! + Aval!
energyb! = energyb! + Bval!
betterA! = Acal! * Aval!
betterB! = Bcal! * Bval!
CalEnergyA! = CalEnergyA! + Acal! * Aval!
CalEnergyB! = CalEnergyB! + Bcal! * Bval!

```

```

LOCATE 16, 5
PRINT " "
LOCATE 16, 5
PRINT USING "#.####^AAA"; betterA!
LOCATE 16, 20
PRINT " "
LOCATE 16, 20
PRINT USING "#.####^AAA"; betterB!
LOCATE 16, 35
PRINT " "
LOCATE 16, 35
PRINT USING "#.####^AAA"; CalEnergyA!
LOCATE 16, 50

```

```

PRINT "      "
LOCATE 16, 50
PRINT USING "#.####^"; CalEnergyB!
PRINT #2, betterA!; ", "; betterB!; ", "; CalEnergyA!; ", "; CalEnergyB!; ", "; Aval!; ", "; energyA! 'store reading to disk, JWC
END IF
END IF 'End of "IF (ibcnt% <> 0)...".
IF (dot1% < 20) THEN 'this IF statement makes the dots following
dot1% = dot1% + 1 'Collecting data" to appear one after another to indicate collecting data
ELSE
dot1% = 1 'after 20 pulses the dots are cleared and start
LOCATE 11, dot0% + 1 'over again
PRINT "      "
END IF

LOOP WHILE INKEY$ = ""



---


This loop is the actual collection of data
for ONE (1) probe present


---


ELSE
IF ch$ = "B" THEN 'Use variables for probe A even
AJoules$ = BJoules$ 'if actually using probe B (JWC)
Acal! = Bcal!
RANAS$ = RANB$
END IF
DO
CALL IBWRT(Dev15%, CMD$) 'Write command to Rm-6600
CALL IBRD(Dev15%, rd$) 'read energy meter
LOCATE 11, (dot0% + dot1%)
PRINT ""
LOCATE 16, 5 ' \ this prints a blank over energy A & B data to get rid
PRINT "      " ' / of the old values and to print nothing when no data is taken
LOCATE 16, 5
PRINT "      "
LOCATE 16, 60
PRINT "      " ' gets rid of X's which indicates over-range
overrangeA$ = " "
IF (ibcnt% <> 0) THEN 'Check if any data was taken
IF (INSTR(rd$, "OR") <> 0) THEN
rd$ = " " + AJoules$ + " "
overrangeA$ = ch$ + "X"
energyA! = energyA! + VAL(rd$)
CalEnergyA! = CalEnergyA! + Acal! * VAL(rd$)
CALL ibonl(Dev15%, 1)
CALL ibtmo(Dev15%, 11) 'changes default timeout in IBRD to 1s
CALL IBWRT(Dev15%, RANAS$) 'send range to detector
CALL IBWAIT(Gp0%, CPL%)
ELSE
rd$ = LEFT$(rd$, ibcnt%)
energyA! = energyA! + VAL(rd$)
CalEnergyA! = CalEnergyA! + VAL(rd$)
END IF
Aval! = VAL(rd$)
betterA! = Acal! * Aval!
LOCATE 16, 62
PRINT overrangeA$
LOCATE 16, 5
PRINT USING "#.####^"; betterA!
LOCATE 16, 35
PRINT USING "#.####^"; CalEnergyA!
PRINT #2, betterA!; ", "; CalEnergyA!; ", "; overrangeA$
END IF
IF (dot1% < 20) THEN 'this IF statement makes the dots following
dot1% = dot1% + 1 'Collecting data" to appear one after another to indicate collecting data
ELSE
dot1% = 1 'after 20 pulses the dots are cleared and start
LOCATE 11, dot0% + 1 'over again
PRINT "      "
END IF

```

```

LOOP WHILE INKEY$ = ""
  END IF

  CALL ibtmo(Dev15%, 14)      'set timeout to longer time
  CLOSE #2                  'stop writing to disk
  LOCATE 11, 1              'this line and the next line erases "Collecting Data ...."
  PRINT "                    "
  LOCATE 23, 1
  INPUT "Data collection complete. Do you want to go again (Y/N) ?"; ans$
  ans$ = UCASE$(ans$)
  LOOP WHILE ans$ = "Y"
  PRINT ""

```

' To end the program, call the lbclr routine to Clear the device and put
' it in Local mode. Call the lbonl function to disable the hardware and
' software.

StopIt:

```

CALL IBCLR(Dev15%)          'Clear the device, go local
CALL lbonl(Dev15%, (0))    'Place device offline (0)
LOCATE 25, 1
END

```

'The following handles file naming/access errors

Handler:

```

SELECT CASE ERR
CASE 52
  PRINT "Bad file name! Please try again!"
  errcode% = 1
  CLOSE
  RESUME NEXT

CASE 53
  notfound% = 0
  RESUME NEXT

CASE 64
  PRINT "Bad file name! Please try again!"
  errcode% = 1
  CLOSE
  RESUME NEXT

CASE 76
  PRINT path$; " is an invalid path!!"
  PRINT "Please try again!"
  errcode% = 1
  CLOSE
  RESUME NEXT

CASE 55

  PRINT "File already open! Do you wish to close that file"
  PRINT "and write over it (Y/N)?"
  DO
    closeit$ = UCASE$(INKEY$)
    LOOP UNTIL (closeit$ = "Y") OR (closeit$ = "N")
    IF closeit$ = "Y" THEN
      CLOSE #2
      RESUME NEXT
    ELSE
      CLOSE #2
      errcode% = 1
      RESUME NEXT
    END IF
  END IF

CASE 58

```



```

PRINT "File already exists! Do you wish to over write it (Y/N)? "
DO
  overwrite$ = UCASE$(INKEY$)
  LOOP UNTIL (overwrite$ = "Y") OR (overwrite$ = "N")
  IF overwrite$ = "N" THEN
    errcode% = 1
    CLOSE #2
  END IF
  RESUME NEXT

CASE ELSE
  RESUME
END SELECT

```

```

' A routine at this location would analyze the fault code returned in the
' Dev15's (Rm-6600) status byte and take appropriate action.
'
SUB Dev15Error STATIC
  PRINT "Device 15 GPIB Error, Call LPC at 315-797-4492"
END SUB

```

```

' A routine at this location would notify you that the lbfnd call failed,
' and refer you to the handler software configuration procedures.
'
SUB FindErr STATIC
  PRINT "lbfnd ERROR consult National Instruments' manual for installation"
END SUB

```

```

SUB NameCheck (name$, path$, notfound%, errcode%)
  name1$ = name$
  LOCATE 1, 1
  PRINT "          "
  PRINT "          "
  LOCATE 15, 1
  PRINT "          "
  LOCATE 16, 1
  PRINT "          "
  LOCATE 18, 1
  PRINT "          "
  errcode% = 0
  temp% = 0

```

```

' Seperate the path and the filename
'
ON ERROR GOTO Handler      'enable error trapping when checking for
                             'existing filename
LOCATE 1, 1

```

```

' Check if file already exists
'
CHDIR path$
IF LEN(path$) = 3 THEN
  filename$ = path$ + name$
ELSE
  filename$ = path$ + "\" + name$
END IF
FILES filename$           'if the file is not found,notfound% =0 in Handler:
CLS
IF notfound% = 1 THEN
  PRINT "The file "; name$; " already exists in the directory"
  PRINT path$
  INPUT "Do you wish to over-write the existing file (Y/N) "; overwrite$
  overwrite$ = UCASE$(overwrite$)
  IF overwrite$ <> "Y" THEN
    errcode% = 1
    EXIT SUB
  END IF
END IF
END IF
dot% = INSTR(name$, ".")  'check to see if extension added

```

```

IF (dot% > 9) THEN errcode% = 1    'if the position of '.' is past 9, then the filename is too long
IF (dot% <> 0) THEN
  ext$ = MID$(name$, dot% + 1)
  IF (LEN(ext$) > 3) THEN errcode% = 1    'check if extension is too long
  name$ = MID$(name$, 1, dot% - 1) 'let the name be only the part up to the '.'
END IF
IF (LEN(name$) > 8) THEN errcode% = 1    'if no extension, check the length of the name
IF (LEN(name$) = 0) THEN
  LOCATE 15, 1
  PRINT "YOU FOOL! You were supposed to enter a filename! Try again!"
  errcode% = 1
  EXIT SUB
END IF

' this is a partial check for invalid characters in a filename
IF INSTR(name$, " ") THEN
  LOCATE 16, 1
  PRINT "Spaces are not allowed in filenames! Try again!"
  errcode% = 1
END IF
IF errcode% = 1 THEN
  LOCATE 18, 1
  PRINT "The filename you selected was too long, please try again "
  PRINT "You may only have 8 characters plus a 3 letter extension "
  PRINT ""
  PRINT "Example:      xxxxxxxx.xxx "
  EXIT SUB
END IF
name$ = name1$    'if everything is OK, set filename back to original, before I messed with it.
END SUB

```

```

SUB PathCheck (path$, errcode%)
ON ERROR GOTO Handler
IF LCASE$(LEFT$(path$, 1)) = "a" OR LCASE$(LEFT$(path$, 1)) = "b" THEN
  CLS
  LOCATE 1, 1
  PRINT "I DON'T SAVE TO FLOPPY DIRVES, YOU DOLT!!! "
  PRINT ""
  PRINT " Hit any key to try again... "
  DO
  LOOP WHILE INKEY$ = ""
  errcode% = 1
  EXIT SUB
END IF
CHDIR path$
END SUB

```

```

SUB SetRange (Channel$, j$, range$, Joules$)
PRINT ""
PRINT " This is for detector "; Channel$
PRINT ""
LOCATE 10, 15
PRINT "a) 30" + CHR$(230) + "J"    'CHR$(230) is a 'mu'
LOCATE 11, 15
PRINT "b) 300" + CHR$(230) + "J"    'CHR$(230) is a 'mu'
LOCATE 12, 15
PRINT "c) 3mJ "
LOCATE 13, 15
PRINT "d) 30mJ "
LOCATE 14, 15
PRINT "e) 300mJ"
LOCATE 15, 15
PRINT "f) 1J"
LOCATE 16, 20
PRINT "Enter choice (a,b,c,d,e,f) "
DO
  choice$ = LCASE$(INKEY$)
  LOOP UNTIL (choice$ = "a") OR (choice$ = "b") OR (choice$ = "c") OR (choice$ = "d") OR (choice$ = "e") OR (choice$ = "f")

```

```
IF (choice$ = "a") THEN
j$ = "1"
range$ = "30" + CHR$(230) + "J"
Joules$ = "0.000030"
  ELSEIF (choice$ = "b") THEN
j$ = "2"
range$ = "300" + CHR$(230) + "J"
Joules$ = "0.000300"
  ELSEIF (choice$ = "c") THEN
j$ = "3"
range$ = "3mJ"
Joules$ = "0.003"
  ELSEIF (choice$ = "d") THEN
j$ = "4"
range$ = "30mJ"
Joules$ = "0.030"
  ELSEIF (choice$ = "e") THEN
j$ = "5"
range$ = "300mJ"
Joules$ = "0.300"
  ELSEIF (choice$ = "f") THEN
j$ = "6"
range$ = "1J"
Joules$ = "1"
  ELSE
j$ = "1"
range$ = "30" + CHR$(230) + "J"
Joules$ = "0.000030"
  END IF
END SUB
```

APPENDIX B

PREVIOUS PUBLICATION

This appendix contains a reprint of the paper written by the author and published in the 1996 *SPIE Proceedings*, volume 2671, pages 243-250, titled "Indocyanine green degradation during high-intensity laser irradiation." The text in this paper has been reformatted and the graphs and figures have been reprinted to fit the specifications of the thesis. Other than the above mentioned formatting changes, the content of the article has been preserved, along with the original references.

Indocyanine green degradation during high-intensity laser irradiation

Jason Crull and Steven A. Schafer

Oklahoma State University
Department of Physics
145 Physical Sciences
Stillwater OK 74078-3072

ABSTRACT

It is known that aqueous solutions of indocyanine green (ICG) are not stable—the dye degrades over time, especially in the presence of light. Addition of protein or other partially-hydrophobic compounds (e.g., surfactants) to the solution act to stabilize the ICG, presumably by binding the dye and preventing occurrence of the degradation reaction. Solutions of ICG in other, less polar solvents, such as methanol, are also stable under normal conditions of handling and storage. We have discovered, however, that both protein-stabilized and methanol solutions of ICG will degrade when exposed to high-intensity monochromatic illumination. We irradiated 10 μ M aqueous solutions of ICG, containing human serum albumin (HSA) as a stabilizer, with light from an alexandrite laser (wavelength: 750 nm; pulse energy: 100mJ; pulse repetition rate: 20 Hz). While the HSA did act to slow the degradation process somewhat, even concentrations as high as 3% were not sufficient to prevent measurable degradation after as little as 30 seconds of irradiation. We obtained similar results with methanol solutions. Our results suggest that it is important to consider the type of illumination used during tissue welding in order to control ICG degradation. We present our measurements of the intensity dependence of ICG degradation in the presence of stabilizers. In addition, we discuss nonlinear effects (saturable absorption and multi-photon absorption and fluorescence) exhibited by ICG during high-intensity pulsed irradiation.

Keywords: indocyanine green, tissue welding, photothermolysis, photodegradation

1. INTRODUCTION

In recent years, indocyanine green (ICG) has been used as a selectivity agent in the delivery of laser energy to biological tissues.¹⁻¹⁵ While solutions of ICG in methanol or ethanol are stable, aqueous ICG solutions are unstable, and the ICG degrades over time and especially upon exposure to light.^{16,17} It has been found that the degradation of aqueous ICG is slowed and even eliminated when globular protein, such as human serum albumin (HSA), or a surfactant is added to the solution. Because ICG used as a selective energy absorber in biomedical applications is always associated with abundant free protein, the dye has been presumed to be stable under these conditions. However, the results of a recent study by LaJoie et al.¹⁸ suggest that ICG may photodegrade even in the presence of stabilizing protein, if the illumination intensity is high enough.

We have investigated this phenomenon by irradiating ICG solutions with high-intensity laser light. We have found that both methanol and aqueous + HSA solutions of ICG do photodegrade significantly when exposed to high-intensity illumination. We have also observed multi-photon absorption and fluorescence, as well as saturable absorption effects, in these solutions.

2. MATERIALS AND METHODS

2.1. Sample Preparation

Aqueous ICG solutions were prepared by dissolving laser-grade indocyanine green (IR-125, Kodak) and human serum albumin (Sigma) in distilled water to obtain a final concentration of 10 μM ICG and 3% HSA by weight. Approximately 3.5 ml of the solution was placed in a 4.5 ml-capacity acrylic cuvette having a 10 mm optical path length. A 3 \times 6 mm magnetic stir bar was then placed inside the cuvette and the cuvette sealed with Parafilm-M to retard evaporation.

Methanol solutions were prepared by dissolving IR-125 in methanol to obtain a concentration of 10 μM . As with the aqueous solutions, a magnetic stir bar was inserted along with the solution into a cuvette, and the cuvette sealed with Parafilm-M.

2.2. Experimental Setup--Irradiations

Figure 1 depicts the experimental setup used to expose the ICG solutions to a controlled amount of laser energy. The energy source is a pulsed alexandrite laser (Light Age PAL-101; wavelength: 750 nm; pulse repetition rate: 20 Hz; pulse energy: \sim 100 mJ; pulse width: \sim 60 μs). A fraction of the beam from the laser is split off using a glass slide as a beam splitter; this side beam is directed to a radiometer (Laser Precision RJP-735) which monitors the energy delivered by the laser during sample irradiation.

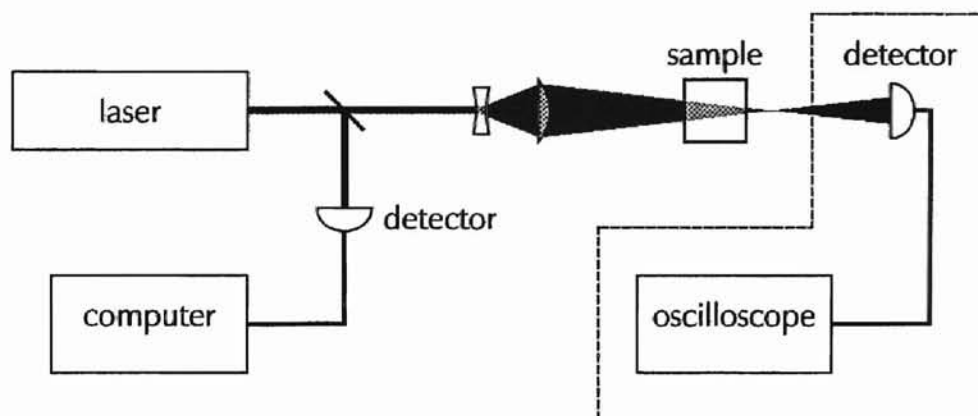


Figure 1. Experimental setup for irradiation of ICG solutions. The components enclosed by the dashed line are used only for the saturable absorption measurement.

The main portion of the beam proceeds through a diverging lens (to increase the spot size) and then through a cylindrical lens which collimates the beam into an elliptical shape. The elliptical beam then strikes the sample; the incident beam spot size is approximately 5 \times 20 mm. Care is taken to ensure that all of the light strikes the ICG solution, and none is lost around the periphery. A magnetic stirrer mixes the ICG solution during the irradiation to ensure that all of the solution is uniformly exposed to the laser light. The accumulated delivered energy is monitored in real time using the radiometer, and the irradiation is terminated when the desired energy dose has been delivered.

The effect of shorter laser pulses on the degradation of ICG was investigated using the same setup as above, with the only change being that the laser's Q-switch was enabled. With the Q-switch on, the pulse width is reduced from 60 μ s to 100 ns; however, the total energy per pulse is unchanged. Thus, the peak optical power is $\sim 600\times$ higher during Q-switched irradiation.

The energy delivery rate was 2W for all irradiations; the maximum energy dose was ~ 6 kJ. Thus, the maximum irradiation time was ~ 3000 s.

Saturable absorption measurements were also performed using the setup in Figure 1, with the addition of a high-speed photodetector (New Focus 1801) placed behind the ICG sample. The output of the detector was fed to an oscilloscope (Hewlett-Packard 5450A); the laser pulse width (full-width half-maximum) was measured using the oscilloscope's built-in measurement functions.

2.3. Experimental Setup--Spectrophotometry

At roughly equal intervals during irradiation, the cuvette containing the ICG sample was removed from the irradiation setup and inserted into the single-beam spectrophotometer shown in Figure 2. The infrared lamp (an electrically-heated wire) emits light in the wavelength range of interest for ICG optical absorption (600-900 nm). A condenser lens and a rectangular aperture (16 \times 5 mm) focus the light onto the cuvette; the spot size at the cuvette is approximately 4 mm \times 15 mm. After passing through the cuvette, the light enters the spectrometer (Instruments SA HR320) through a 50 μ m slit. The spectrum is imaged by a thermoelectrically cooled CCD camera (Photometrics CH 250; 1317 \times 1035 pixels).

Camera exposure time for optimum signal/noise ratio was ~ 5 s. Immediately after measurement of the light intensity passing through the ICG solution, the cuvette was replaced with one containing only the corresponding solvent (either water or methanol), and a second exposure made. The image obtained from the second exposure served as a reference--at a given wavelength, the ratio of the ICG signal to the reference signal is directly related to the optical absorbance by

$$A = -\log_{10}(I_{\text{ICG}}/I_{\text{reference}}), \quad (1)$$

where A is the optical absorbance, and I_{ICG} and $I_{\text{reference}}$ are the measured intensities of the signal and reference, respectively.

A part of the entrance slit is masked off to provide a "dark zone" in the CCD image. Any residual signal in this dark zone can be attributed to stray light and CCD dark current; this information is used to correct the data and significantly improve the signal/noise ratio of the resulting absorption spectra. Using this correction technique, the instrument is capable of measuring absorbance values as high as approximately 3.5.

After completion of an irradiation experiment (during which time several CCD images have been acquired), the images of the light transmitted through the ICG solutions are processed by computer to obtain absorbance spectra, as presented below.

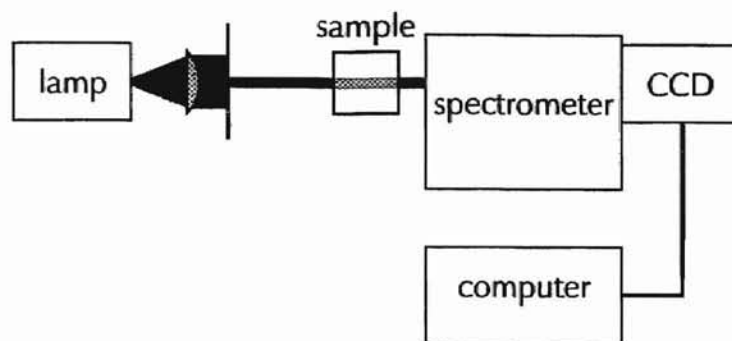


Figure 2. Experimental setup for spectrophotometric measurement of ICG solution optical absorbance.

3. RESULTS AND DISCUSSION

Figures 3-5 show the reduction in optical absorbance of three ICG solutions (aqueous + HSA, methanol, and methanol/Q-switched laser) as a consequence of laser irradiation. As can be seen, even small exposures ($\leq 50 \text{ J ml}^{-1}$) lead to measurable degradation of the ICG.

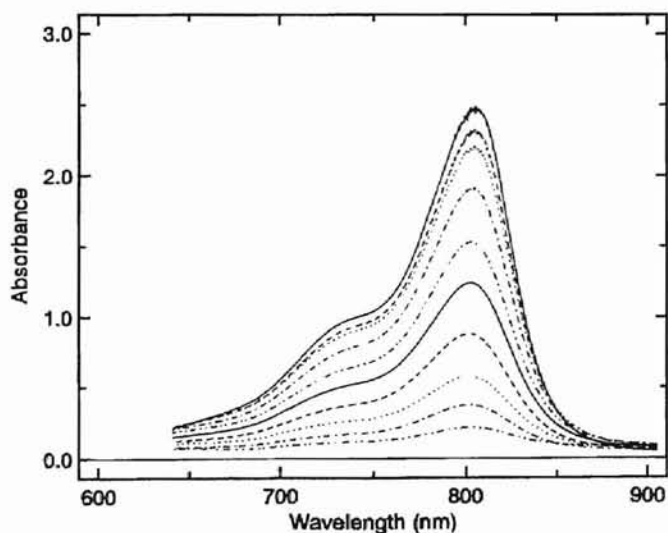


Figure 3. Optical absorbance spectra of photodegraded $10 \mu\text{M}$ aqueous ICG + HSA solution. From highest to lowest absorbance, delivered energy dose is 0, 12, 28, 58, 101, 146, 207, 280, 376 and 496 J ml^{-1} .

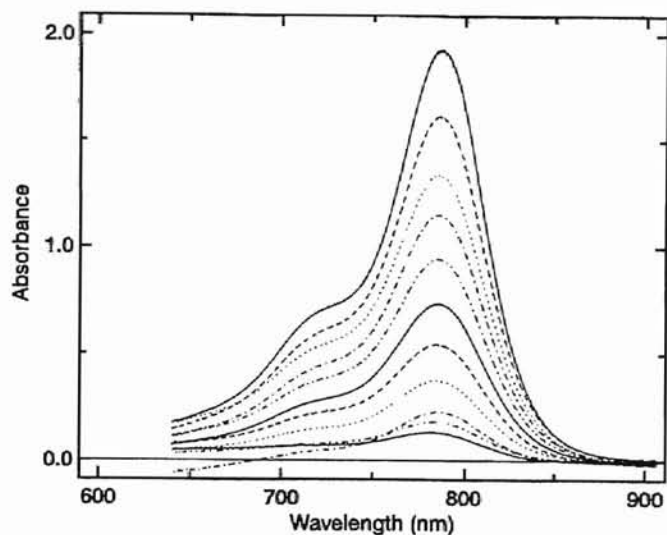


Figure 4. Optical absorbance spectra of photodegraded 10 μM methanol ICG solution. From highest to lowest absorbance, delivered energy dose is 0, 91, 211, 343, 493, 674, 861, 1059, 1269, 1480 and 1696 J ml^{-1} .

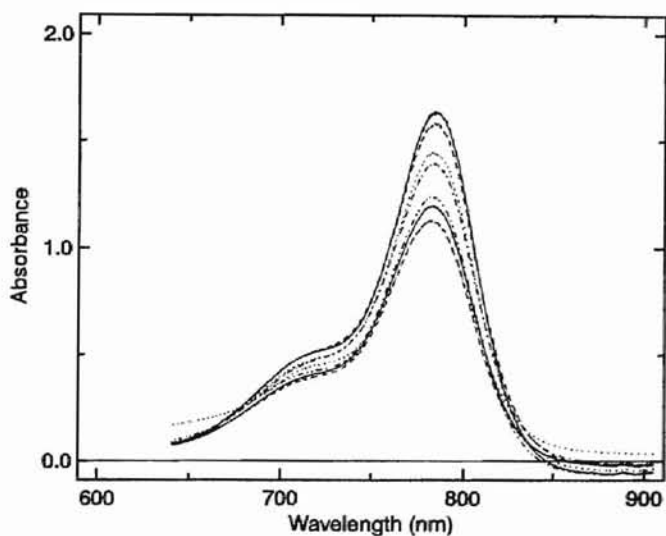


Figure 5. Optical absorbance spectra of photodegraded 10 μM methanol ICG solution; Q-switched irradiation. From highest to lowest absorbance, delivered energy dose is 0, 60, 151, 253, 374, 494, 644 and 766 J ml^{-1} .

In order to model the degradation behavior, we first note that while the energy *delivery* rate (*i.e.*, incident power) remains constant during an irradiation, the energy *absorption* rate does not, because the absorption coefficient decreases significantly during the course of the irradiation. If we assume that the degradation rate is proportional to the energy absorption rate, we can write

$$\frac{d\alpha}{dE} = -k(1 - e^{-\alpha x}), \quad (2)$$

where α is the absorption coefficient of the solution, E represents delivered energy, x is the path length of the cuvette, and k is a constant of proportionality. The quantity $1 - e^{-\alpha x}$ represents the fraction of the incident energy absorbed by the solution.

We find, however, that Equation 2 does not accurately fit the experimental data. One possible explanation for the discrepancy would be that the degradation rate is not simply proportional to the energy absorption rate, but contains other factors as well. For example, if the degradation reaction involves ICG dimers, the degradation rate would be proportional to the ICG concentration as well as to the energy deposition rate,

$$\frac{d\alpha}{dE} = -k(1 - e^{-\alpha x})C, \quad (3)$$

where C is the ICG concentration. From Beer's Law, we know that $\alpha \propto C$, so we can rewrite Equation 3 as

$$\frac{d\alpha}{dE} = -k'(1 - e^{-\alpha x})\alpha. \quad (4)$$

Similarly, if the degradation involves ICG trimers, then $da/dE = -k''(1 - e^{-\alpha x})\alpha^2$, and so on. The generalized form of this relationship is of course

$$\frac{d\alpha}{dE} = -k(1 - e^{-\alpha x})\alpha^{m-1}. \quad (5)$$

where we have dropped the prime superscripts on k , and m represents the number of ICG molecules involved in the degradation reaction.

Since ICG is known to exist in various oligomerized forms in solution,¹⁷ it is not unreasonable that one or more of these oligomers might participate in the degradation reaction. Indeed, we find that the inclusion of the additional factor α^{m-1} in Equation 5 dramatically improves the agreement between the model and the experimental data. The degradation rate data, derived from the spectra shown in Figures 3-5, are shown along with the best-fit curves calculated using Equation 5, in Figures 6-8, respectively.

For photodegradation of ICG in aqueous + HSA solution (Figure 6) and methanol solution (Figure 7), the "oligomerization exponent," m , is ~ 1.5 . Thus, it appears that the degradation reaction involves at least monomer and dimer forms of ICG, with possible contribution from higher oligomers. Because the units of k depend on m , different values of k obtained under different experimental conditions are not directly comparable, unless the corresponding values of m are equal. Nevertheless, since the values of m are similar in the two cases, we can conclude from the model fit that the degradation rate of ICG in aqueous + HSA solution is roughly four times larger than in methanol solution.

In the case of Q-switched irradiation, the oligomerized exponent is much larger, $m \approx 4.3$. While this may be partly the result of the oligomeric characteristics of the degradation reaction, it is also undoubtedly related to nonlinear (multi-photon) absorption of the incident light. To first order, the

factor $(1 - e^{-\alpha x})$ is approximately αx ; thus, for example, a two-photon absorption/degradation process, which would require that the degradation rate be proportional to $(1 - e^{-\alpha x})^2$, would increase the apparent oligomerization exponent by 1.

Figure 8 also shows that the degradation rate of a methanol solution of ICG when exposed to Q-switched laser pulses is much lower than when exposed to longer pulses. Using the saturable absorption observation setup shown in Figure 1, we measured the pulse width of the Q-switched pulses after they had traversed the sample. The pulse width of the light directly from the laser (sample removed) was 94 ns; however, when a 10 μM methanol solution of ICG was placed in the beam path, the pulse width decreased to 77 ns. This pulse-shortening behavior is indicative of saturable absorption. A 100 mJ pulse of 750 nm light contains 4×10^{19} photons, while 3.5 ml of a 10 μM ICG solution contains only 2×10^{16} ICG molecules. Thus, if the excited singlet state lifetime of ICG is long compared to the laser pulse width, it is expected that absorption saturation would occur.

We also observed substantial visible fluorescence during irradiation with Q-switched laser pulses. this fluorescence was easily seen by the naked eye, and through protective laser goggles designed to block 750 nm light. since the fluorescence emission is at wavelengths shorter than that of the incident radiation, a multi-photon absorption phenomenon must be involved. Most likely, the fluorescence is a result of two-photon absorption (375 nm equivalent) into the weak ICG absorption band centered near 350 nm.

Both saturated absorption and fluorescence act to reduce the amount of light energy available for photodegradation, thus explaining the much lower degradation rate observed during Q-switched irradiation.

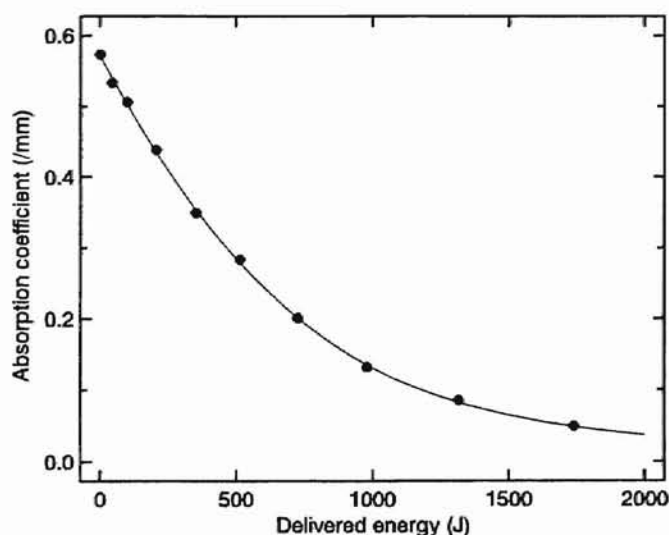


Figure 6. Photodegradation of 10 μM ICG in aqueous + HSA solution. Best-fit parameters are $\alpha_0 = 0.57 \text{ mm}^{-1}$, $k = 0.0011$, $m = 1.67$.

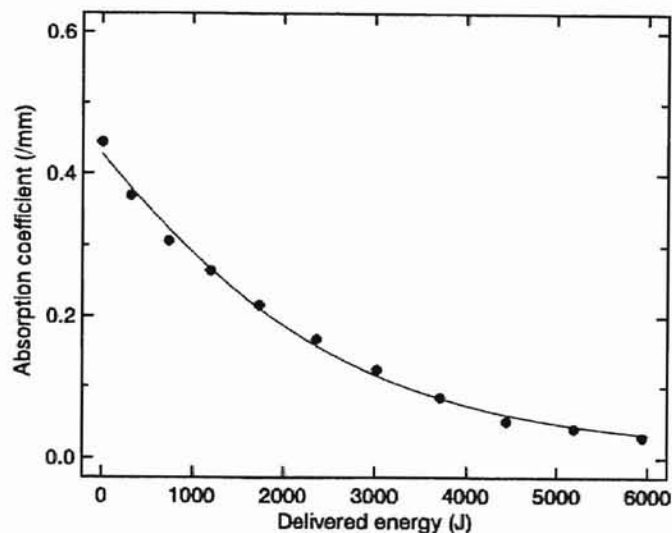


Figure 7. Photodegradation of 10 μM ICG in methanol solution. Best-fit parameters are $\alpha_0 = 0.43 \text{ mm}^{-1}$, $k = 0.00024$, $m = 1.52$.

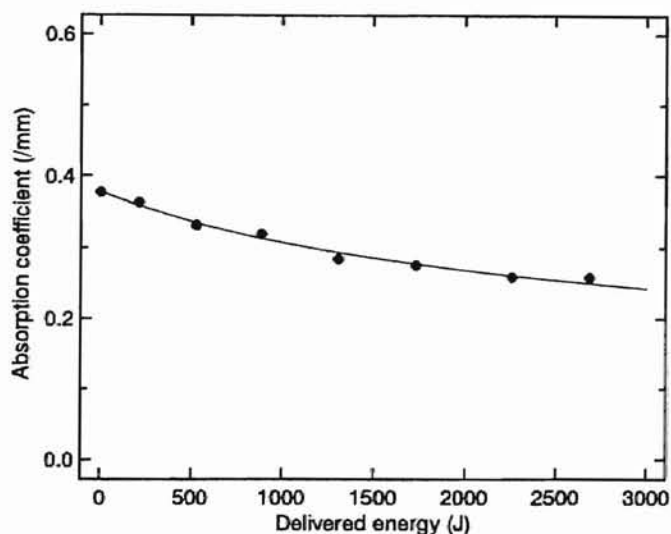


Figure 7. Photodegradation of 10 μM ICG in methanol solution; Q-switched irradiation. Best-fit parameters are $\alpha_0 = 0.38 \text{ mm}^{-1}$, $k = 0.0027$, $m = 4.33$.

4. SUMMARY

We have demonstrated that aqueous + HSA and methanol solutions of ICG will photodegrade when exposed to intense laser radiation, and that aqueous + HSA solutions degrade significantly more rapidly than do methanol solutions. We have also observed two nonlinear optical phenomena, saturable absorption and multi-photon absorption and fluorescence, during very high-intensity irradiation of ICG solutions. All three phenomena need to be taken into consideration by researchers contemplating the use of high-intensity pulsed laser light to excite ICG in biological tissues.

We plan to continue our investigation of these phenomena and to fully characterize the photodegradation of ICG solutions as a function of solvent, deposited light energy, and energy deposition rate.

5. ACKNOWLEDGMENTS

this work was supported by a grant from the Presbyterian Health Foundation. Dr. J.F. Zhou provided considerable assistance with the spectrophotometer and related data acquisition and analysis software.

6. REFERENCES

1. N. Maozami, M.C. Oz, L.S. Bass and M.R. Treat, Reinforcement of colonic anastomoses with a laser and dye-enhanced fibrinogen, *Arch. Surg.* **125**, pp. 1452-1454, 1990.
2. M.C. Oz, J.P. Johnson, S. Parangi, R.S. Chuck, C.C. Marboe, L.S. Bass, R. Nowygrod and M.R. Treat, Tissue soldering by use of indocyanine green dye-enhanced fibrinogen with the near infrared diode laser, *J. Vasc. Surg.* **11**, pp. 718-725, 1990.
3. T. M. Wider, S.K. Libutti, D.P. Greenwald, M.C. Oz, J.S. Yager, M.R. Treat and N.E. Hugo, Skin closure with dye-enhanced laser welding and fibrinogen, *Plastic Reconst. Surg.* **88**, pp. 1018-1025, 1991.
4. J.S. Auteri, M.C. Oz, V. Jeevanandam, J.A. Sanchez, M.R. Treat and C.R. Smith, Laser activation of tissue sealant in hand-sewn canine esophageal closure, *J. Thorac. Cardiovasc. Surg.* **103**, pp. 781-783, 1992.
5. L.S. Bass, N. Maozami, J. Pocsidio, M.C. Oz, P. LoGerfo and M.R. Treat, Changes in type I collagen following laser welding, *Lasers Surg. Med.* **12**, pp. 500-505, 1992.
6. S.D. DeCoste, W. Farinelli, T. Flotte and R.R. Anderson, Dye-enhanced laser welding for skin closure, *Lasers Surg. Med.* **12**, pp. 25-32, 1992.
7. D.P. Poppas, T.J. Choma, C.T. Rooke, S.D. Klioze and S.M. Schlossberg, Preparation of human albumin solder for laser tissue welding, *Lasers Surg. Med.* **13**, pp. 557-580, 1993.
8. L.S. Bass, N. Moazami, A. Avellino, W. Trosaborg and M.R. Treat, Feasibility studies for laser solder neuroorrhaphy, *SPIE Proc.*, **2128**, pp. 472-475, 1994.
9. U.M. Reali, R. Gelli, v. Fiannotti, F. Gori, R. Pini, F. Toncelli and U. Vanni, diode laser-assisted microvascular anastomosis: clinical and histological analysis on long period follow up, *SPIE Proc.*, **2128**, pp. 476-483, 1994.
10. J.R. Mourant, G.D. Anderson, I.J. Bigio and T.M. Johnson, Laser welding of bone: successful *in vitro* experiments, *SPIE Proc.*, **2128**, pp. 484-488, 1994.

11. M.L. Kayton, S.K. Libutti, M Bessler, J.D.F. Allendorf, S.D. Eiref, G. Marx, X.Mou, A. Morales, M.R. Treat and R. Nowygrod, A comparison of laser-activated tissue solders and thrombin-activated cryoprecipitate for wound closure, *SPIE Proc.*, **2128**, pp. 527-531, 1994.
12. D. Dimitrov, L.S. Bass and M.R. Treat, Thermal breakdown properties of indocyanine green, *SPIE Proc.*, **2395**, pp. 486-489, 1995.
13. S. Thomsen, E. Chan, I. Stubig, T. Menovsky and A.J. Welch, Importance of wound stabilization in early wound healing of laser skin welds, *SPIE Proc.*, **2395**, pp. 490-496, 1995.
14. R. Trickett, A. Lauto, J. Dawes and E. Owen, Laser activated protein solder for peripheral nerve repair, *SPIE Proc.*, **2395**, pp. 542-546, 1995.
15. K.E. Bartels, R.J. Morton, D.T. Dickey, E.L. Stair, M.E. Payne, S.A. Schafer and R.E. Nordquist, Use of diode laser energy (808 nm) for selective photothermolysis of contaminated wounds, *SPIE Proc.*, **2395**, pp. 602-606, 1995.
16. J. Gathje, R.R. Steuer, and K.R.K. Nicholes, Stability studies on indocyanine green, *J. Appl. Physiol.* **29**, pp. 181-185, 1970.
17. J.F. Zhou, M.P. Chin and S.A. Schafer, Aggregation and degradation of indocyanine green, *SPIE Proc.* **2128**, pp. 495-505, 1994.
18. E.N. LaJoie, A.d. Barofsky, K.W. Gergory and S.A. Prahl, Welding artificial biomaterial with a pulsed diode laser and indocyanine green dye, *SPIE Proc.*, **2395**, pp. 508-516, 1995.

VITA

JASON WAYNE CRULL

Candidate for the Degree of

Master of Science

Thesis: DEGRADATION BEHAVIOR OF INDOCYANINE GREEN DYE DURING
HIGH INTENSITY LASER IRRADIATION.

Major Field: Physics

Biographical:

Personal Data: Born in Oklahoma City, Oklahoma, on July 24, 1972, the son of
R. Wayne and Janis Crull.

Education: Graduated from Guthrie High School, Guthrie, Oklahoma in May 1990;
received Bachelor of Science degree in Engineering Physics from the
University of Central Oklahoma, Edmond, Oklahoma, in December 1994.
Completed the requirements for the Master of Science degree with a major in
Physics at Oklahoma State University in December 1997.

Professional Memberships: Society of Photo-Optical Instrumentation Engineers,
SPIE; Society of Physics Students, SPS; Sigma Pi Sigma, ΣΠΣ.